NEW APPROACHES TO IMPROVE THE PERFORMANCE OF THE PEM BASED FUEL CELL POWER SYSTEMS

A Dissertation

by

WOOJIN CHOI

Submitted to the Office of Graduate Studies of
Texas A&M University
in partial fulfillment of the requirements for the degree of

DOCTOR OF PHILOSOPHY

August 2004

Major Subject: Electrical Engineering

NEW APPROACHES TO IMPROVE THE PERFORMANCE

OF THE PEM BASED FUEL CELL POWER SYSTEMS

A Dissertation

by

WOOJIN CHOI

Submitted to the Office of Graduate Studies of
Texas A&M University
in partial fulfillment of the requirements for the degree of

DOCTOR OF PHILOSOPHY

Approved as to style and content by:

Prasad N. Enjeti (Co-Chair of Committee)	Jo W. Howze (Co-Chair of Committee)
Hamid A. Toliyat (Member)	Emil J. Straube (Member)

Chanan Singh
(Head of Department)

August 2004

Major Subject: Electrical Engineering

ABSTRACT

New Approaches to Improve the Performance of the PEM Based Fuel Cell Power Systems. (August 2004)

Woojin Choi,

B.S., Soongsil University, Seoul, Korea;

M.S., Soongsil University, Seoul, Korea

Co-Chairs of Advisory Committee: Dr. Prasad N. Enjeti
Dr. Jo W. Howze

Fuel cells are expected to play an important role in future power generation. However, significant technical challenges remain and the commercial breakthrough of fuel cells is hindered by the high price of fuel cell components. As is well known, the fuel cells do not provide the robust source characteristics required to effectively follow the load during significant load steps and they have limited overload-handling capability. Further, the performance of the fuel cell is significantly degraded when the CO (Carbon Monoxide) is contained in the hydrogen fuel.

In this thesis several new approaches to improve the performance of PEM based fuel cell power systems are discussed. In the first section an impedance model of the Proton Exchange Membrane Fuel Cell Stack (PEMFCS) is first proposed. This equivalent circuit model of the fuel cell stack is derived by a frequency response analysis (FRA) technique to evaluate the effects of the ripple current generated by the

power-conditioning unit. Experimental results are presented to show the effects of the ripple currents.

In the second section, a fuel cell powered UPS (Uninterruptible Power Supply) system is proposed. In this approach, two PEM Fuel Cell modules along with suitable DC/DC and DC/AC power electronic converter modules are employed. A Supercapacitor module is also employed to compensate for instantaneous power fluctuations including overload and to overcome the slow dynamics of the fuel processor such as reformers. A complete design example for a 1-kVA system is presented.

In the third section, an advanced power converter topology is proposed to significantly improve the CO tolerance on PEM based fuel cell power systems. An additional two-stage dc-dc converter with a supercapacitor module is connected to the fuel cell to draw a low frequency (0.5Hz) pulsating current of the specific amplitude (20-30[A]) from the fuel cell stack. CO on the catalyst surface can be electro-oxidized by using this technique, and thereby the CO tolerance of the system can be significantly improved. Simulation and experimental results show the validity and feasibility of the proposed scheme.

To My God

For His Grace, Mercy, Guidance and All the Support

To My Parents:

Ki-Woong Choi and Ok-Yeon Park

For Their Endless Sacrifice, Love and Prayers

To My Wife and Son:

Suyeol Kim and Samuel Hyun Choi

Who Are My Beloved.

ACKNOWLEDGMENTS

I would like to express my heartfelt gratitude to Dr. Enjeti. His professionalism in his academic and research activities has broadened my knowledge in power electronics and power quality. I want to express my sincere appreciation to the other members for serving on my committee; Dr. Howze, Dr. Toliyat and Dr. Straube.

I would like to thank my parents, wife and son for their love, support and encouragement in all my endeavors.

And for all things, I thank the Lord.

TABLE OF CONTENTS

CHAPTER Page

LIST OF FIGURES

FIGURE Page

FIGURE Page

LIST OF TABLES

CHAPTER I

INTRODUCTION

1.1 Introduction

Increasing environmental awareness and imminent fossil-fuel-supply shortages are forcing society to develop and adopt a combination of clean and highly efficient power-generation system. During the past century, the world has witnessed a lot of ecological disasters on an unprecedented scale. Greenhouse effect discussions over the last decade have led to general acceptance of the theory that carbon dioxide (CO_2) emissions cause atmospheric heating, and global studies have conclusively shown that the earth's fossil fuel resources should be better maintained in order to secure a sustainable future. This consensus has led to the legislation of emission penalties in several countries [1].

The oil is becoming scarce and may be considered to achieve its peak production with in the next few years. The idealized potential energy depletion curve shows that oil is expected to last hardly for more than 100 years [2]. Further, the outbreak of the gulf wars II reemphasized the global importance of the world's most traded commodity,

---

The citations in this dissertation follow the style of *IEEE Transactions on Industry Applications*.

crude oil, and made this valuable feedstock the focus of attention. Now it has become a trend for most rich nations to reduce their dependency on oil by diversification of primary energy sources. Another significant trend is decentralization of power production, since people now realize that the limited fossil fuel reserves should be used as efficiently as possible, with minimum losses during production as well as transmission and end use.

In this aspect, the fuel cells are emerging as a highly promising alternative to conventional power generation due to their high efficiency, lower environmental impact, reliability, compactness, modularity, quiet operation and fuel flexibility. Furthermore, fuel cell systems can provide both power and heat with cogeneration efficiencies as high as 80% [3]. A fuel cell is an electrochemical device that combines hydrogen fuel and oxygen from the air to produce electricity, heat and water. Fuel cells operate without combustion, so they are virtually pollution free. Since the fuel is converted directly to electricity, a fuel cell can operate at much higher efficiencies than internal combustion engines, extracting more electricity from the same amount of fuel. The fuel cell itself has no moving parts - making it a quiet and reliable source of power. As hydrogen flows into the fuel cell anode, platinum coating on the anode helps to separate the gas into protons (hydrogen ions) and electrons. The electrolyte in the center allows only the protons to pass through the electrolyte to the cathode side of the fuel cell. The electrons cannot pass through this electrolyte and flow through an external circuit in the form of electric current. As oxygen flows into the fuel cell cathode, another platinum coating helps the oxygen, protons, and electrons combine to produce pure water and heat. Individual fuel

cells can be then combined into a fuel cell stack. The number of fuel cells in the stack determines the total voltage, and the surface area of each cell determines the total current. Multiplying the voltage by the current yields the total electrical power generated.

With the significant advantages over the conventional power source, as described above, their usage is being expanded to accommodate the needs for various application fields such as,

- Stationary power installations for utilities, factories, emergency power (UPS) for hospitals, communications facilities, credit card centers, police stations, banks and computer installations.
- Diverse military applications.
- Domestic power supplies for individual residences.
- Mobile phones, laptop computers and other personal electronic devices.
- Transportation - particularly cars and buses but also in boats, trains, planes, scooters and bicycles, as well as highway road signs.
- Portable power for building sites, camping and vending machines.
- Landfills and waste water treatment plants (which are using fuel cells to convert the methane gas they produce into electricity).

Although the potential benefits of fuel cells are significant, many challenges, technical and otherwise, must be overcome before fuel cell will be a successful,

competitive alternative to the conventional power sources for consumers. These challenges can be summarized as followings.

- Cost: Cost is the greatest challenge to fuel cell development and adaptation, and it is a factor in almost all other fuel cell challenges as well. Several fuel cell designs require expensive, precious metal catalysts such as Pt, while others require costly materials that are resistant to extremely high temperatures. Costs are also associated with fuel cell durability and operating lifetime, fuel delivery and storage, power conditioner, and other aspects of fuel cell use.
- Power Quality: Fuel cells do not provide a stiff power source. There are inherent voltage variations from fuel cells according to the load and fuel cells do not respond to the load change quickly due to its delay time for fuel flow rates to adjust. This phenomenon becomes more serious if the fuel cell is associated with the reformer for the conversion of hydrogen-rich fuels into pure hydrogen. Thus the voltage fluctuation is unavoidable unless the auxiliary energy storage device such as batteries and/or supercapacitor is adopted.
- Fuel: A number of fuel-related challenges exist for fuel cells, especially those powered by pure hydrogen. Production of hydrogen is currently more expensive to produce than conventional fuels, such as gasoline, and many of the more cost-effective production methods generate greenhouse gases. And one of the problems in reforming hydrogen-rich gas is the presence of carbon monoxide (CO) in the hydrogen fuel. CO, a by-product of the reforming process, can poison the PEM fuel cell by blocking the catalyst and can drastically decrease the

output voltage and hence the power output. Many natural gas reformers (adiabatic) developed to date can produce as little as 10 parts per million (PPM) of CO. However, these reformers are expensive and thereby become another factor to increase the system cost.

- Durability & Dependability: Another technical challenge facing fuel cells is the need to increase durability and dependability. High-temperature fuel cells, in particular, are prone to material breakdown and shortened operating lifetimes. PEM fuel cells must have effective water management systems to operate dependably and efficiently. Finally, all fuel cells are prone, in varying degrees, to catalyst poisoning, which decreases fuel cell performance and longevity.
- Delivery: The current system for delivering conventional fuels to consumers cannot be used for hydrogen. New infrastructure will have to be developed and deployed. Unfortunately, since several potential technologies are evolving at this stage of development, the exact infrastructure requirements have not been determined.
- Storage: Hydrogen has a low energy density in terms of volume, making it difficult to store amounts adequate for most applications in a reasonable-sized space. This is a particular problem for hydrogen-powered fuel cell vehicles, which must store hydrogen in compact tanks. High-pressure storage tanks are currently being developed, and research is being conducted into the use of other storage technologies such as metal hydrides and carbon nanostructures (materials that can absorb and retain high concentrations of hydrogen).

- Safety: Hydrogen, like gasoline or any other fuel, has safety risks and must be handled with due caution. While we are quite familiar with gasoline, handling hydrogen will be new to most of us. Therefore, developers must optimize new fuel storage and delivery systems for safe everyday use, and consumers must become familiar with hydrogen's properties and risks.
- Public Acceptance**:** Finally, fuel cell technology must be embraced by consumers before its benefits can be realized. This is especially true for transportation, stationary residential, and portable applications, where consumers will interact with fuel cell technology directly. Consumers may have concerns about the dependability and safety of fuel-cell-powered equipment, just as they have about other modern devices when they were introduced.

A great deal of research effort is being made all over the world to overcome these challenges for accelerating the market penetration of the fuel cell. It is expected that some of them are likely to be overcome in the foreseeable future, but the others are not. This dissertation is mainly focused on improving the performance of the fuel cell power conditioning system in terms of cost, power quality, and fuel issue, and thereby suggests the design criteria for the improved, cost-effective fuel cell power conditioning system.

1.2 Historical Background of the Fuel Cell [1]

The history of the fuel cell can be traced back to the nineteenth century and the work of the British judge and scientist, Sir William Robert Grove. His experiments in

1839 on electrolysis - the use of electricity to split water into hydrogen and oxygen - led to the first mention of a device that would later be termed the fuel cell. Grove reasoned that it should be possible to reverse the electrolysis process and generate electricity from the reaction of oxygen with hydrogen. To test this theory he enclosed two platinum strips in separate sealed bottles, one containing hydrogen and one oxygen. When these containers were immersed in dilute sulphuric acid a current began to flow between the two electrodes and water was formed in the gas bottles. In order to increase the voltage produced, Grove linked several of these devices in series and produced what he referred to as a 'gas battery'. The term 'fuel cell' was coined by the chemists Ludwig Mond and Charles Langer in 1889 as they attempted to build the first practical device using air and industrial coal gas. It soon became apparent that there would be many scientific hurdles to overcome if this technology were to be commercialized and early interest in Grove's invention began to diminish. By the end of the century the advent of the internal combustion engine and the widespread exploitation of fossil fuels meant that the fuel cell was relegated to the status of a scientific curiosity.

The next major chapter in the fuel cell story was written by an engineer at Cambridge University, Dr Francis Thomas Bacon, a direct descendent of his 17th century philosopher namesake. In 1932 Bacon resurrected the machine developed by Mond and Langer and carried out a number of modifications to the original design. These included replacing the platinum electrodes with less expensive nickel gauze. He also substituted the sulphuric acid electrolyte for alkali potassium hydroxide, a substance less corrosive to the electrodes. This device, which he named the ‘Bacon Cell’, was in

essence the first alkaline fuel cell (AFC). It would however prove to be another 27 years until he could produce a truly workable fuel cell. In 1959 Bacon demonstrated a machine capable of producing 5 kW of power, enough to power a welding machine. It soon became apparent that Bacon was not the only person working on fuel cells as later that year Harry Karl Ihrig of Allis-Chalmers, a farm equipment manufacturer, demonstrated the first fuel cell powered vehicle. By combining 1008 cells he produced a fuel cell stack which could generate 15 kW and was capable of powering a 20 horsepower tractor. These developments helped pave the way for the commercialization of the fuel cell as we know it today.

The recent history of the fuel cell can be thought of as beginning in the early 1960s. A new US government agency, the National Aeronautics and Space Administration (NASA), was looking for a way to power a series of upcoming manned space flights. NASA had already ruled out using batteries as they were too heavy, solar energy as it was too expensive and nuclear power as it was too risky and began to look around for an alternative. The fuel cell was lighted upon as a possible solution and NASA awarded a number of research contracts to develop a practical working design. This search led to the development of the first Proton Exchange Membrane (PEM). In 1955 Willard Thomas Grubb, a chemist working for General Electric (GE), further modified the original fuel cell design by using a sulphonated polystyrene ion-exchange membrane as the electrolyte. Three years later another GE chemist, Leonard Niedrach, devised a way of depositing platinum on to this membrane and this became known as the 'Grubb-Niedrach fuel cell'. GE went on to develop this technology with NASA, leading

to it being used on the Gemini space project. This was the first commercial use of a fuel cell. In the early 1960s the aircraft manufacturer Pratt & Whitney licensed the Bacon patents for the alkaline fuel cell. The company modified the original design in order to reduce the weight and developed a cell that proved to be longer lasting than the GE PEM design. As a result Pratt & Whitney won a contract from NASA to supply these fuel cells to the Apollo spacecraft and alkali cells have since been used on most subsequent missions, including the Space Shuttle flights. An additional benefit of using fuel cell power is that they produce drinkable water as a by-product. Despite this flurry of interest in space applications, there was little development work at this time on fuel cells for more down to earth applications.

An oil embargo in 1973 kick-started renewed interest in fuel cell power for terrestrial applications as governments looked to reduce their dependence on petroleum imports. A number of companies and government organizations began to undertake serious research into overcoming the obstacles to widespread commercialization of the fuel cell. Throughout the 1970s and 1980s a huge research effort was dedicated to developing the materials needed, identifying the optimum fuel source and drastically reducing the cost of this exotic technology.

Finally, in the 1990s, over 150 years after Grove's experiments, the promise of inexpensive, clean, renewable energy began to look as if it might become reality as the first viable fuel cells were unveiled. Technical breakthroughs during the decade included the launch of the first fuel cell-powered vehicle in 1993 by the Canadian company

Ballard. Two years later a fuel cell stack with a power density of 1 kW per liter was demonstrated by Ballard and Daimler Benz.

For a long time, the price of fuel cell systems was prohibitive and they were used only in special applications, where good performance was the primary concern. In the last 20 years, ongoing research has produced new materials and solutions, which have led to improving fuel cell economies. That, coupled with concern for the environment and earth's limited resources, has led to introduction of commercial applications of fuel cells.

In the last few years we have seen fuel cells installed in hospitals and schools and many of the major automotive companies have unveiled prototype fuel cell powered cars. Trials of fuel cell powered buses have taken place in Chicago and Vancouver with other cities in North America and Europe looking to take delivery of these vehicles in the near future. Over the coming decades concerns over depleting stocks of natural resources and a growing awareness of the environmental damage caused by widespread burning of fossil fuels will help to drive the development of fuel cells for both transport and stationary power sources.

1.3. Overview of the Fuel Cell Technologies

1.3.1. Fundamentals of the Fuel Cell

The fuel cell is an electrochemical device that converts energy into electricity

and heat without combustion. A fuel cell consists of a cathode (negatively charged electrode), an anode (positively charged electrode) and an electrolyte (Fig 1). The anode provides an interface between the fuel and the electrolyte, catalyzes the fuel reaction, and provides a path through which free electrons are conducted to the load via the external circuit. The cathode provides an interface between the oxygen and the electrolyte, catalyzes the oxygen reaction, and provides a path through which free electrons are conducted from the load to the oxygen electrode via the external circuit. The electrolyte acts as the separator between hydrogen and oxygen to prevent mixing and, therefore, preventing direct combustion.

While there are different fuel cell types, all work on the same principle. Hydrogen, or a hydrogen-rich fuel, is fed to the anode where a catalyst separates hydrogen's negatively charged electrons from positively charged ions (protons). At the cathode, oxygen combines with electrons and, in some cases, with species such as protons or water, resulting in water or hydroxide ions, respectively. The electrons from the anode side of the cell cannot pass through the membrane to the positively charged cathode; they must travel around it via an electrical circuit to reach the other side of the cell. This movement of electrons is an electrical current. The amount of power produced by a fuel cell depends upon several factors, such as fuel cell type, cell size, the temperature at which it operates, and the pressure at which the gases are supplied to the cell. Still, a single fuel cell produces enough electricity for only the smallest applications. Therefore, individual fuel cells are typically combined in series into a fuel cell stack. Direct hydrogen fuel cells produce pure water as the only emission. This

water is typically released as water vapor. Fuel cells release less water vapor than internal combustion engines producing the same amount of power.

1.3.2. Thermodynamics [1,4]

The basic reaction for the hydrogen/oxygen fuel cell can be written as (1.1)-(1.3)

Anode reaction: $H_2 \rightarrow 2H+ + 2e-$ (1.1)

Cathode reaction: $½O_2 + 2e- + 2H+ \rightarrow H_2O$ (1.2)

Total reaction: $H_2 + ½O_2 \rightarrow H_2O$ (1.3)

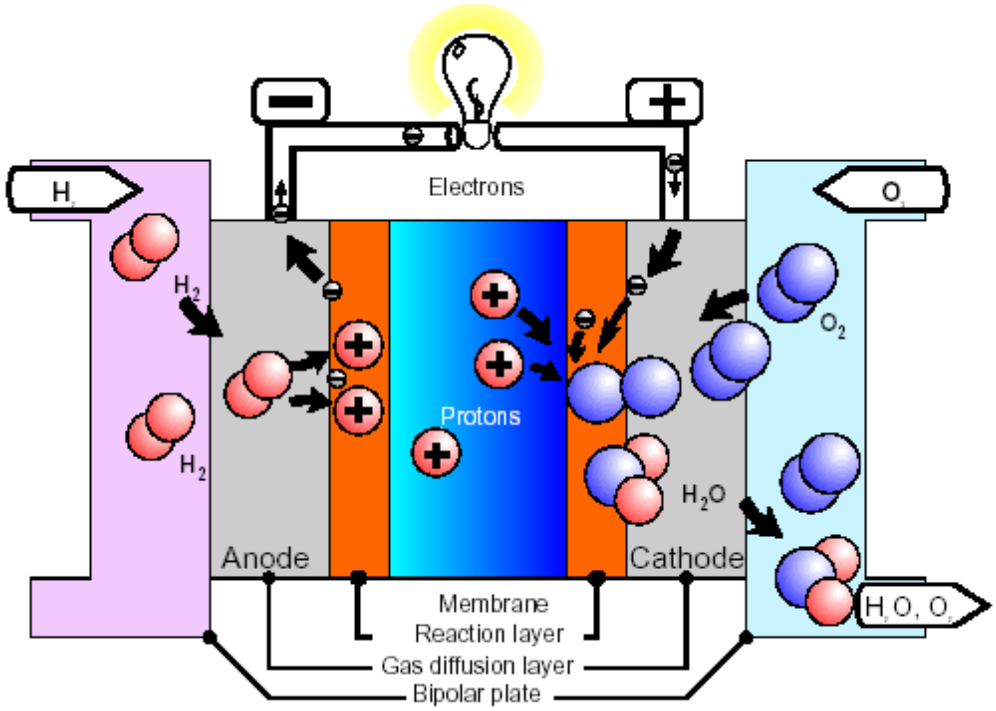

Fig. 1.1 Structure of the fuel cell

Fuel cells convert chemical energy directly into electrical energy (Fig. 1.1). Thus the energy to be released by the reaction can be expressed by the difference between the chemical energy of the reactants and that of the products. The chemical energy of a system can be expressed in terms of several thermodynamic quantities including enthalpy, Helmholtz free energy and Gibbs free energy. In the case of fuel cell, it is the Gibbs free energy that is important. Gibbs free energy is the he total amount of energy that is either used up or released during a chemical reaction. Thus it is the change in enthalpy, calculated by adding up the amount of energy released or used up to break or form chemical bonds during the reaction.

$$\Delta G_f = (\sum \Delta g_f)_{products} - (\sum \Delta g_f)_{reactants} \quad (1.4)$$

where,

ΔG_f: Gibbs free energy change for the reaction defined on a per mole basis of one of the reactants or products.

Δg_f: Gibbs free energy of formation

In order to determine the maximum electrical energy that can be extracted from a chemical reaction, it is needed to find the relationship between chemical energy content of fuel-oxidant system and the maximum electrical work that can be performed. For an electrochemical reaction, the maximum electrical work obtained is related to equilibrium potential as follows:

Maximum electrical work = $nFEo$ (1.5)

where,

n = number of electrons participating in the reaction

F = Faraday's Constant (96, 485 Coulombs)

Eo = Equilibrium potential (also called the reversible potential or theoretical open circuit potential/voltage, i.e. OCP/OCV)

The molar free energy change of reaction in terms of Gibbs free energy is related to the maximum electrical work according to the following relationship.

$$\Delta G_f = nFEo \quad (1.6)$$

Gibbs free energy of formation of common chemical species is available in standard thermodynamics textbooks. The JANAF (Joint Army Navy Armed Forces) Thermochemical Tables (1986) provide thermochemical data, including Gibbs free energy of formation, for hundreds of chemical species. [5]

The Gibbs free energy change for the reaction occurring in a hydrogen-oxygen fuel cell according to the reaction equation (1.3) can be calculated as follows:

$$\Delta G_f = (\Delta g_f)_{H_2O} - (\Delta g_f)_{H_2} - \tfrac{1}{2} (\Delta g_f)_{O_2} \quad (1.7)$$

The above equation can be calculated as (1.8) by using the value found from the molar thermodynamic properties table [5].

$$\Delta G_f = -237{,}129\ [J/mol] \tag{1.8}$$

Therefore, theoretical maximum equilibrium potential can be calculated from (1.6) and (1.8) as follows.

$$E_0 = \frac{\Delta G_f}{nF} = \frac{237129\ [J/mol]}{2 * 96485\ [Coulombs/mol]} = 1.23\ [V] \tag{1.9}$$

1.3.3. Causes of Voltage Drop

Even though the theoretical maximum open circuit voltage is 1.23 [V], it is found that the actual output voltage is less than this, often considerably less. Figure 1.2 show the performance of a typical single cell operating at 40 °C, at normal air pressure. As seen in the figure, the rapid initial fall in voltage is observed and after then the voltage falls slowly. At higher current, the voltage again falls rapidly. This voltage drop results from three major causes described below.

1. Activation losses: These are caused by the slowness of the reaction taking place on the surface of the electrodes. A proportion of the voltage generated is lost in driving the chemical reaction that transfers the electrons to or from the electrode.

2. Ohmic losses: This voltage drop is straightforward resistance to the flow of electrons through the material of the electrodes and the various interconnections, as well as the resistance to the flow of ions through the electrolyte. This voltage drop is essentially proportional to the current, linear and so called ohmic losses.

3. Concentration losses or mass transport: These result from the change in concentration of the reactants at the surface of the electrodes as the fuel is used. This is also called mass transport because the reduction in concentration is the results of the failure to transport sufficient reactant to the electrode.

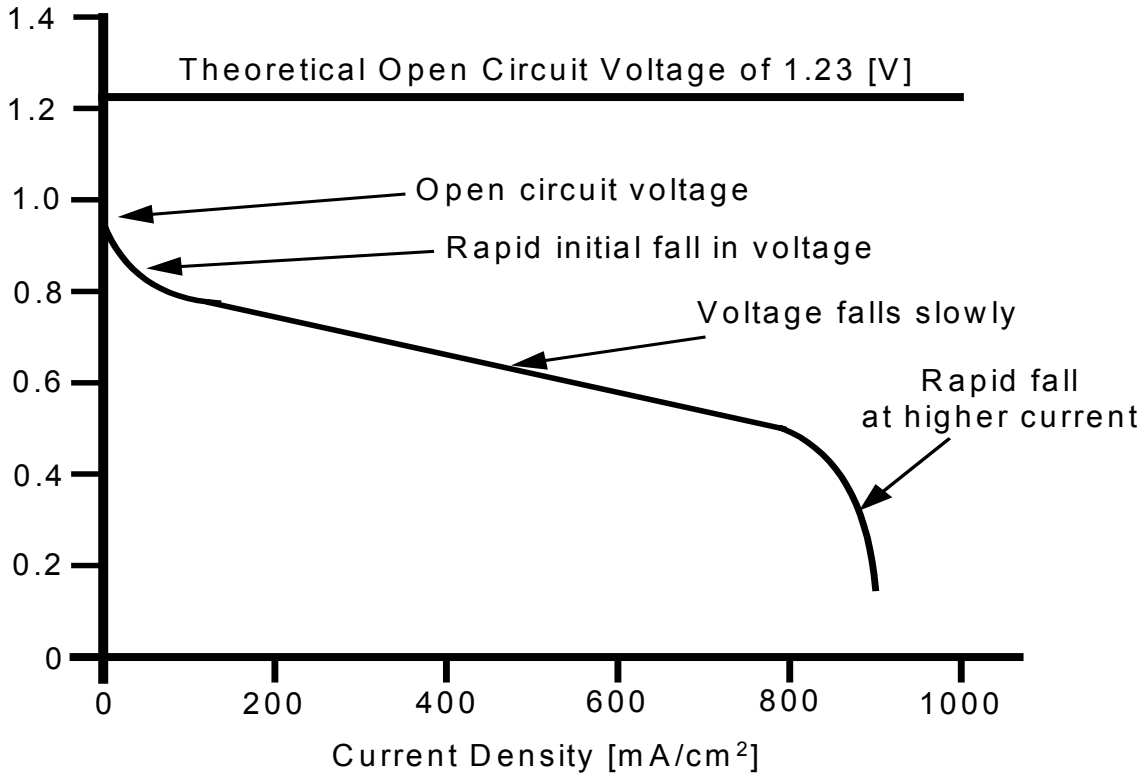

Fig. 1.2 Typical voltage vs. current density curve of the low temperature fuel cell

1.3.4. Types of the Fuel Cell

Fuel cells are classified primarily by the kind of electrolyte they employ. This determines the kind of chemical reactions that take place in the cell, the kind of catalysts required, the temperature range in which the cell operates, the fuel required, and other factors. These characteristics, in turn, affect the applications for which these cells are most suitable. There are several types of fuel cells currently under development, each with its own advantages, limitations, and potential applications. A few of the most promising types include

- Alkaline Fuel Cell (AFC)
- Proton Exchange Membrane Fuel Cell (PEMFC)
- Phosphoric Acid Fuel Cell (PAFC)
- Solid Oxide Fuel Cell (SOFC)
- Molten Carbonate Fuel Cell (MCFC)
- Direct Methanol Fuel Cell (DMFC)

Alkaline fuel cell: Alkaline fuel cells (AFCs) were one of the first fuel cell technologies developed, and the first type widely used in the U.S. space program to produce electrical energy and water onboard spacecraft. AFCs are high-performance fuel cells, efficiencies of 60 percent in space applications, due to the rate at which chemical reactions take place in the cell. The disadvantage of this fuel cell type is that it is easily

poisoned by carbon dioxide (CO2). In fact, even the small amount of CO2 in the air can affect the cell's operation, making it necessary to purify both the hydrogen and oxygen used in the cell.

Proton exchange membrane fuel cells: Proton exchange membrane fuel cells (PEMFCs) deliver high power density and offer the advantages of low weight and volume, compared to other fuel cells. PEM fuel cells use a solid polymer as an electrolyte and porous carbon electrodes containing a platinum catalyst. Due to this noble-metal catalyst, the system becomes costly. The platinum catalyst is also extremely sensitive to CO poisoning, making it necessary to employ an additional reactor to reduce CO in the fuel gas if the hydrogen is derived from an alcohol or hydrocarbon fuel, thereby adds cost to the system. PEM fuel cells are used primarily for transportation applications and some stationary applications due to their fast startup time, low sensitivity to orientation, and favorable power-to-weight ratio, and they are particularly suitable for use in passenger vehicles, such as cars and buses.

Phosphoric acid fuel cells: Phosphoric acid fuel cells (PAFCs) use liquid phosphoric acid as an electrolyte and porous carbon electrodes containing a platinum catalyst. This “first generation" of modern fuel cells is considered one of the most mature cell types and the first to be used commercially. This type of fuel cell is typically used for stationary power generation, but some PAFCs have been used to power large vehicles such as city buses. PAFCs are more tolerant of impurities in the reformate than PEM cells. They are 85 percent efficient when used for the co-generation of electricity and heat, but less powerful than other fuel cells, given the same weight and volume. As a

result, these fuel cells are typically large and heavy. PAFCs are also expensive. Like PEM fuel cells, PAFCs require an expensive platinum catalyst, which raises the cost of the fuel cell.

Solid oxide fuel cells: Solid oxide fuel cells (SOFCs) use a hard, non-porous ceramic compound as the electrolyte. Since the electrolyte is a solid, the cells do not have to be constructed in the plate-like configuration typical of other fuel cell types. SOFCs are expected to be around 50-60 percent efficient and could reach 85 percent efficiency with co-generation. Since the Solid oxide fuel cells operate at very high temperatures—around 1,000ºC, they do not require the precious-metal catalyst. It also allows SOFCs to reform fuels internally, which enables the use of a variety of fuels and reduces the cost associated with adding a reformer to the system. SOFCs are also the most sulfur-resistant fuel cell type and are not poisoned by carbon monoxide (CO), which can even be used as fuel. However, high-temperature operation has disadvantages. It results in a slow startup and requires significant thermal shielding to retain heat and protect personnel, which may be acceptable for utility applications but not for transportation and small portable applications. The high operating temperatures also place stringent durability requirements on materials. The development of low-cost materials with high durability at cell operating temperatures is the key technical challenge facing this technology.

Molten carbonate fuel cells: Molten carbonate fuel cells (MCFCs) are currently being developed for natural gas and coal-based power plants for electrical utility, industrial, and military applications. MCFCs are high-temperature fuel cells that use an

electrolyte composed of a molten carbonate salt mixture suspended in a porous, chemically inert ceramic lithium aluminum oxide (LiAlO2) matrix. Since they operate at extremely high temperatures of 650ºC and above, non-precious metals can be used as catalysts at the anode and cathode, thereby reducing costs. Molten carbonate fuel cells can reach efficiencies approaching 60 percent, considerably higher than the 37-42 percent efficiencies of a phosphoric acid fuel cell plant. When the waste heat is captured and used, overall fuel efficiencies can be as high as 85 percent. Unlike other fuel cells, MCFCs don't require an external reformer to convert more energy-dense fuels to hydrogen. Due to the high temperatures at which they operate, these fuels are converted to hydrogen within the fuel cell itself by a process called internal reforming, which also reduces cost. Molten carbonate fuel cells are not prone to carbon monoxide or carbon dioxide "poisoning"—they can even use carbon dioxides as fuel—making them more attractive for fueling with gases made from coal. The primary disadvantage of current MCFC technology is durability. The high temperatures at which these cells operate and the corrosive electrolyte used accelerate component breakdown and corrosion, decreasing cell life.

Direct methanol fuel cells: Direct methanol fuel cell technology is relatively new compared to that of fuel cells powered by pure hydrogen. Most fuel cells are powered by hydrogen, which can be fed to the fuel cell system directly or can be generated within the fuel cell system by reforming hydrogen-rich fuels such as methanol, ethanol, and hydrocarbon fuels. Direct methanol fuel cells (DMFCs), however, are powered by pure methanol, which is mixed with steam and fed directly to the fuel cell

anode. Direct methanol fuel cells do not have many of the fuel storage problems typical of some fuel cells since methanol has a higher energy density than hydrogen—though less than gasoline or diesel fuel. Methanol is also easier to transport and supply to the public using our current infrastructure since it is a liquid, like gasoline. A comparison of the fuel cell types is summarized in the Table 1.1.

Table 1.1. Comparison of the fuel cell types

	AFC	PEMFC	PAFC	MCFC	SOFC	DMFC
Electrolyte	Potassium Hydroxide Solution	Solid Polymer Membrane	Liquid Phosphoric Acid	Morten Carbonate Salt	Solid Metal Oxide	Solid Polymer Membrane
Operating Temperature	80-120°C	60-100 °C	150-200 °C	650°C	800-1000°C	60-100 °C
Efficiency	60%	35-50 %	35-50 %	45-60%	45-60%	35-40%
Power Range (kW_{el})	0.3-5	0.05 - 250	50-10,000	200-100,000	2-100,000	0.1-100
Mobile Ion	OH^-	H^+	H^+	CO_3^{2-}	O^{2-}	H^+
Favored Application	Space Vehicle	Residential, Ground Vehicle	CHP	CHP, CC	Residential, CHP, CC	Portable

CHP: Combined Heat Power

CC: Combined cycle

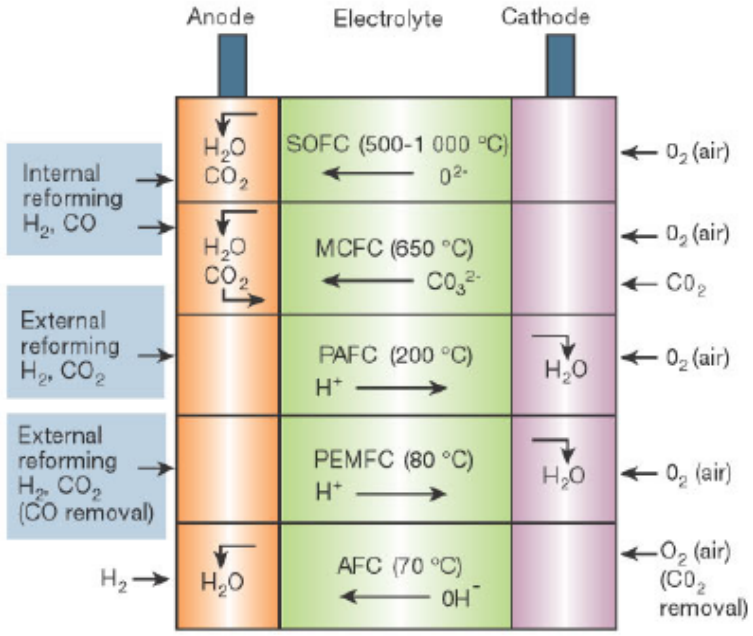

Fig.1.3 Electrochemical reactions for each type of the fuel cells

Figure 1.3 shows the electrochemical reactions for each type of the fuel cells, As seen in the figure, for polymer electrolyte membrane fuel cell (PEMFC), direct methanol fuel cell (DMFC) and phosphoric acid fuel cells (PAFC), protons move through the electrolyte to the cathode to combine with oxygen and electrons, producing water and heat. For alkaline (AFC), molten carbonate fuel cell (MCFC), and solid oxide fuel cell (SOFC), negative ions travel through the electrolyte to the anode where they combine with hydrogen to generate water and electrons.

1.4 Problems Associated with the Fuel Cell and Reformer

As mentioned earlier in the section 1.1, there are several hurdles that have to be

overcome for the wide spread applications and the successful commercialization of the fuel cell system. This section is focused on discussing the problems, which are important from electrical performance point of view and can be solved by the power electronic approaches. The main problems to which the power electronics can make a contribution are summarized as follows.

1. Cost: To produce the useful AC power from the low DC voltage of the fuel cells, it is essential to employ the power conditioning system including DC-DC converter, energy storage device, DC-AC inverter and AC filter. With large fuel cell systems, power electronics make up anywhere from 25% to 35% of the system cost, with many systems being at least one-third. This is a very significant portion of the cost, compared to other technologies. Most successful applications find ways to bring down the cost of the power electronics. Thus it is essential to develop the low cost, high performance topologies for the fuel cell system to accelerate the market penetration.

2. Slow response and start-up of the fuel cell: The fuel cell power response is limited by the air and hydrogen feed, flow and pressure regulation, and heat and water management. As current is instantaneously drawn from the load, heat and water is generated, whereas oxygen is depleted. During this transient, the fuel cell stack breathing control system is required to maintain optimal temperature, membrane hydration, and partial pressure of the reactants across the membrane in order to avoid detrimental degradation of the stack voltage, and thus, efficiency reduction. These critical fuel cell parameters can be controlled for a wide range of current, and thus power, by a series of actuators such as valves, pumps, compressor motors, expander vanes, fan motors,

humidifiers and condensers. Thus the dynamic response of the fuel cell system is actually affected by the response time of those components.

In the case of PEM fuel cells, the water plays an important role inside. Thus the water management is one of the most important functions of the fuel cell control system. The amount of reactant flow and the water injected into the anode and cathode flow stream affect the humidity of the membrane. Dry membrane and flooded fuels cause high polarization losses. Therefore, it is necessary to get the membrane hydrated suitably before the start-up of the fuel cell and, depending on the technology, it takes several seconds to several minutes. In the case of high temperature fuel cells, thermal expansion demands a uniform and slow heating process at startup, that will cause very long startup times typically, several hours are to be expected.

Therefore, high temperature fuel cells with longer start-up time are not suitable for the emergency back-up power application. However, short period of start-up time and/or slow dynamics of the low termperature fuel cells can be compensated by using auxiliary power starage devices such as batteries, supercapacitors and flywheels.

3. Ripple Current: Fig. 1.4 shows the block diagram of the fuel cell power generation unit for supplying 120/240V, 60Hz load and Fig. 1.5 shows its simplified diagram for ripple current calculation. For simplicity, fictitious L-C high-frequency filters will be used at the dc side as well as the ac side, as shown in Fig 1.5. With the assumption that the switching frequency is almost infinity, the values of L and C components approach zero, and hence the energy stored in the filter is negligible. Having

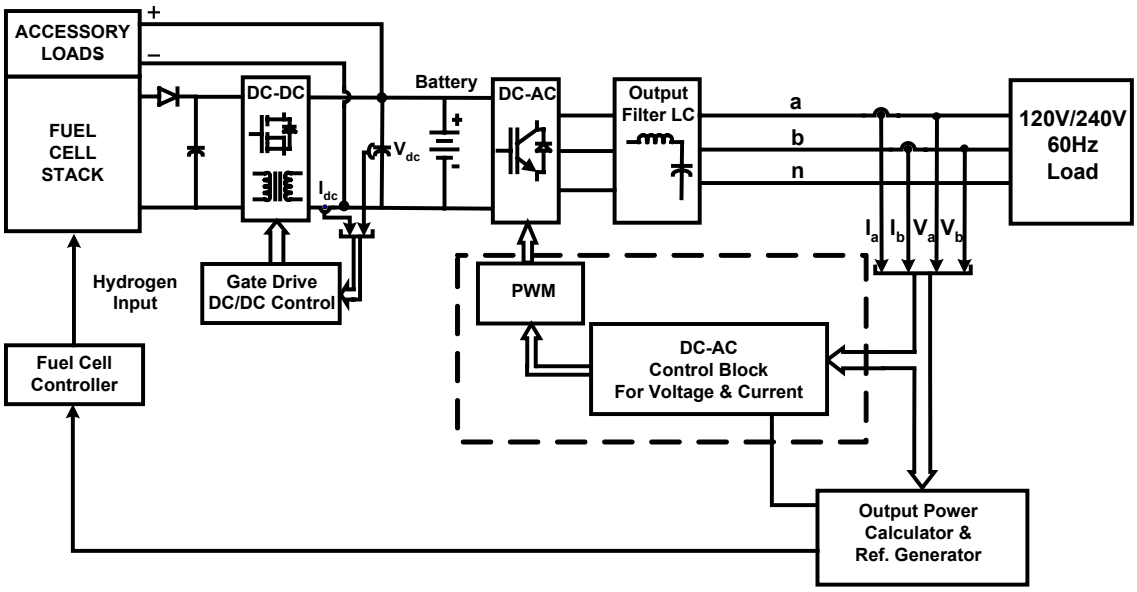

Fig. 1.4 Block diagram of a fuel cell power generation unit for supplying 120V/240V, 60Hz load

made these assumptions, energy balance equation can be written as (1.12). It is clear from equation (1.13) that the current drawn by a load from the fuel cell is not a constant dc but has a second harmonic of the fundamental frequency at the inverter output.

$$v_o = \sqrt{2}V_o \sin \omega_1 t\,, \tag{1.10}$$

$$i_o = \sqrt{2}I_o \sin(\omega_1 t - \phi) \tag{1.11}$$

$$v_{fc}\, i^*_{fc} = v_o(t) i_o(t) = \sqrt{2}V_o \sin \omega_1 \sqrt{2}I_o \sin(\omega_1 t - \phi) \tag{1.12}$$

$$i^*_{fc} = \frac{V_o I_o}{V_{fc}} \cos\phi - \frac{V_o I_o}{V_{fc}} \cos(2\omega_1 - \phi) \tag{1.13}$$

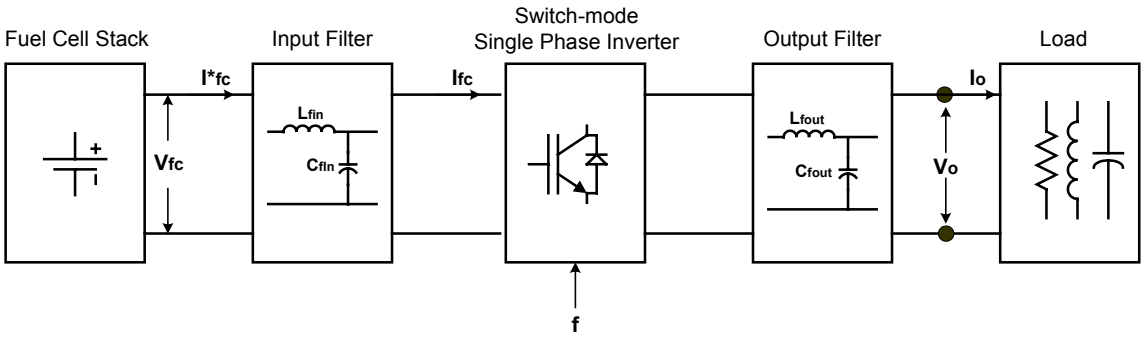

Fig. 1.5 Simplified block diagram of a fuel cell power generation unit for supplying 120V/240V, 60Hz load

The effect of the ripple current on the performance of a fuel cell stack has not been investigated thoroughly and so far remains uncertain. Many of the fuel cell manufacturers have specified the limit for the ripple current in their instruction manual. It is typically in the range of 5 % to 25% RMS of the rated DC full load current. However, no explanation is shown as to how the limit was decided. In the design of the power-conditioning unit for fuel cells, an important variable is the amount of ripple current that can be drawn from a fuel cell without causing any adverse affect. Both the magnitude and frequency of the ripple is important. Thus it is crucial to know the relationship between the ripple currents and the fuel cell performance, and this is the essential information for the design of the fuel cell power conditioning system.

4. Fuel Purity: Fuel flexibility is one of the advantages of the fuel cell system over the conventional power source. Fuel cell systems can be fueled with hydrogen-rich fuels, such as methanol, natural gas, gasoline, or gasified coal as well as pure hydrogen. Since these hydrogen-rich fuels have a higher energy density than that of pure hydrogen, it is advantageous to store the fuel in these forms rather than to store the fuel in the form

of pure gas. This can provide a significant advantage to the fuel cell power system such as stationary, mobile and vehicular applications. However, the reforming process also has several disadvantages as follows.

- Reformers add to the complexity, cost, and maintenance demands of fuel cell systems.
- If the reformer allows carbon monoxide to reach the fuel cell anode, it can gradually decrease the performance of the catalyst and hence the cell, especially in the case of PEM fuel cell. Expensive reforming system is required to keep the CO concentration in the fuel below the acceptable level.
- Reformers also produce carbon dioxide (a prominent greenhouse gas) and other air pollutants, but less than typical fossil combustion processes.

Therefore, it is required to develop the fuel cell stack tolerant of CO to reduce the requirement of the fuel processing system and hence the cost of the system.

1.5 Previous Work

It has been shown in the previous chapter that several technical challenges have to be solved for the fuel cell to play an important role in the future power production and to accelerate the market penetration. In order to make the fuel cell system more competitive with conventional power system a number of solutions have been proposed

to overcome those challenges. In this chapter, some of these methods are reviewed and discussed.

1.5.1. Conventional Modeling Technique and Evaluation of the Effects of Ripple Current

Reference [6] provides a first attempt to examine the impact of inverter load dynamics on the PEM fuel cell. Since it is suggested that the varying reactant condition surrounding the cell governs, at least in part, the lifetime of the fuel cell, this study investigate about the effects of the ripple current to the reactant utilization. To evaluate these effects a dynamic model for the bulk condition within the stack, as well as a one-dimensional model for the detailed mass transport occurring within the electrode of a cell is proposed with the series of the dynamic equations. In this work, the inverter load is imposed as a boundary condition to the models and the effects of the ripple current is evaluated in the range of the frequency between 30 Hz and 1250Hz. Figure 1.6 shows the overview of the Simulink model of the PEM fuel cell stack used in the study.

However, this model has several disadvantages. First, it requires all the design parameters for simulation, which are not easy to obtain due to proprietary nature of the technology. Second, as mentioned above, this model uses the predetermined pattern of the load current as an input to the fuel cell model to compute the internal variable such as partial pressure of the reactants and the output voltage. Thus it is not suitable for

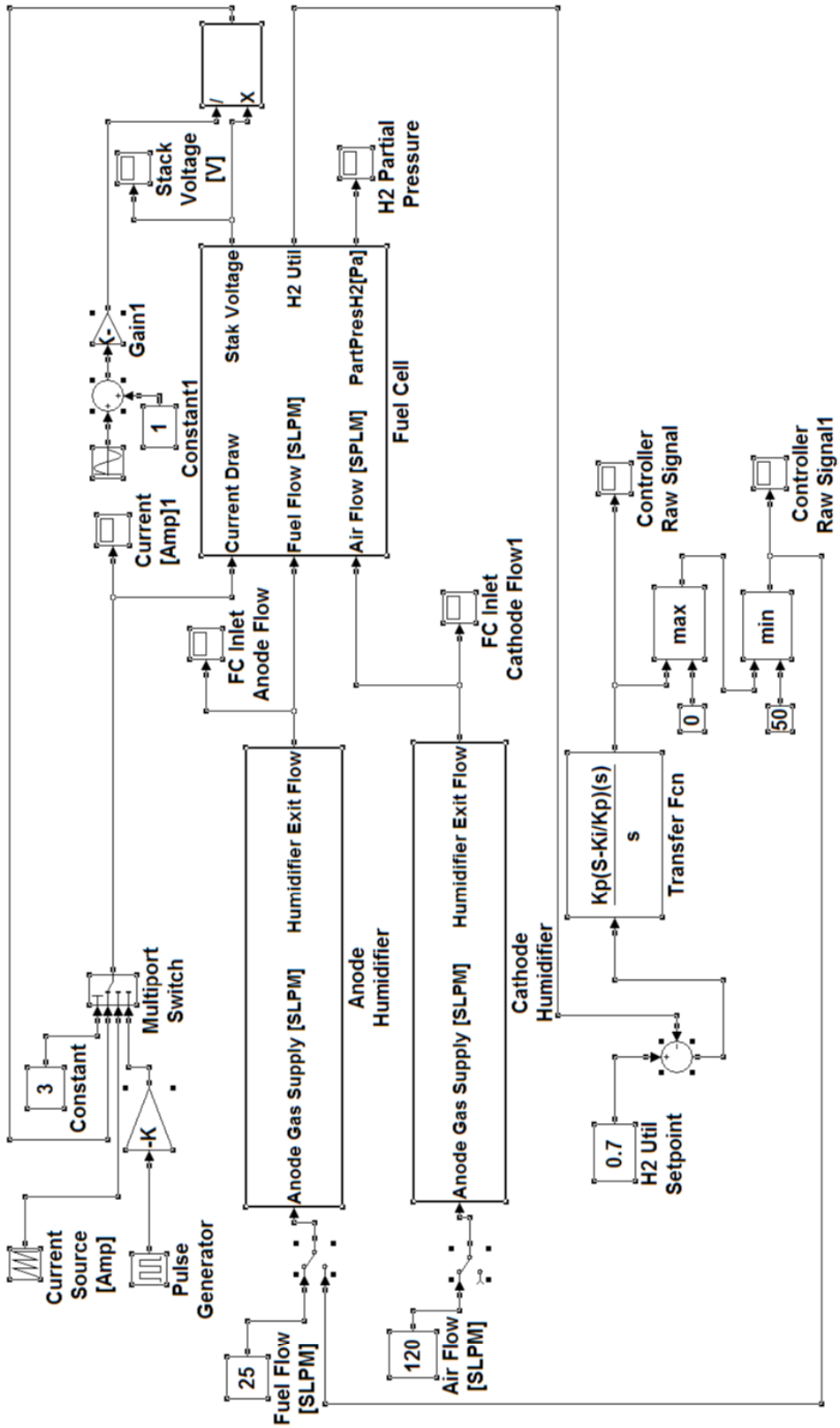

Fig .1.6 Overview of the Simulink model of the PEM fuel cell stack [6]

observing the electrical phenomena occurring when the fuel cell interacts with its power-conditioning unit (PCU). Third, most of the blocks in the model include complex chemical equations, which are not easy to solve.

1.5.2. Conventional UPS Systems and Fuel Cell Powered UPS Systems

In this section, the structures of the conventional UPS systems are briefly reviewed. The advantages and disadvantages of each type of the UPS systems are summarized in term of the topology, control, system complexity and cost.

Figure 1.7 shows the conventional UPS system. In this system, the load is connected directly to the utility through the transfer switch. The system monitors the utility voltage and the transfer switch transfers the load to the UPS system when the power outage occurs. The auxiliary energy storage device can be batteries, supercapacitor, flywheel or superconducting magnet. In any case, the energy is stored in

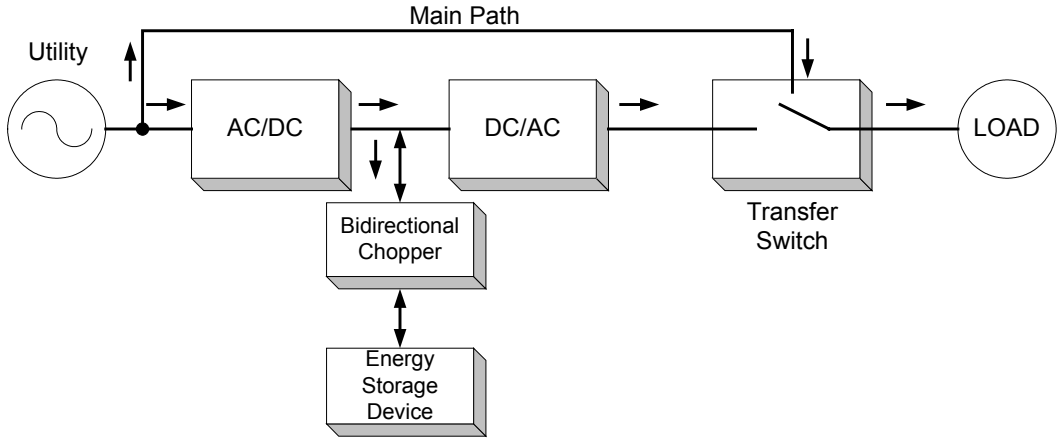

Fig 1.7 Block diagram of the conventional UPS system

the auxiliary energy storage device during the normal operation and this stored energy is utilized to supply the load during the power outage. The AC/DC converter takes care of this charging process. However the double conversion performed in the main power path results in a reduced efficiency.

Battery based UPS, which uses the batteries as the auxiliary energy storage device, has an advantage that the control and the operation are simple. But it has the disadvantage that the permanent and expensive maintenance is required to achieve the peak performance. Also, since the batteries often contain toxic heavy metals such as cadmium, mercury, and lead and may cause serious environmental problems if they are discarded without special care.

Flywheel based UPS is essentially the same approach as the battery based UPS. However it is different in that the energy is stored in the form of mechanical kinetic energy and the amount of energy that can be stored in the flywheel depends on its speed and inertia. It is advantageous that the flywheel does not require an exhaustive maintenance and the required footprint and weight is less. However it requires providing protection due to hazard potential of the high speeds of rotor.

Superconductor based UPS can be used for high power capacity UPS system due to its good handle of high power bursts and highly repetitive charge and discharge cycles. Superconducting magnet is used to store the energy and the stored energy is released through a power electronic converter to supply the load. However a sophisticated cooling system is required to maintain cryogenic temperature yielding in high cost and safety concerns.

While the conventional UPS systems are equipped with the passive energy storage device, fuel cell powered UPS systems adopt the fuel cell, an active energy generator. Unlike the batteries, flywheel or superconducting magnet, the fuel cells can continuously provide power as long as the reactants are supplied. This feature is especially useful under the condition where the duration of the power outage is uncertain. Several approaches have been suggested for the design of the fuel cell powered UPS system [7-10].

While the references [7-9] mainly discuss the conceptional design, the reference [10] shows the design and the actual implementation of system. Figure 1.8 shows the block diagram of the UPS suggested in the reference [10]. In this scheme, the power supplied from the utility is transferred to the load via UPS.

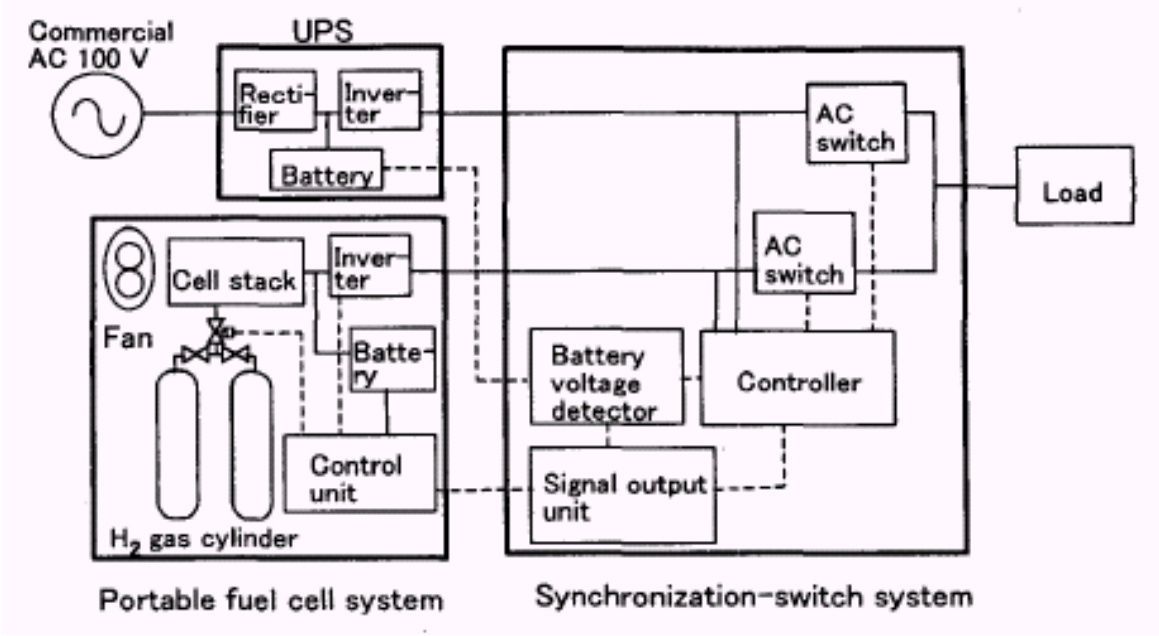

Fig 1.8 Block diagram of the conventional fuel cell powered UPS [10]

When the power outage occurs, energy stored in the battery is used to support the load. The voltage of the battery becomes progressively lower as the power outage continues. When the voltage becomes lower than the pre-determined value, then the signal-output unit outputs an operation signal to the fuel cell system. The fuel cell system begins to warm up and incorporated inverter starts to generate the 100 V AC power. Power transfer is performed by the synchronization-switch system. However, since this system requires the power conditioning stage for both batteries and fuel cell, the system is expensive. Further, it is disadvantageous in term of efficiency that the power is always processed by the UPS.

Figure 1.9 shows the UPS system topology suggested by the reference [7]. In this proposed scheme, a bi-directional dc/dc converter with a battery module is used as an active filter to compensate for the power mismatch between the fuel cell and load. However, this approach also employs the problematic batteries in the system and thus the system is not environmentally clean.

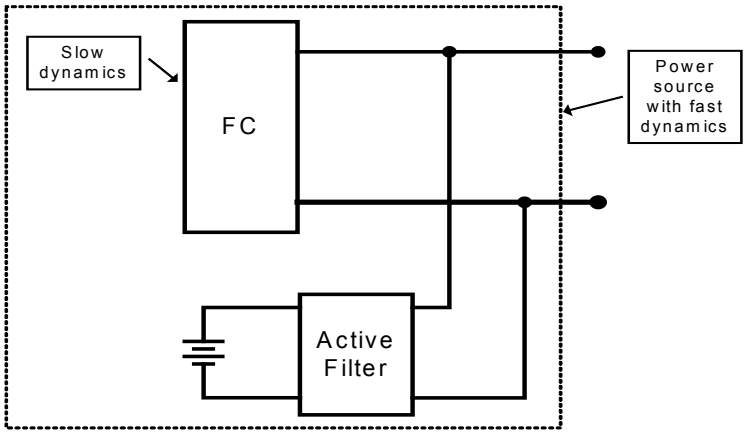

Fig 1.9 Fuel cell powered UPS system with fuel cell/active filter combination [7]

1.5.3. CO Tolerant PEM Fuel Cells

While the high temperature fuel cells (because of their high operating temperature) can directly operate on hydrogen-rich fuels, the low temperature fuel cells require external reforming of a hydrogen-rich fuel to produce hydrogen. However the former cannot be practically employed for vehicular and small-scale application due to size and operating problems. PEM fuel cells are currently considered to be the most promising fuel cells for vehicular and small-scale applications. Hydrogen is the best fuel for PEM fuel cells. Unfortunately, however, hydrogen cannot be obtained directly mines or drilling; it has to be produced via chemical processing of other fuels such as fossil fuels, methanol, ammonia and water. Hence the PEM fuel cell is essentially consist of two distinct units, the PEM fuel cell stack and the fuel reformer, which produces hydrogen.

One of the most important problems that the PEM fuel cells are confronting is their extremely low tolerance for CO. For example, PEM fuel cell requires less than 10 ppm CO in the hydrogen stream. The CO concentration higher than this causes the significant voltage drop and hence the output power. Although the reformers developed to date can satisfy this conditions, these are too expensive and the amount of CO produced is not always consistent

In response to this concern, several solutions have been suggested to increase the CO tolerance of the fuel cell. One solution is to use alloyed catalysts, which exhibit improved CO-tolerance [11]. However, this is not an adequate way for the CO

concentration higher than 10 ppm. In the presence of higher CO concentration, the oxidant bleeding technique can be used [12]. This technique uses oxidants such as air, oxygen, or hydrogen peroxide chemically oxidizes CO to CO2 to lower the CO concentration. However, since only a small part of the oxidants participates in the oxidation process, the remaining oxidant chemically combusts with hydrogen. This combustion reaction lowers the fuel efficiency [11,12].

Recently, a research with another interesting approach has been published about this topic. [13]. The results show that increasing the anode over-potential can significantly increases the CO tolerance of the PEM fuel cells. This technique is based on the electrochemical oxidation of adsorbed CO to CO_2, which frees the surface of the catalyst from poisoning species. In this research, experiments were performed on a single PEM fuel cell and the effectiveness of the current pulse to increase the CO tolerance was proven. However, this technique has not been applied to the PEM fuel cell stack and the power electronic topology to achieve this technique has not yet been suggested.

1.6 Research Objectives

As discussed in this chapter, several challenges should be overcome in order for the fuel cell to play an important role as a primary power source. In response to the challenges presented in this chapter, the objective of this research work is to propose

new schemes to improve the performance of the PEM based fuel cell power system and thereby making the system more competitive and acceptable.

Though the amount of ripple current that can be drawn from the fuel cell stack is an important variable in the design of power conditioning unit, the effect of the ripple current on the performance of a fuel cell stack has not been investigated thoroughly and so far remains uncertain. In the first study, an equivalent circuit model of the PEM fuel cell stack is developed. It is essential to derive the equivalent impedance model of the fuel cell stack to illuminate the relationship between the ripple current and the performance of the fuel cell. Frequency Response Analysis (FRA) technique is used to develop the equivalent circuit and the validity of the model is proven by the experiments. Maximum ripple current allowable is suggested for the single-phase 60 Hz fuel cell power systems.

In the second study, fuel cell powered UPS system is proposed. This study is focused on discussing the suitable topology for the fuel cell UPS system and details about the design and operation of the system. For the emergency power application such as UPS, seamless power supply is essential to ensure the power quality for the critical load. However, instantaneous power fluctuation is unavoidable for the system employing reformers due to their slow dynamics. Thus in this study a compensation scheme is suggested by using an auxiliary energy storage device such as the supercapacitor module, and line-interactive topology is adopted due to several minutes of the start-up time. A complete design example for 1 kVA UPS system is presented and the simulation results are shown to prove the feasibility of the system.

In the third study, an advanced power electronic scheme is proposed to increase the CO tolerance of the PEM fuel cell power system. As discussed in this chapter, the output power of the PEM fuel cell is reduced if the CO is present in the hydrogen fuel and the reduced output power of the fuel cell can be restored by drawing the pulse current from the fuel cell stack. Thus the research objective of this study is to develop the suitable power converter topology to achieve this goal. An add-on solution composed of two-stage dc/dc converters and a supercapcitor module is suggested. Experimental results and the simulation results prove the validity of the proposed method and system.

1.7 Dissertation Outline

The content of this dissertation is composed of five chapters as followings. Chapter I introduces the potentials, kinds and principles of the fuel cells. In addition several challenges associated with the fuel cell are described in detail. A review of the previous work performed in the area is also presented. Their advantages and disadvantages are discussed.

In Chapter II, an impedance model of the PEM fuel cell stack is developed to evaluate the effects of the ripple current. In order to show the relationship between the ripple current and the performance of the fuel cell the power loss computed based on the impedance model are compared to those obtained from the experiments.

In Chapter III, a novel fuel cell powered UPS system is proposed. The proposed topology and its operation are detailed. Design examples are presented along with simulations results.

Chapter IV presents an advanced power electronic scheme to improve the CO tolerance of the PEM fuel cell system. Experimental results show the effects of the proposed method and simulation results show the feasibility of the proposed scheme.

Chapter V summarizes the contributions of this research work to the area of PEM based power system design and performance improvement. Some suggestions are also included for future work.

CHAPTER II

DEVELOPMENT OF AN EQUIVALENT CIRCUIT MODEL OF A FUEL CELL TO EVALUATE THE EFFECTS OF INVERTER RIPPLE CURRENT

2.1 Introduction

In the 21st century, fuel cells appear poised to meet the power needs of a variety of applications. Fuel cells are electrochemical devices that convert chemical energy to electricity and thermal energy. Fuel cell systems are available to meet the needs of applications ranging from portable electronics to utility power plants. In addition to the fuel cell stack itself; a fuel cell system includes a fuel processor and subsystems to manage air, water, thermal energy, and power. The overall system is efficient at full and part-load, scaleable to a wide range of sizes, environmentally friendly, and potentially competitive with conventional technology in first cost. Promising applications for fuel cells include portable power, transportation, building cogeneration, and distributed power for utilities. For portable power, a fuel cell coupled with a fuel container can offer

*Reprinted with permission from "An Experimental Evaluation of the Effects of Ripple Current Generated by the Power Conditioning Stage on a Proton Exchange Membrane Fuel Cell Stack" by W. Choi, G. Joung, Jo.W. Howze and P. N. Enjeti, 2004. Journal of Materials Engineering and Performance, vol. 13(3), 257-264. 2004

a higher energy storage density and more convenience than conventional battery systems. In transportation applications, fuel cells offer higher efficiency and better part-load performance than conventional engines. In stationary power applications, low emissions permit fuel cells to be located in high power density areas where they can supplement the existing utility grid. Furthermore, fuel cell systems can be directly connected to a building to provide both power and heat with cogeneration efficiencies as high as 80%.

Various attempts have been made to model Proton Exchange Membrane Fuel Cell Stack (PEMFCS). Almost all-recent endeavors of modeling [14-17], have neglected the effects of inverter load due to reasons of simplicity. Several modeling methods have been suggested in literature [14-17]. However, these modeling methods require fuel cell design parameters, which are not easy to obtain due to proprietary nature of the technology. Furthermore, most of the models include complex chemical equations, which are not easy to solve, and are not suitable for observing the electrical phenomena occurring when the fuel cell interacts with its power conditioning unit (PCU).

Since the fuel cell produces DC electricity, a power conditioning stage is essential to produce commercial AC power (120/240V, 60Hz). A typical fuel cell PCU employs switch-mode dc-dc and dc-ac converters (Fig 2.1). Important variables for the design of the PCU are: (a) variation of fuel cell terminal voltage from no-load to full load; (b) the amount of ripple current the fuel cell can tolerate. A large variation in fuel cell terminal voltage from no-load to full load, results in larger volt-amp rating of the PCU. Also, for fuel cells powering single-phase loads (60Hz), the ripple current is twice

the output frequency i.e. 120Hz. The effect of the ripple current on the performance of a fuel cell stack has not been investigated thoroughly and so far remains uncertain [6].

Development of an equivalent circuit for a fuel cell by conducting a series of tests, to predict the electrical performance: voltage regulation, rating of the PCU, dynamic behavior and the effects of inverter ripple current is essential. A clear understanding of various factors including additional losses (if any) due to ripple current can contribute to better design of next generation fuel cell power systems.

In this chapter, test results from three commercially available (Avista Lab SR-12, Ballard Nexa and BCS-Tech) PEM fuel cells are fully analyzed. The proposed study employs an equivalent circuit of the PEM stack derived by frequency response analysis (FRA) technique. The test results are then expressed in per-unit quantities to facilitate easy comparison. The relationship between ripple current and fuel cell stack performance such as power loss and fuel consumption is investigated.

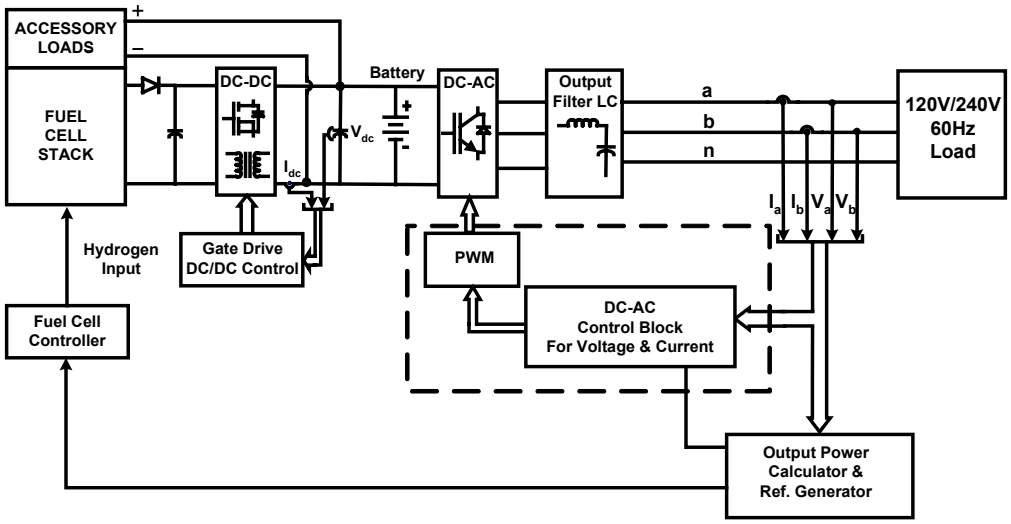

Fig. 2.1 Block diagram of a fuel cell power generation unit for supplying 120V/240V, 60Hz load

2.2 Modeling of the Fuel Cell Stack with Frequency Response Analysis (FRA) Technique

Fig. 2.2 shows the experimental setup to evaluate the performance of the fuel cell stack under test. The setup consists of Proton Exchange Membrane Fuel Cell Stack (PEMFCS), Programmable Electronic Load (PEL, Chroma 63201), Frequency Response Analyzer (FRA, Venable Model 260), current/voltage probes (Tektronix AM503B Current Amplifier and A6303 Current Probe, Tektronix P5205 Differential Voltage Probe), and a computer with the analysis software. The test setup is used to perform both DC and AC tests described in the next sections.

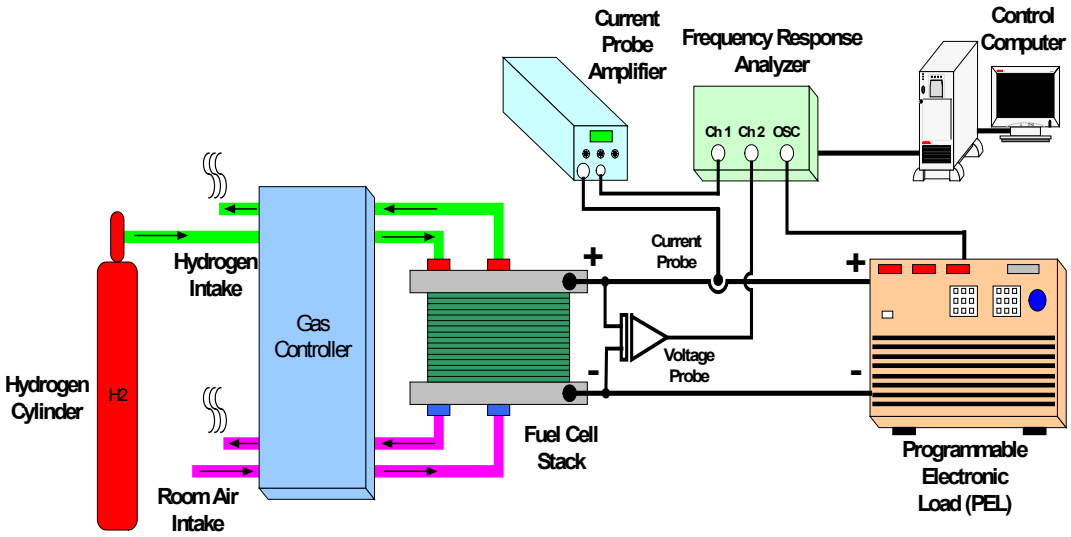

Fig. 2.2 Frequency response analysis technique: experimental setup for the fuel cell stack

2.2.1. DC Equivalent Circuit

In this test, the fuel cell is supplied with the hydrogen and the electrical load (DC) is varied from zero to full load (rated). The fuel cell terminal voltage variation is plotted for various output current settings (Fig. 2.3). The V-I curve (or polarization curve) is somewhat nonlinear for lower values of current and exhibits a near linear behavior for load current > 25%. If we neglect the initial non-linearity, a simplified electrical equivalent circuit for the fuel cell can be obtained by calculating the slope of the V-I curve (Fig. 2.3). Fig. 2.4 shows the equivalent circuit with a resistance in series with a DC voltage source.

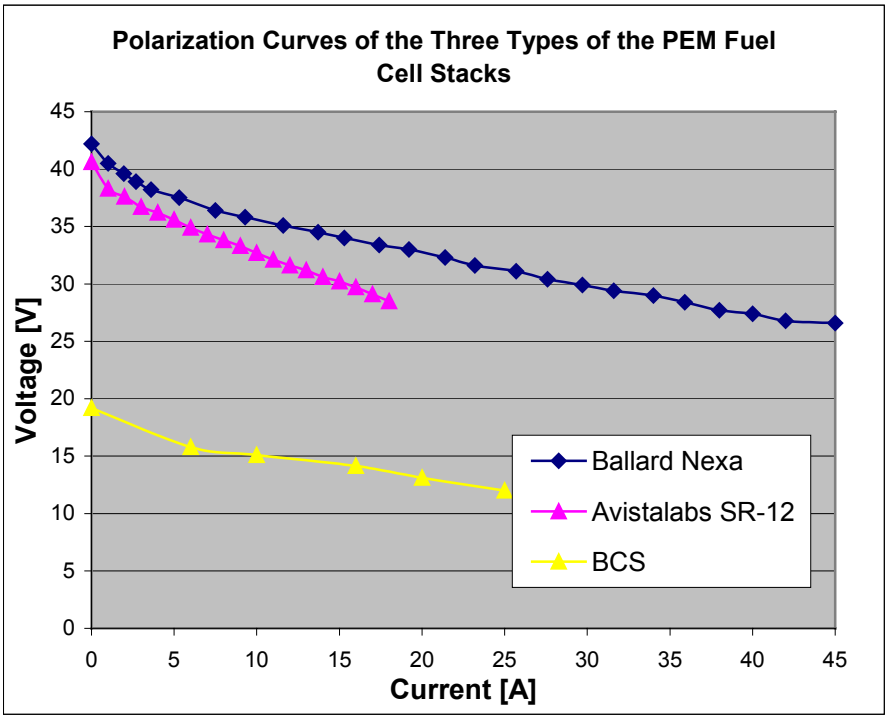

Fig. 2.3 Polarization (V-I) curves of the three types of the PEM fuel cell stacks

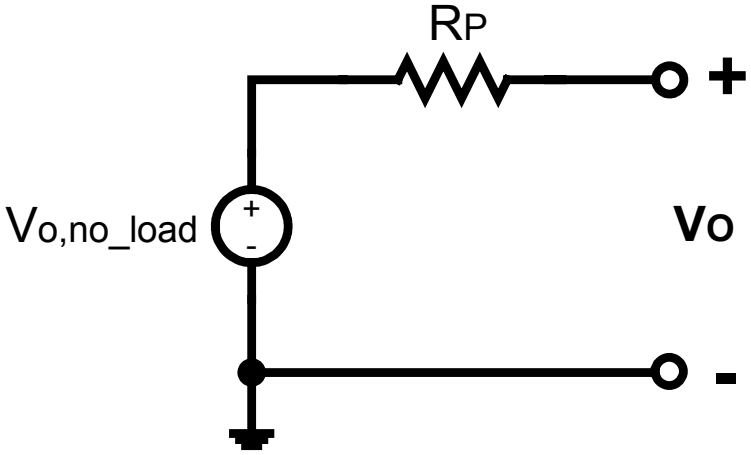

Fig. 2.4 DC equivalent circuit of the fuel cell stack

To facilitate the comparison between different ratings of fuel cells with different output voltage and current ratings, a per-unit system is developed. The Table 2.1 shows the base definitions of per-unit quantities for the fuel cells under test.

Table 2.1 Basic definitions of per-unit quantities for the fuel cell under test

Fuel Cell Type	$V_{o,no\text{-}load}$ [V]	V_{base} [V]	I_{base} [A]	P_{base} [W]	R_{base} [Ω]
SR-12	40.6	28.9	17.3	500	1.67
Nexa	42.2	26.6	45	1200	0.59
BCS	19.2	12	25	300	0.48

Where,

V_{base}: Fuel cell stack voltage at the full load

I_{base} : Rated (full load) current (rms.)

P_{base} : Rated output power

Z_{base}= V_{base} / I_{base}: Base impedance (2.1)

The resistance R_P shown in fuel cell equivalent circuit (DC) can be represented in per-unit as,

$$R_{P,Per-unit} = \frac{R_P}{Z_{base}} \tag{2.2}$$

Since the fuel cell V-I curve shows a wide variation in output voltage (V_o) from no load to full load, a voltage regulation factor (VRF) is defined:

$$VRF = \frac{V_{o,no-load} - V_{o,full-load}}{V_{o,full-load}} \tag{2.3}$$

It can be shown from (2.1)-(2.3) that,

$$VRF = R_{P,\ Per-unit} \tag{2.4}$$

$R_{P,\ Per\text{-}unit}$ and VRF for each fuel cell stack can be calculated from Table 2.1. A fuel cell

stack, which has a lower $R_{P,Per\text{-}unit}$ and VRF is considered to be better from the electrical performance point of view, since the variation in output voltage from no-load to full load is minimal. Since a PCU is connected to the fuel cell output terminals, a larger VRF (variation in fuel cell output voltage) results in a larger volt-amp (VA) rating of the PCU. The VA rating of the PCU can be calculated as,

$$VA = V_{o,no-load} * I_{full-load} \tag{2.5}$$

Expressing (2.5) in per-unit, we have,

$$VA_{per-unit} = \frac{V_{o,no-load} * I_{full-load}}{V_{base} * I_{base}} \tag{2.6}$$

It can be shown from (2.1), (2.3) and (2.6) that,

$$VA_{per-unit} = VRF + 1 \tag{2.7}$$

From (2.7) it is clear that a higher value of VRF results in higher rating (VA) of the power conditioning unit. Table 2.2 shows the corresponding VA ratings of the PCU for the fuel cells tested. A lower VA rating of the PCU is indicative of: the higher power semiconductor switching device and passive L-C component utilization (within the PCU) and the lower cost of the PCU.

Table 2.2 VA ratings of the PCU for the fuel cells tested

Fuel Cell Type	$R_{P,\ Per\text{-}unit}$ (or VRF) see Eqn (2.1)-(2.3)	VA ratings of the PCU in per-unit
SR-12	0.4 (or 40 [%])	1.4 (or 140[%])
Nexa	0.586 (or 58.6 [%])	1.586 (or 158.6 [%])
BCS	0.6 (or 60 [%])	1.6 (or 160[%])

2.2.2 AC Equivalent Circuit

The objective of this test is to obtain the ac impedance of the fuel cell stack from zero to 10kHz frequency. In this test (Fig. 2.2) the fuel cell is operated at a certain DC operating point on the V-I curve, and a small magnitude of sinusoidal ac current is superimposed. The current and corresponding voltage at fuel cell terminals is recorded. From this data, the ac impedance of the fuel cell is computed. The above test is repeated from zero to 10kHz frequency and the frequency response of fuel cell internal impedance is computed. Fig. 2.5 shows the magnitude and phase plot of the SR-12 fuel cell stack internal impedance variation from zero to 10kHz (for a dc current of 18A, when perturbed by a sinusoidal ac current of 1A in magnitude).

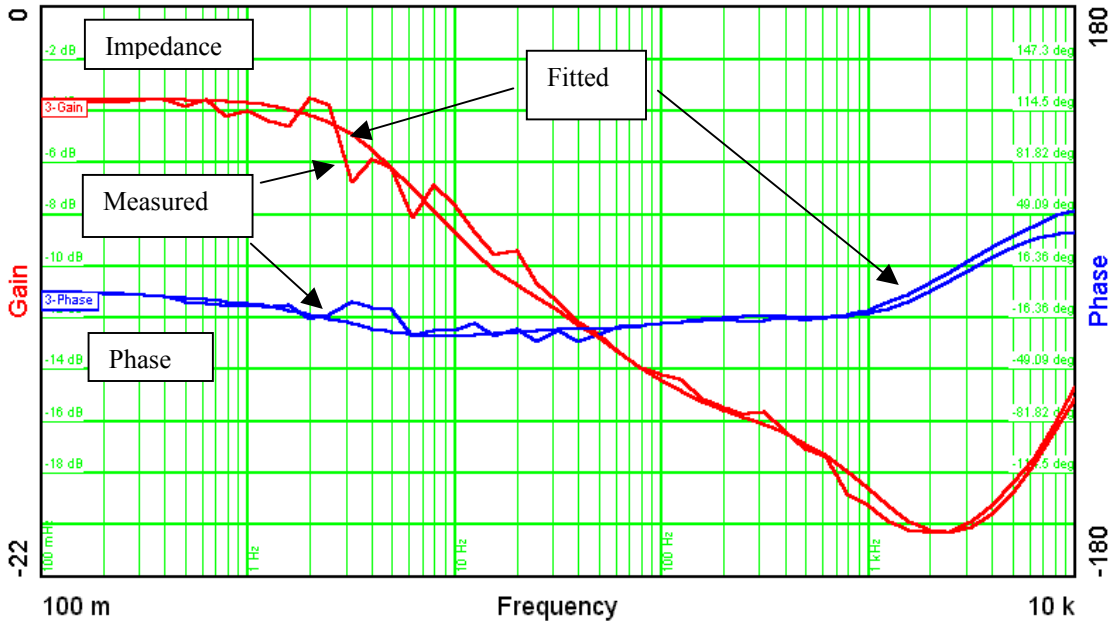

Fig. 2.5 Measured impedance spectrum of the PEMFCS and its curve fitting results

The above impedance test is repeated at different operating points on the fuel cell V-I curve. Fig. 2.6 (a) and 2.6 (b) show the Nyquist impedance plot of the computed impedance variation for SR-12 and Nexa PEMFCS respectively. From Fig. 2.6 (a) and 2.6 (b) it can be seen that the ac impedance variation of SR-12 is smaller than that of Ballard-Nexa fuel cell. The smaller variation in ac impedance for SR-12 (in Fig. 2.6 (a)) can be attributed to its lower VRF value (see Table 2.2).

With the above measured impedance data, an electrical equivalent circuit of the fuel cell internal impedance is obtained as follows. Since one semicircle in the Nyquist impedance plot (Fig. 2.6 (a) and (b)) corresponds to a single time constant (R-C), closer observation of Fig. 2.6 (a) and (b) shows the existence of three such time constants.

Further, the diameter of each semicircle is a representative of the resistor value and the vertex corresponds to the characteristic frequency. Using the above-described approach and the curve fitting technique, an electric equivalent circuit of the fuel cell and its parameters at a certain operating point is obtained from the measured data and is shown in Fig. 2.7 and Table 2.3. The equivalent circuit consists of R-C branches obtained from parameter extraction. The fitted curve (see Fig. 2.5), which represents the frequency response (obtained from the equivalent circuit (Fig. 2.7)) shows close agreement with the measured frequency data. It is clear from Fig. 2.7 that for dc conditions (zero frequency) the equivalent circuit parameters match the steady state V-I data shown in Fig. 2.3.

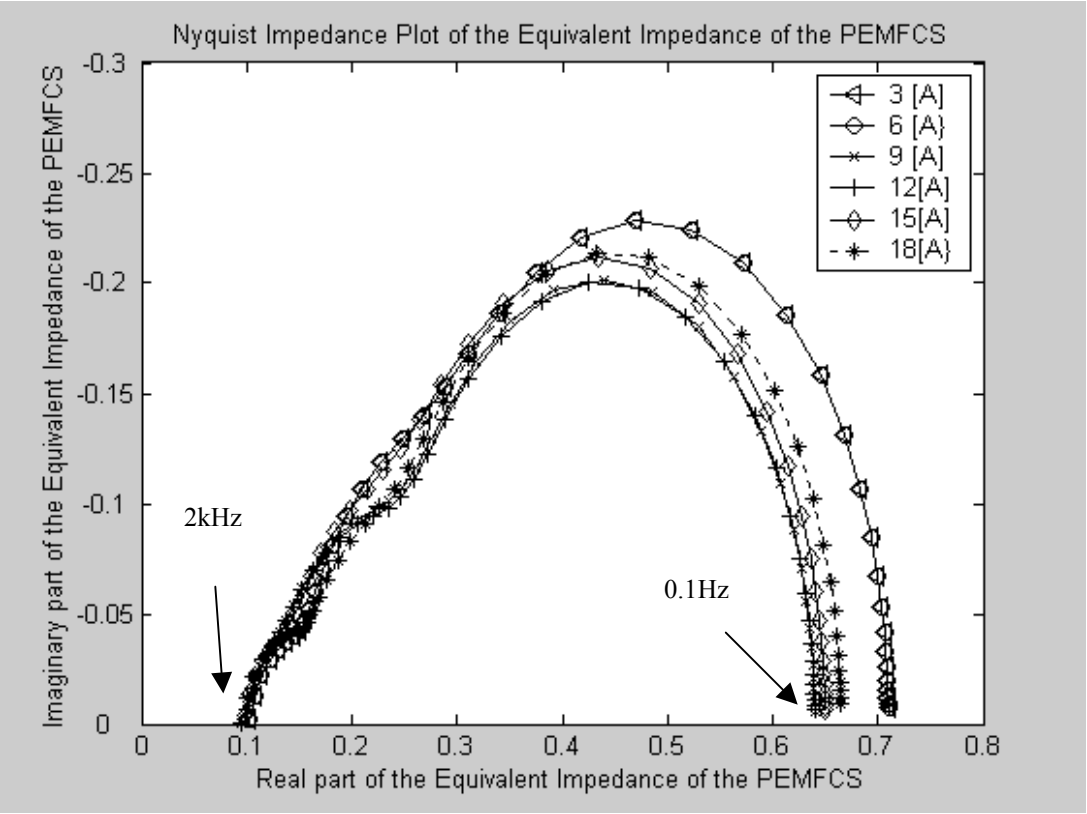

Fig. 2.6 (a) Nyquist impedance plot of the Avistalabs SR-12 PEMFCS at the different operating points

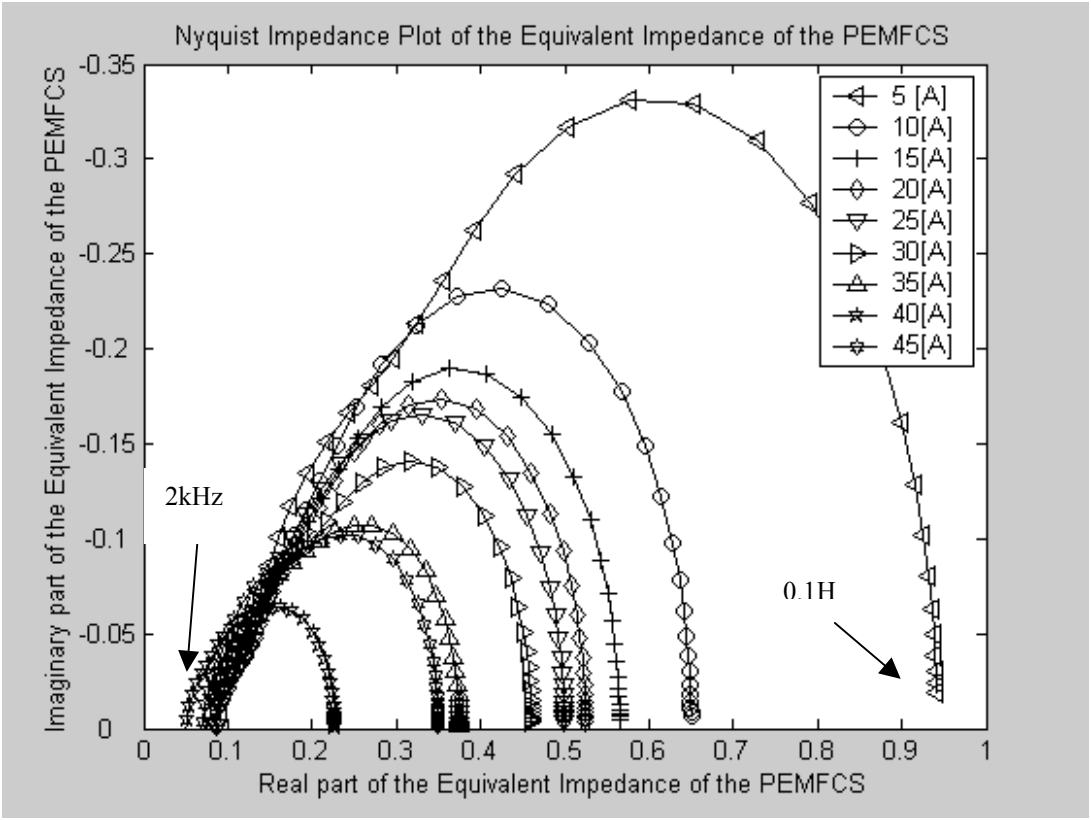

Fig. 2.6 (b) Nyquist impedance plot of the Ballard Nexa PEMFCS at the different operating points

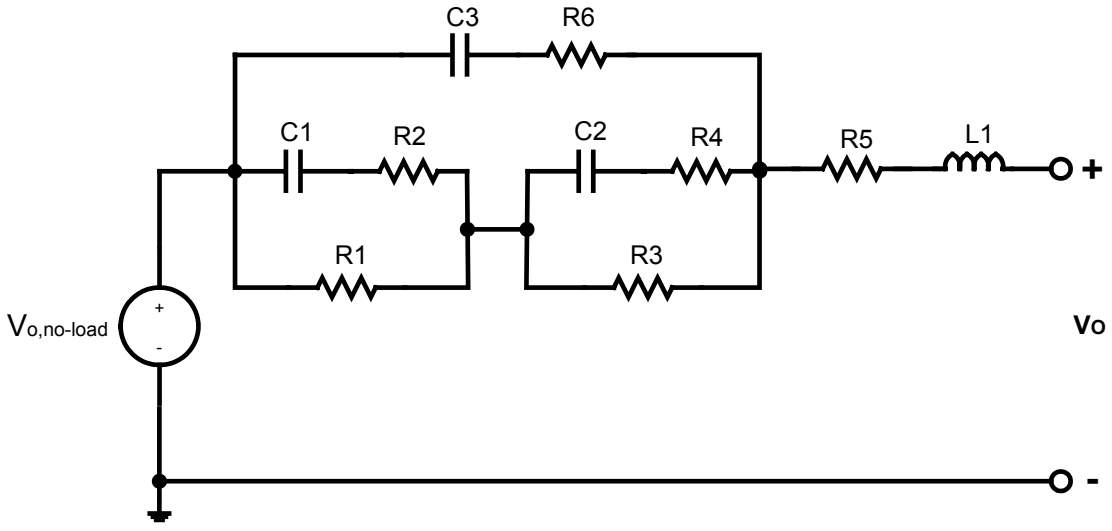

Fig. 2.7 Equivalent circuit of the PEMFCS at a certain operating point

Table 2.3 Equivalent circuit parameters for each fuel cell

Fuel Cell Type	R1 [Ω]	R2 [Ω]	R3 [Ω]	R4 [Ω]	R5 [Ω]	R6 [mΩ]	C1 [mF]	C2 [mF]	C3 [mF]	L1 [μH]
SR12	**0.41**	**0.0115**	**0.17**	**0.15**	**0.085**	**0.07**	**80**	**9**	**2.5**	**2**
Nexa	**0.15**	**0.0115**	**0.15**	**0.15**	**0.065**	**0.07**	**70**	**7.5**	**5.5**	**4.8**

2.3 Evaluation of the Effect of the Inverter Ripple Current

An important variable in the design of the power conditioning unit for fuel cell is the amount of ripple current that can be drawn from a fuel cell without causing any adverse affect. Since the reactant utilization is known to impact the mechanical nature of a fuel cell, it is suggested in [6] that the varying reactant conditions surrounding the cell (due to ripple current) govern, at least in part, the life time of the cells. Both the magnitude and frequency of the ripple current is important.

For fuel cells powering single-phase loads (60Hz), the ripple current of concern is twice the output frequency i.e. 120Hz [18]. A limit of 0.15 per-unit (i.e. 15% of its rated current) from 10% to 100% load is specified in [19]. Further, Ballard Nexa specifications indicate a limit of 24.7% RMS (35% peak-peak) for 120Hz ripple current. It should be noted that switching frequency (20-60kHz) components in the DC-DC converter is easily filtered via a small high frequency capacitive filter.

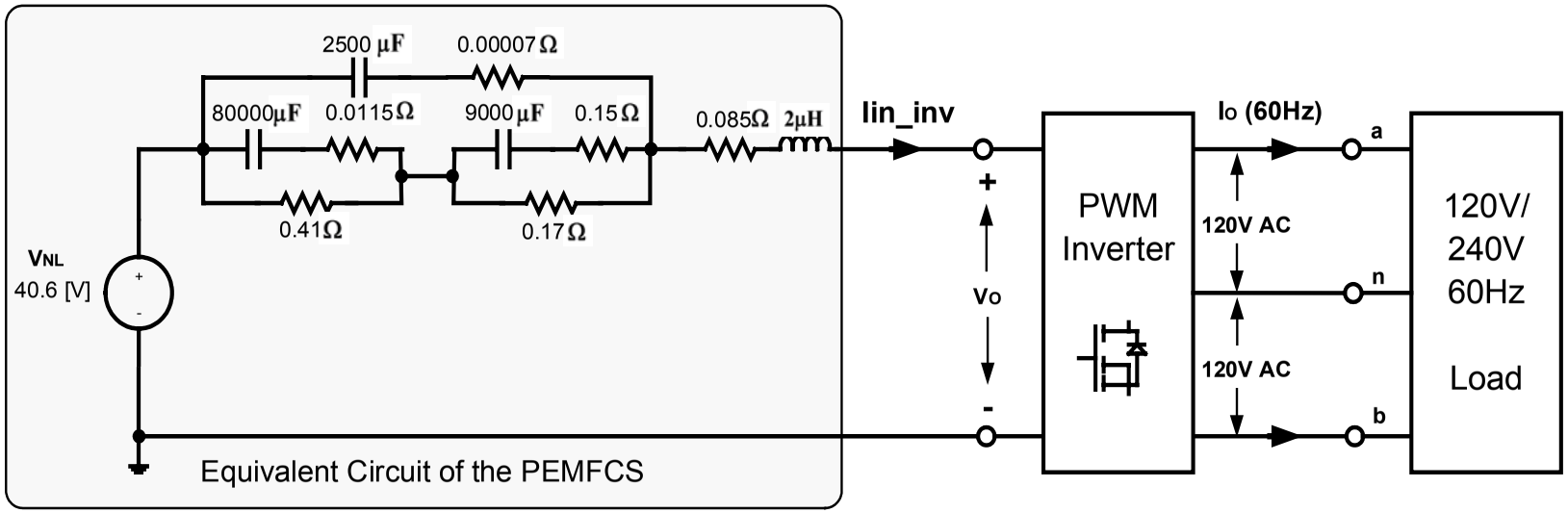

Fig. 2.8 Interconnection of the fuel cell equivalent circuit with the power conditioning unit to facilitate the evaluation of the effect of ripple current

Fig 2.8 shows the interconnection of the fuel cell equivalent circuit with the PCU. The PCU may be composed of any combination of switch-mode dc-dc converters, dc-ac inverters, filters and isolation transformers depending on the topology adopted [18]. Fig. 2.9 and Table 2.4 show the ac equivalent circuit and its parameters of the fuel cell at 120Hz frequency. This figure is obtained by setting f = 120Hz in Fig. 2.7.

From Fig. 2.9 and table 2.4, the impedance of the fuel cell stack at 120Hz at the rated operating condition is,

$$Z_{120HZ} = 0.1717 - j0.06 = 0.1818\angle\text{-}19.26^\circ \quad \text{(SR-12)}$$
$$= 0.1115 - j0.061 = 0.1271\angle\text{-}28.68^\circ \quad \text{(Nexa)} \qquad (2.8)$$

From the per-unit quantities defined in (2.1) we have,

$$Z_{120Hz,per-unit} = \frac{Z_{120Hz}}{Z_{base}} = R_{120Hz,per\text{-}unit} - jX_{120Hz,per\text{-}unit}$$
$$= 0.1028 - j0.0359 = 0.1089\angle\text{-}19.26^\circ \quad \text{(SR-12)}$$
$$= 0.1889 - j0.1034 = 0.2153\angle\text{-}28.69^\circ \text{ (Nexa)} \qquad (2.9)$$

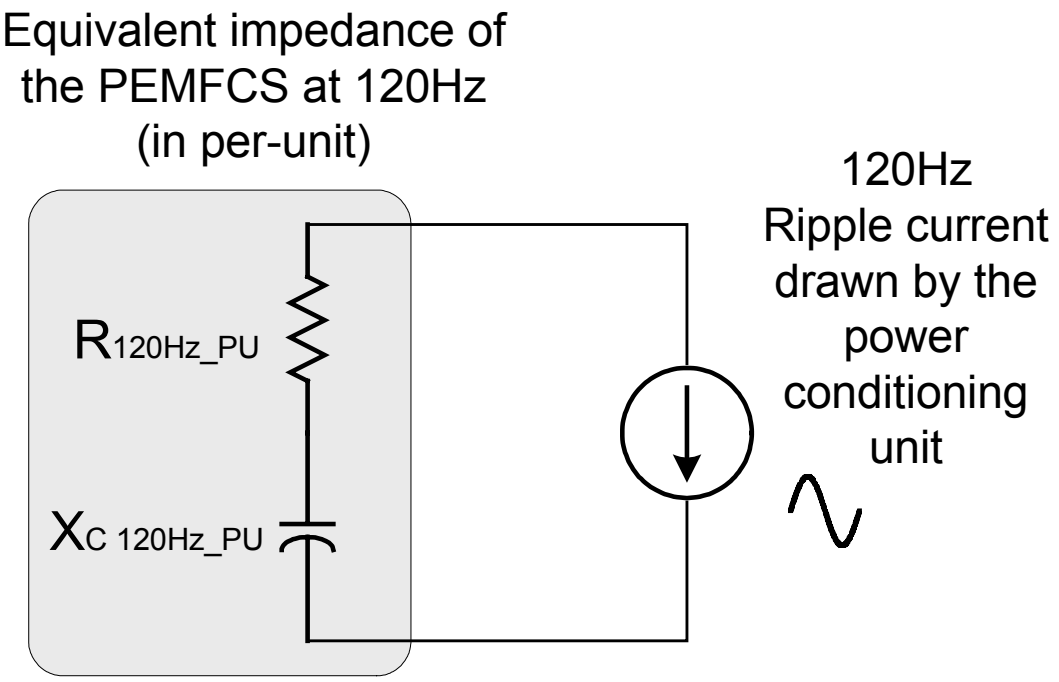

Fig. 2.9 AC equivalent circuit of the fuel cell stack at 120Hz

From (2.9) and Fig. 2.9 it is clear that the 120Hz ripple current drawn by the PCU contributes to a loss equal to $I^2_{Ripple} * R_{120Hz}$. This loss can be interpreted as a reduction in the available output power from the fuel cell. The per-unit reduction in fuel cell output power due to ripple current can be computed as,

$$P_{Loss,per-unit} = I^2_{Ripple,per-unit} * R_{120Hz,per-unit} \tag{2.10}$$

In addition to power reduction, the ripple current (120Hz) also contributes to ac voltage ripple (120Hz) at the fuel cell output terminals. The magnitude of the ac ripple voltage also can be computed from Fig. 2.9 as,

$$V_{Ripple,per-unit} = I_{Ripple,per-unit} * Z_{120Hz,per-unit} \quad (2.11)$$

Table 2.4 AC equivalent circuit parameters of the fuel cell stack at 120Hz

Fuel Cell Type	R_{120HZ}	X_{C_120HZ}	R_{120HZ_PU}	X_{C120HZ_PU}
SR- 12	**0.1717 [Ω]**	**0.06 [Ω]**	**0.1028**	**0.0359**
Nexa	**0.1115 [Ω]**	**0.061 [Ω]**	**0.1889**	**0.1034**

2.4 Experimental Results and Discussions

Several experiments were conducted on the PEMFCS setup (Fig. 2.2). Fig. 2.10 (a) shows the 120Hz impedance variation for different DC current loading conditions of the fuel cells. It is noted that the impedance of the PEMFCS is minimum around 90% loading condition. From the figure, it can be observed that SR-12 shows almost no variation on its 120Hz resistance value over the 20-100% operating point, while the Nexa shows a variation of 37%. This implies that the power reduction due to ripple current is almost the same at every operating point in the case of SR-12, however it becomes severe in the lower range of the operating point in the case of Nexa. Fig 2.10 (b) shows the variation of the AC resistance of the PMEFCS.

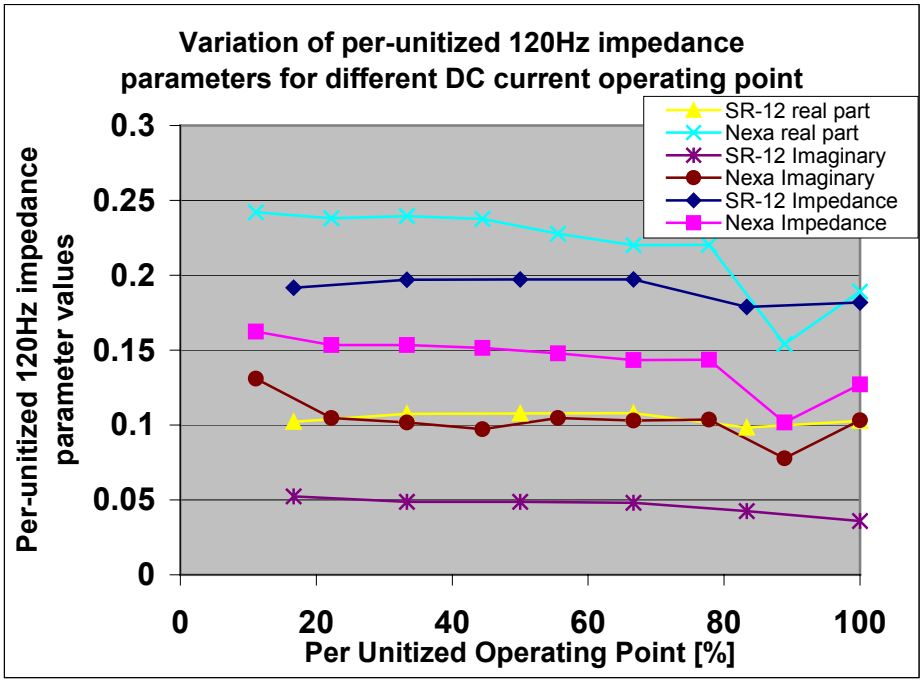

Fig. 2.10 (a) Variation of 120Hz impedance parameters for different DC current loading conditions

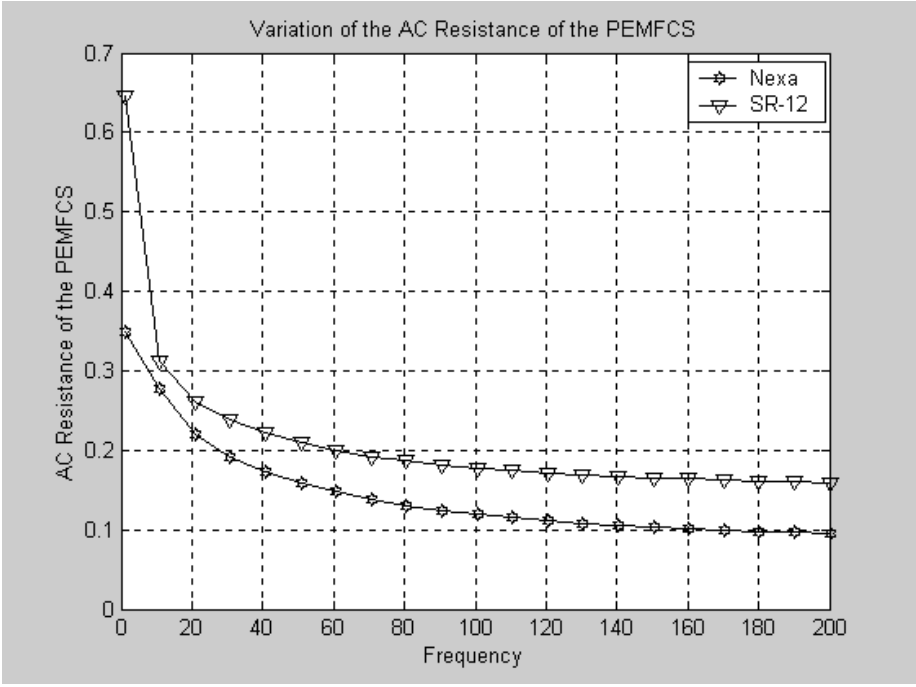

Fig. 2.10 (b) Variation of the AC resistance of the PEMFCS at the rated condition

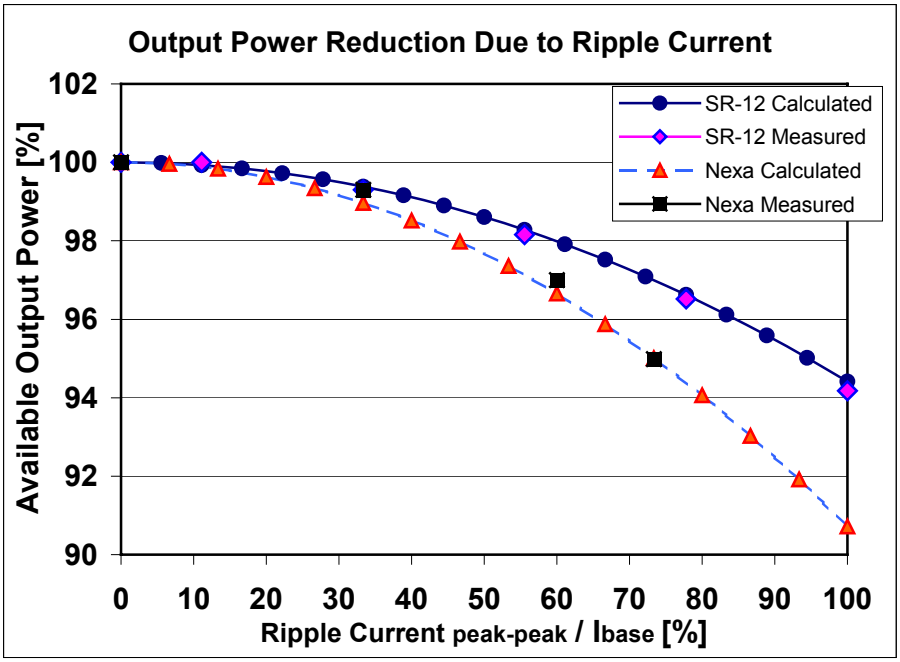

Fig. 2.11 Relationship between output power reduction and ripple current at the rated condition

Fig. 2.11 shows the variation of fuel cell available power (at the rated condition) as a function of ripple current as predicted by equation (2.10) and the measured results. It is noted that under the extreme case of 100% ripple (120Hz), the available power is reduced by 5.86% in SR-12 and 9.4% in Nexa, respectively. Further, for 30% ripple the reduction in output power from SR-12 is 0.5% and 0.84% from Nexa.

Fig. 2.12 (a) and Fig 2.13 (a) show the terminal voltage, current, hydrogen input flow rate and fuel cell output power when the fuel cell is supplying a DC load. Fig. 2.12 (b) and Fig. 2.13 (b) show the fuel cell terminal voltage distortion when supplying a ripple current of 120Hz superimposed on the DC current. Fig. 2.12 (c) and Fig. 2.13 (c) confirm the power reduction due to the ripple current with no change in the hydrogen input flow rate.

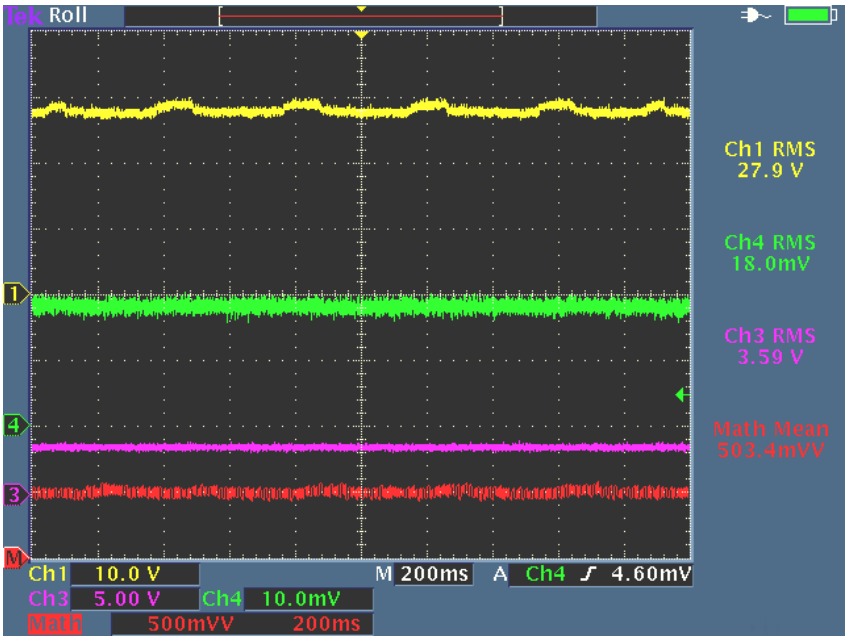

Fig. 2.12 (a) SR-12 outputs with no ripple current (SR-12 loaded by a constant load (18[A]). Channel-1: PEMFCS voltage [10V/div], Channel-4: PEMFCS current [10A/div], Channel-3: Hydrogen flow rate [10SLM/div], Channel-M: PEMFCS output power [500W/div], P_o = 503.4 [W])

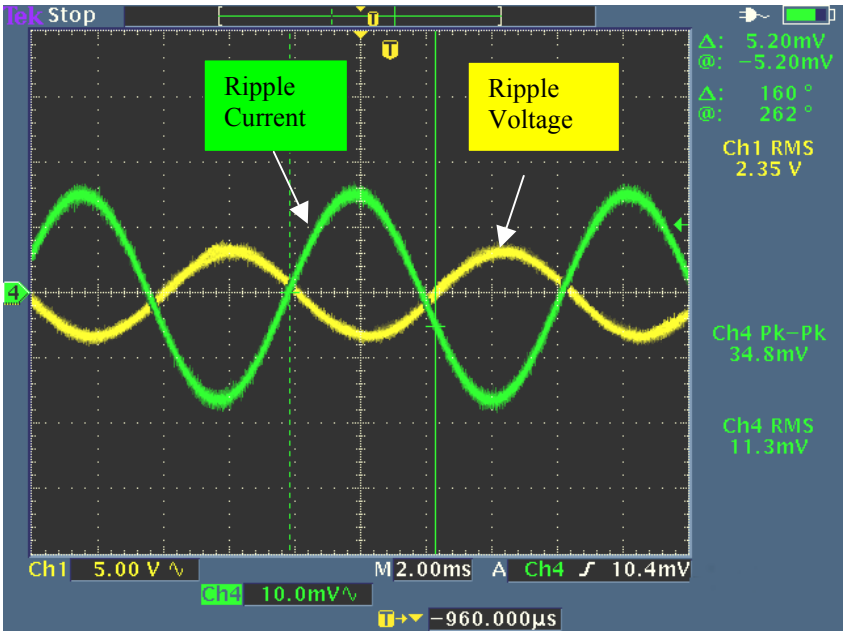

Fig. 2.12 (b) Effect of the ripple current for SR-12 (voltage distortion) (SR-12 Fuel cell terminal voltage and the ripple current for: 120Hz ripple current (17.3[A], peak-to-peak value) at the DC operating point of 18 [A], P_o = 473.9 [W], Hydrogen flow rate: 7.18[SLM/min])

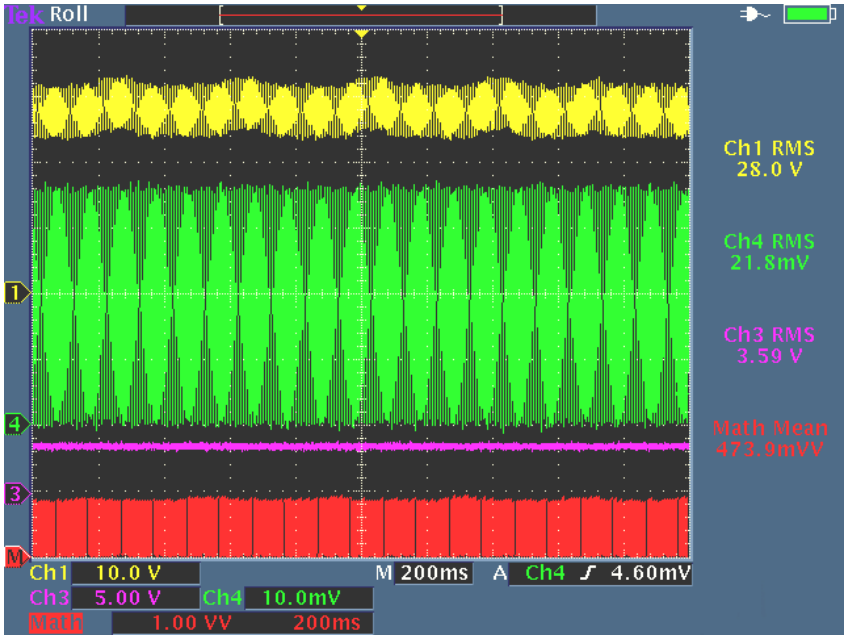

Fig. 2.12 (c) Effect of the ripple current for SR-12 (power reduction) (SR-12 loaded by a constant load (18[A]) and a 120Hz ripple (18[A] peak-to-peak). Channel-1: PEMFCS voltage [10V/div], Channel-4: PEMFCS current [10A/div], Channel-3: Hydrogen flow rate [10SLM/div], Channel-M: PEMFCS output power, [1kW/div], P_o = 473.9 [W])

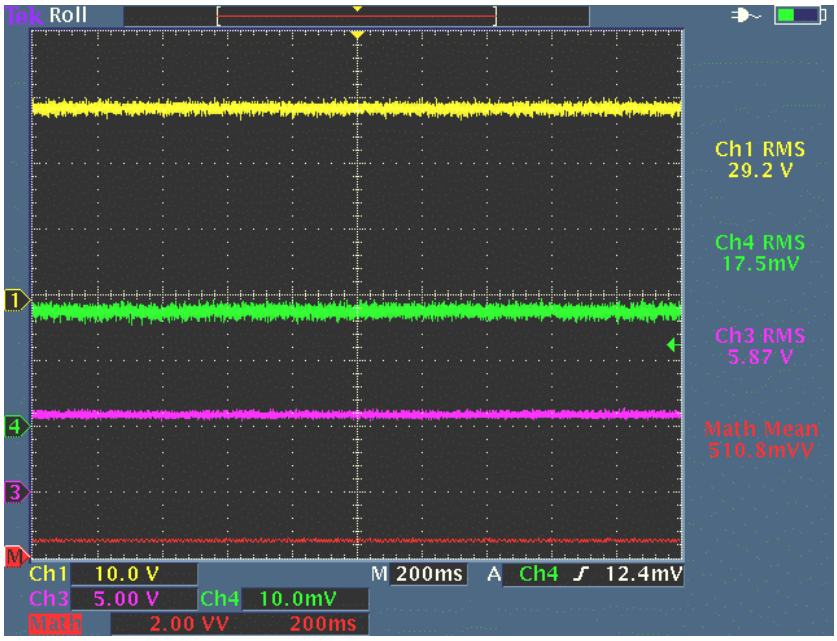

Fig. 2.13 (a). Nexa outputs with no ripple current (Nexa loaded by a constant load (35[A]). Channel-1: PEMFCS voltage [10V/div], Channel-4: PEMFCS current [20A/div], Channel-3: Hydrogen flow rate [10SLM/div], Channel-M: PEMFCS output power [2kW/div], P_o = 1021.6 [W])

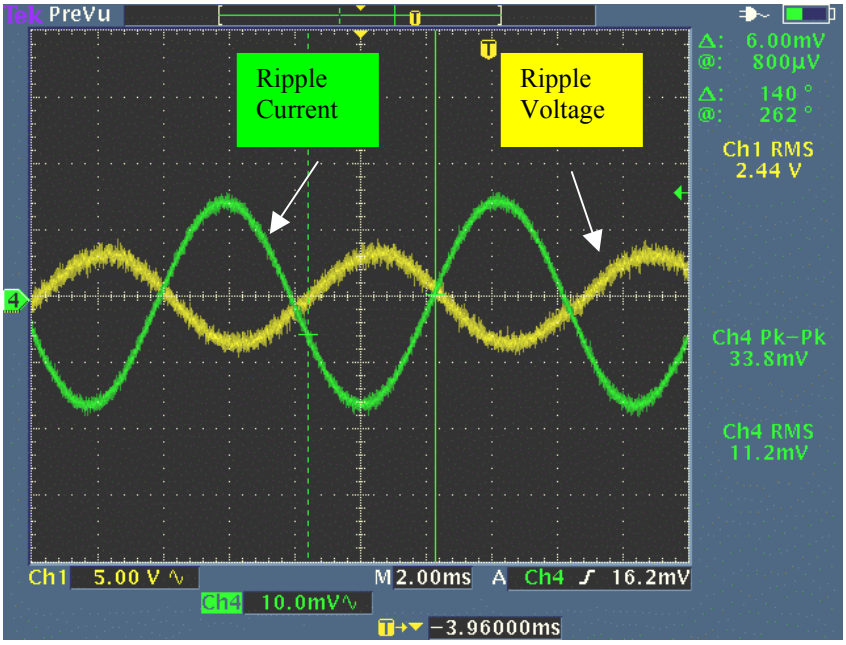

Fig. 2.13 (b) Effect of the ripple current for Nexa (voltage distortion) (Nexa Fuel cell terminal voltage and the ripple current for: 120HZ ripple current (30.2[A], peak-to-peak value) at the DC operating point of 35 [A], P_o = 967.6 [W], Hydrogen flow rate: 11.74[SLM/min])

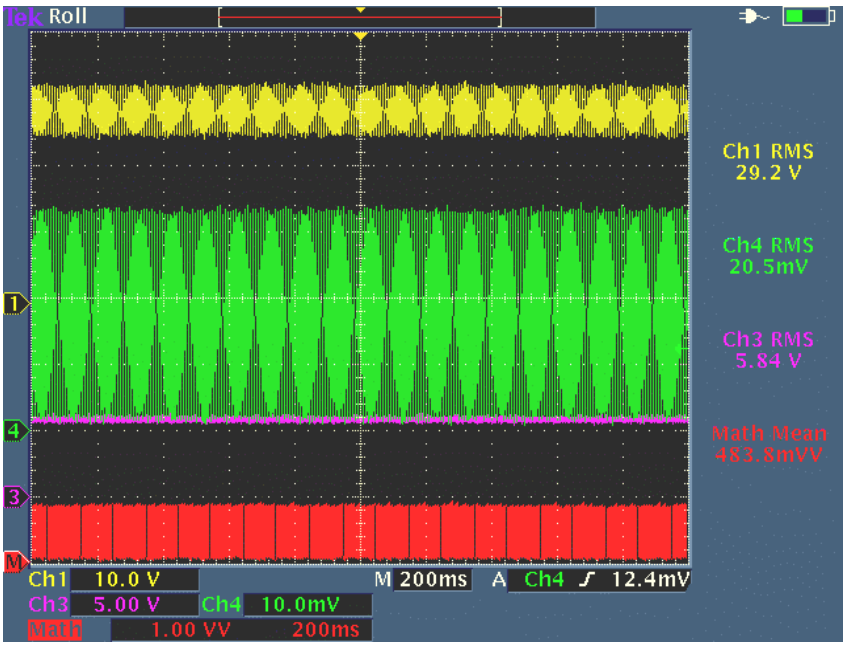

Fig. 2.13 (c) Effect of the ripple current for Nexa (power reduction) (Nexa loaded by a constant load (35[A]) and a 120Hz ripple (30.2[A] peak-to-peak). Channel-1: PEMFCS voltage [10V/div], Channel-4: PEMFCS current [10A/div], Channel-3: Hydrogen flow rate [10SLM/div], Channel-M: PEMFCS output power, [2kW/div], P_o = 967.6 [W])

2.5 Conclusion

In this chapter an impedance model of the PEMFCS has been developed by experiments. Experimental results show that the developed model is suitable to explain the electrical characteristics of the fuel cell when connected to a power conditioning unit (PCU). The relationship between the fuel cell output voltage variation and the Volt-Amp rating of the PCU has been shown. It has been shown experimentally that the PCU ripple current (120Hz) can contribute to a reduction in the fuel cell available output power and increased distortion of terminal voltage. Limiting the low frequency (120Hz) fuel cell ripple current between 30% and 40% has been shown to result in less than 0.5% to 1.5% reduction in fuel cell output power and therefore may be acceptable. Restricting the ripple current below these values will require a more robust input L-C filter within the PCU. Additional losses within PCU's L-C filter then become a concern and contribute to a lower PCU efficiency. The results presented in this chapter can be used to further optimize the overall efficiency and cost of the fuel cell and its PCU.

CHAPTER III

FUEL CELL POWERED UPS SYSTEMS: DESIGN CONSIDERATIONS

3.1 Introduction

Conventional uninterruptible power supply systems (UPS) employ engine generators and/or batteries as their main power sources to provide the electric power for critical functions or loads when the normal supply, i.e. utility power, is not available [7][20]. Typical UPS systems consist of rechargeable batteries such as sealed lead-acid (SSLA) or nickel cadmium (Ni-Cd). However, these batteries contain toxic heavy metals such as cadmium, mercury, and lead and may cause serious environmental problems if they are discarded without special care [9].

Fuel cells are emerging as an attractive power source by virtue of their inherently clean, efficient and reliable service [5][21]. As the demand for various applications such as remote generation, backup power generation and distributed generation increases, their use is spreading widely. Accordingly, their prices are steadily reducing and this is further accelerating their penetration into market [7]. Among various kinds of fuel cells, PEMFCs (Proton Exchange Membrane Fuel Cells) are compact and lightweight; provide a high output power density at room temperature, plus ease of start-up and shut down in system operation [5]. Further, unlike batteries, fuel cells can continuously provide power

as long as the reactants are supplied. This feature is especially useful under the condition where the duration of the power outage is uncertain.

It is important for the UPS system to be able to immediately take over the full load at the power outage or out-of-tolerance situation to avoid any data loss, uncontrolled system shutdown or malfunctioning of the devices. Some critical applications do not allow even several tens of millisecond power interruption. As is well known, fuel processors have a delay as much as several tens of seconds, and fuel cell cannot take over the full load if its membrane is not properly humidified. For this reason, a supercapacitor module is employed to compensate for these response delays by supplying the required instantaneous energy, which is stored during the normal operation. This energy can be used to handle overload conditions as well.

In this chapter, design considerations of a 1-kVA fuel cell powered line-interactive UPS system employing modular (fuel cell & power converter) blocks is discussed (Fig. 3.1). A design example for the DC/DC boost converter and sizing of the supercapacitor as well as fuel calculations are presented and the validity of the design is verified through the simulation.

3.2 Proposed Fuel Cell Powered UPS System Architecture

Fig. 3.1 shows the block diagram of the proposed approach. The approach consists of two boost converters with fuel cells and one bi-directional converter with a supercapacitor. Normally, the utility power is transferred to the load through the static

switch module (SSM). At the initial start, fuel cells charge the supercapacitor through the bi-directional converter, and then supply 10% of the rated load along with the utility. In the event of power outage or out-of-tolerance, however, the controller turns the SSM off, thereby the fuel cell and their power converter modules start to power the full load alone.

At the moment of the transition from the normal mode to fuel cell powering mode, the system is not able to take over the full load due to the slow dynamics of the fuel processor. This proposed topology overcomes this drawback by placing the supercapacitor and bi-directional converter module in parallel with the fuel cell and power converter modules. This module transfers the energy that was stored in the supercapacitor during the normal mode operation, to the load at the initial start to make

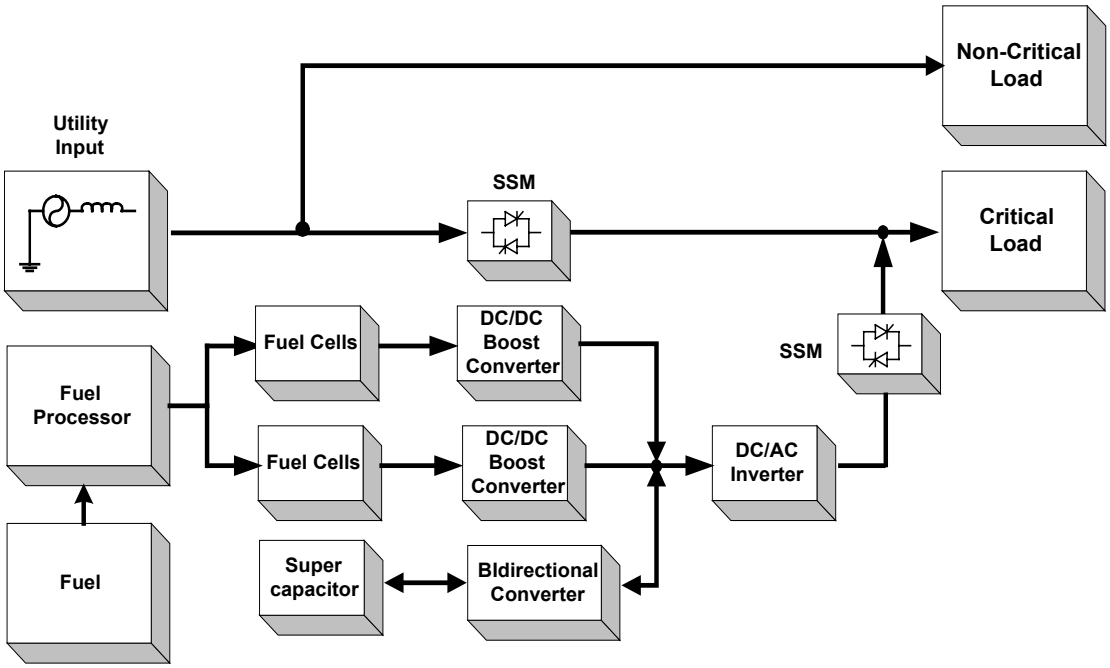

Fig. 3.1 Proposed fuel cell powered line-interactive uninterruptible power supply system

up the instantaneous power shortage. This stored energy can also be used to handle the transient power shortage due to load step changes and/or overload conditions for a short time. When the transient situation is over, the fuel cells supply the minimum power to the load and at the same time recharges the supercapacitor. The control circuit monitors the utility and the fuel cells status continuously. When the system detects a utility disturbance condition, it controls the fuel cell and power converter modules to supply more power. After the disturbance, the controller connects the utility to the load through the synchronization process. The advantages of the proposed approach over conventional UPS systems are as follows:

1. Due to the absence of batteries and an engine generator, it is environmentally friendly, clean and quiet.
2. In the proposed fuel cell powered UPS, the amount of power availability is a function of Hydrogen availability. This is an advantage compared to the battery based UPS whose state-of-charge (SOC) is not always precisely known.
3. No delay time is required to take over the full load when the power disturbance occurs due to fast discharging characteristics of the supercapacitor.
4. The system possesses good overload handling capability with the supercapacitor.

5. Continuous power generation is possible as long as the reactant gases are supplied to the fuel cells.

Fig. 3.2 shows the detailed circuit of the proposed Architecture. The DC/DC conversion stage of this architecture consists of two fuel cells employing boost converters, a supercapacitor employing bi-directional buck-boost converter and a low voltage DC bus capacitor. An additional DC/DC converter and a high frequency isolation transformer are employed to form the high voltage DC link. At the initial start-up, two fuel cells charge the supercapacitor through the MOSFET S3 and DC bus capacitor as well. Under normal operating conditions, two boost converters supply 10% of the rated power to the load. However, when the load changes suddenly, the UPS system is not able to respond promptly to the power demand change due to its delay time for fuel flow rates to adjust. In this situation, the system controls the switch S4 to supply the DC bus by the boost operation.

This control topology is also useful for handling the instantaneous overload situation. If the load demands more than the rated power momentarily, the stored energy in the supercapacitor can be utilized to supply the load, thereby preventing the fuel cell from being overloaded. It is obvious that system delay or voltage drop is unavoidable without this auxiliary power system in the condition of sudden load change and/or overload. The DC/AC conversion stage of this architecture consists of a DC/AC IGBT inverter and produces the high quality sinusoidal 120/240V output voltage based on the

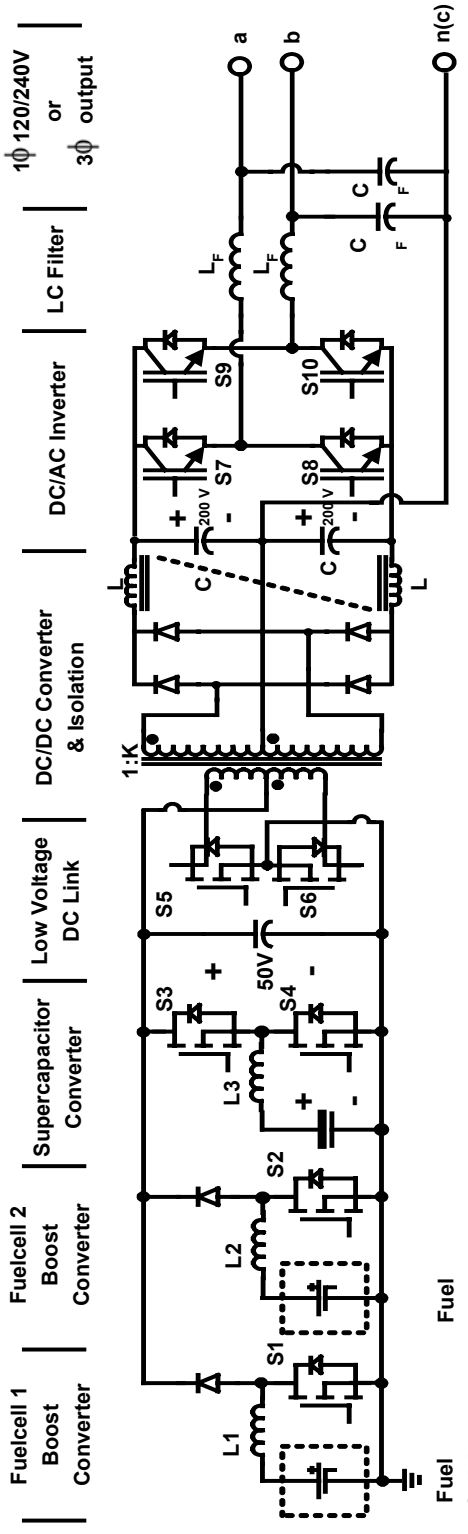

Fig 3.2. Circuit Topology of the Proposed Fuel Cell Powered UPS System

neutral point produced by the switch S5 and S6 in a controlled manner or 3-phase AC output. In this architecture, though the additional DC converter stage results in reduced system efficiency, it is attractive in that this approach does not require a low frequency transformer, which is bulky and heavy.

3.3 DC-Bus Control Scheme

Figure 3.3 shows the block diagram of the parallel DC-DC boost converter control scheme. In the figure DC/DC converters 1 and 2 are combined with fuel cells 1 and 2, and DC/DC converter 3 is combined with a supercapacitor. The control scheme is composed of one voltage control loop and three independent current control loops and the DC bus voltage is controlled by a PI controller to generate the system current command. Power available signal from the fuel cell indicates the available power from the fuel cell at the moment and thereby available current command is calculated. In the situation of a power shortage or instantaneous overload current sharing controller

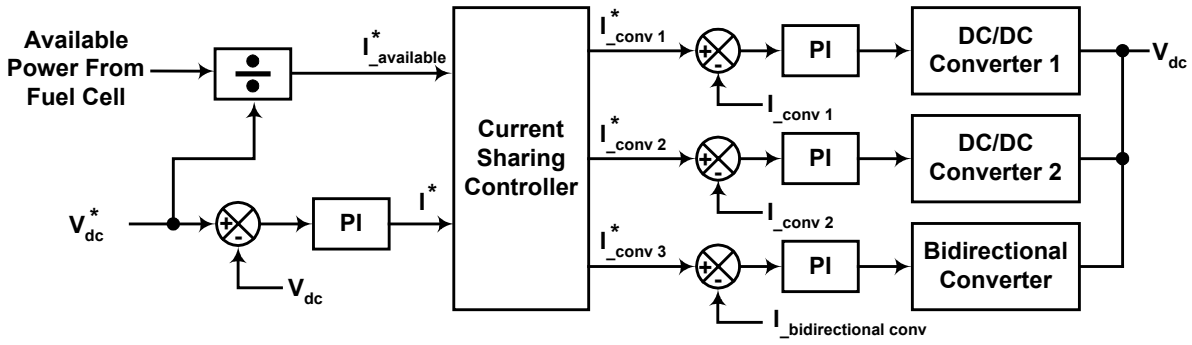

Fig 3.3 Block diagram of the parallel DC-DC converter control scheme

calculates the appropriate current command values for each converter and sends it to them.

3.4 Simulation Results

Fig.3.4 shows the simulation results for the DC/DC converters incorporated with the fuel cells and supercapacitor when the power outage occurs. Initially, the DC/DC converter and fuel cell modules are powering the 10% of the load and then load changes suddenly from 10% to 100%. In this condition, the system is not able to respond fast enough to supply the load. The top trace is the 'power available signal' indicating the amount of power available from the fuel cells. In this simulation, it is assumed for convenience that the reformer and fuel cell stack have 6-second response delay. Therefore, it takes 6 seconds for the fuel cell and associated reformer to produce enough power to supply 100% load from the moment of a power outage. The second and third traces show inductor (L1 and L2) current waveforms for boost converters 1and 2. Each converter is sharing the load equally in the range of the available power. The fourth trace is the inductor (L3) current waveform showing that power from the supercapacitor is making up for the power shortage during the transient. The supercapacitor is discharging to supply the load. The bottom trace shows the DC bus voltage being maintained stable during the transient. After the transient, the supercapacitor is recharged.

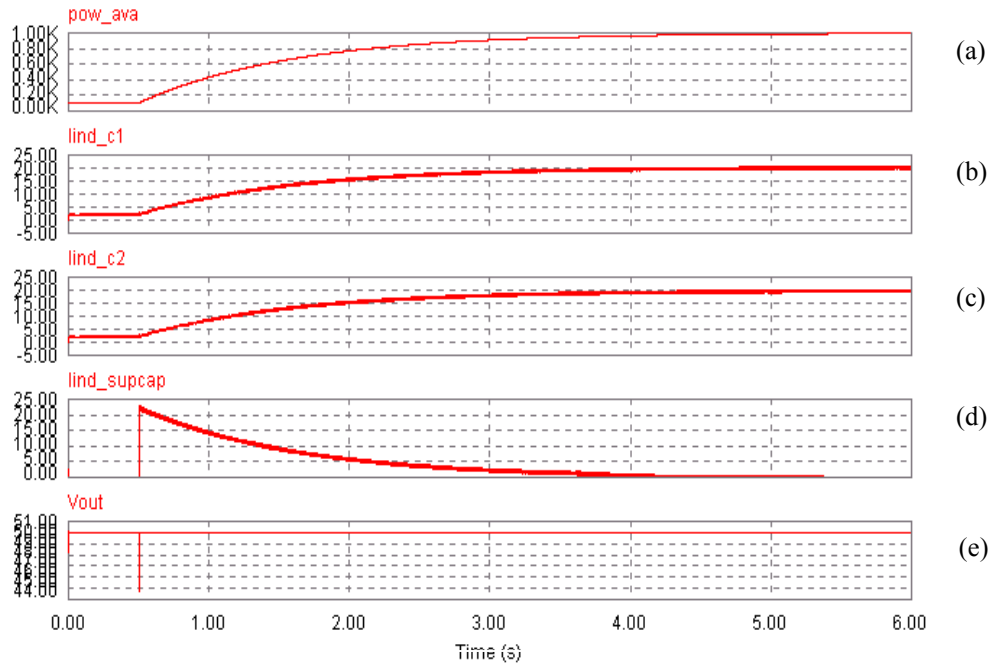

Fig. 3.4 Simulation results (Compensation for the reformer delay). (a) Power available signal form the fuel cell (b) Inductor current of converter 1 (c) Inductor current of converter 2 (d) Inductor current of bi-directional converter (e) DC bus voltage

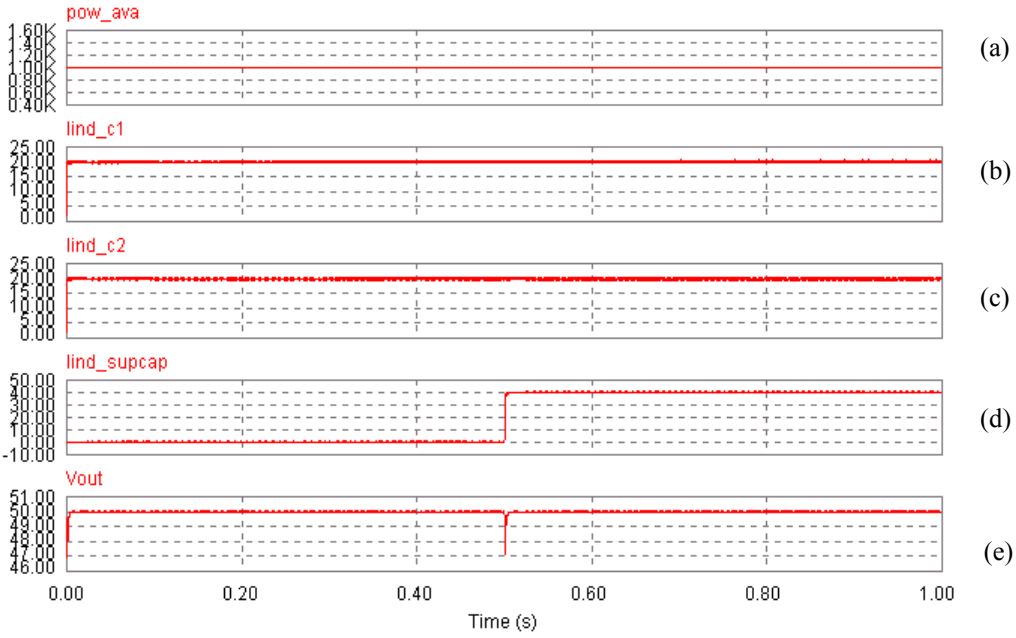

Fig 3.5 Simulation results (Compensation for the instantaneous overload). (a) Power available signal form the fuel cell (b) Inductor current of converter 1 (c) Inductor current of converter 2 (d) Inductor current of bi-directional converter (e) DC bus voltage

Fig 3.5. shows the simulation results when the load changes from 100% to 200% for a short time. At the beginning, two converters are powering the 100% load equally and the load increased to 200% in 0.5 second. In this condition, the supercapacitor is discharging its stored energy to supply the overloaded portion. The first and second traces show that the two boost converters 1 and 2 are not overloaded.

3.5 Design Example

3.5.1 Specification of Proposed Fuel Cell Powered UPS

- Rated Power: 1 KVA
- Normal Output Power: 10% rated power with utility power available
- Fuel Reformer Time Constant: < 20 sec
- Output Voltage: 120VAC ± 5%
- Output Voltage Frequency: 60HZ ± 0.1%
- THD (Total Harmonic Distortion): < 2%
- Overload Rating: 200% for 10 sec.

In this design example, all the calculations are done based on a PEMFC (Proton Exchange Membrane Fuel Cell).

3.5.2. Required Fuel Calculation for 1-hr Power Outage and Normal Mode Operation [5][22]

In this section hydrogen consumption is calculated for the 1kW PEMFC stack.

The basic chemical equation for a fuel cell reaction can be expressed as,

$$2H_2 + O_2 = 2H_2O \tag{3.1}$$

The rate of Hydrogen fuel usage in a single cell is related to current by,

$$Q_{\_H_2} = \frac{I}{Z \cdot F} \text{ [moles / sec]} \tag{3.2}$$

where,

$Q_{\_H2}$: Hydrogen flow rate

F: Faraday constant 96485[coulombs/mole]

Z: Number of electrons participating in the reaction

Thus, the Hydrogen flow rate required to generate 1 ampere for one cell can be calculated by,

$$Q_{U\_H_2} = \frac{I}{Z*F*I*K} = \frac{1[\frac{coulomb}{sec}]*60[\frac{sec}{min}]*22.4[\frac{SL}{mol}]}{2*96485[\frac{coulombs}{mol}]*1[A]*1[cell]} = 0.007[\frac{SLM}{A\cdot Cell}] \quad (3.3)$$

where,

K: Number of cells

SLM: Standard liter per minute

For the parasitic power to run the control system of the fuel cell, it is estimated that the fuel cell is required to generate about 10% more power than needed. Thus, the hydrogen flow rate needed for 1kW fuel cell stack can be calculated as follows.

$$Q_{T\_H2} = Q_{U\_H_2} * \frac{P*1.1}{V_{cell}} * N*S = 0.007* \frac{1000*1.1}{25} *48*1.05 = 15.5[SLM] \quad (3.4)$$

where,

$Q_{\_T\_H2}$: Hydrogen flow rate needed to generate total power

V_{cell}: Fuel cell output voltage at the rated load

N: Number of cells

S: Stoichiometry

Therefore, the total amount of Hydrogen to be consumed for a 1kVA UPS system during a 1-hour power outage can be calculated as,

$$Q_{T\_H2}[\mathrm{SLM}] * 60[\mathrm{min}] = 15.5 * 60 = 931[\mathrm{L}] \tag{3.5}$$

If the Hydrogen is stored in the cylinder as a compressed gas at 25°C (298.15[K]), its weight and volume at 150 atm (2205 [psi]) can be calculated as follows. The weight of Hydrogen is given by,

$$\frac{931[\mathrm{L}] * 2[\frac{\mathrm{g}}{\mathrm{mole}}]}{22.4[\frac{\mathrm{L}}{\mathrm{mole}}]} = 83[\mathrm{g}] \tag{3.6}$$

Since Hydrogen gas normally takes up 3 weight percent when it is contained in a cylinder as a compressed gas, the total weight of the compressed Hydrogen gas and its cylinder is

$$\frac{83[\mathrm{g}]}{3[\mathrm{wt}\%]} = 2766[\mathrm{g}] \tag{3.7}$$

The volume of the Hydrogen at 150[atm] can be calculated by eq. (3.8-3.10) The number of moles of Hydrogen in a certain volume (931[L] in this case) can be calculated as,

$$n = \frac{P \cdot V}{R \cdot T} = \frac{1[atm] * 931[L] * 10^{3}[cm^{3} / L]}{82.06[\frac{cm3 \cdot atm}{mol \cdot K}] * 298.15[K]} = 38[moles] \quad (3.8)$$

where,

n: Number of moles

P: Pressure [atm]

V: Volume of the gas [cm^3]

R: Gas constant

T: Temperature [K]

The volume of one mole of Hydrogen at 150[atm] can be calculated from the virial equation [22-23] as

$$V_{\_U} = \frac{R \cdot T}{P} + B = \frac{82.06\ [\frac{cm3 \cdot atm}{mol \cdot K}] * 298.15\ [K]}{150\ [atm]} + 15.4[\frac{cm3}{mol}] = 178.5[\frac{cm^3}{mole}] \quad (3.9)$$

where,

$V_{\_U}$: Volume of one mole of Hydrogen at a certain pressure

B: Virial constant at 298.15[K]

Thus, the total volume of the Hydrogen at 25[°C] at 150 [atm] is

$$V_{\_U} * n = 178.5[\frac{cm^3}{mole}] * 38[mole] * 10^{-3}[\frac{L}{cm^3}] = 6.78[L] \quad (3.10)$$

The proposed line-interactive UPS system is assumed to supply 10% of the rated load. Thus the Hydrogen needed for normal mode operation is 93-Liters per hour.

3.5.3. DC/DC Converter Design

The DC/DC converter is designed according to the following calculations [24]:

- Switching frequency; Fs= 100 [kHz]
- Critical load; 10% of the full load for continuous current mode

  I_out_crit = Po/Vo*0.1= 1[A]
- Output voltage ripple ; 1% output voltage ripple

  Vr = Vo*0.01 = 0.5 [V]
- Output power of each converter; Po = 500 [W]
- Input voltage; Vs = 25-39 [V]
- Output voltage; Vo = 50 [V]
- Maximum output voltage / Input voltage ratio; M=50/25=2
- Output current; Io=Po/Vo=10 [A]
- Maximum input current; $Is_{\_max}$ = 500/25 =20 [A]
- Minimum inductance

  Lc=Vo*(M-1)/(Iout_crit*Fs*2*M^3) = 32.15 [uH]
- Worst-case peak current

  Ipk = Io*(M((+M-1)/(2*Io*Lc*Fs/Vo*M^2))) =22 [A]

- Output dc capacitance

  $Co = (Ipk^2 * Lc) / (2*Vr*(Vo-Vs)) = 600$ [uF]

3.5.4. Sizing the Supercapacitor

The energy stored in a supercapacitor is given by:

$$W_j = \frac{1}{2} CV^2 \tag{3.11}$$

Since the energy stored in a supercapacitor is directly proportional to the square of the voltage, a drop in 30% of its voltage (1pu to 0.7pu) represents the release of 50% of the stored energy. Further, losses in the DC/DC boost converter powering the supercapacitor along with the internal losses due to the equivalent series resistance (ESR) also need to be accounted for. Adopting this discharge strategy, the following equation can be written:

$$\frac{1}{2}[CV_{sup}^2 - C(0.7V_{sup})^2] * k = P_{shortage} * t \tag{3.12}$$

where, C is the required capacitance of the supercapacitor, k is the efficiency, which is less than 1 due to loss. $P_{shortage}$ is the amount of power shortage (watts) due to

the system delay or overload and "t" is the specified duration for those events. In the proposed approach, the fuel cell and associated reformer are assumed to have 20 seconds of response delay. Therefore, as shown in the simulation (Fig. 3.4), supercapacitor needs to make up for the power shortage, which is the power difference between the required power for the load and available power from the fuel cells. For the proposed system, we have $P_{shortage}$=500[W]; t=20[seconds] and let k=0.9. Assuming a supercapacitor of 40[V] rating, the required capacitance value can be calculated by substituting these values in Eqn. (3.12), and

$$C = \frac{4 \cdot P_{shortage} \cdot t}{k * V_{sup}^2} = \frac{4 \cdot 500 \cdot 20}{0.9 * 40^2} = 27.8[F] \tag{3.13}$$

This can be achieved by connecting 16 of commercially available supercapacitors (450F, 2.5V) in series. Detailed specification for the supercapacitor is presented in the Table 3.1.

3.5.5 Fuel Cell System Setup

Fig. 3.6 shows the experimental setup installed in the Power Electronics & Fuel Cell Power System Laboratory of the Texas A&M University. Hydrogen is stored in the

Table 3.1. Specification of supercapacitor, BCAP0013 (Maxwell Technologies)

Capacitance	450 Farads (±20%)
Maximum ESR(25°C)	2.4 mohms
Specific Power Density	3400 (W/kg)
Voltage(Cont.)	2.5 V
Voltage(Peak)	2.8 V
Maximum current	180 A
Dimensions	50 x 97 mm
Weight	190 g
Volume	.15 L
Temperature (Operating & Storage)	-35°C to 65°C
Leakage Current (12 hours, 25°C)	3 mA

Table 3.2 Specification of 500W PEM fuel cell stack, SR-12 (Avista Labs)

Power Output (Cont.)	500 W
Output Voltage	25-39 VDC
Fuel Source	Hydrogen
Fuel Consumption	7.0L/min 500W (<1.0L/min @ no load)
System Start Time	7 minutes @room temperature
Turndown Ratio	500W to no load, infinity
Operating Temperature	5°C to 35°C
Dimension(W x D x H)	22.3” x 24.2” x 13.6”
Weight	44kg w/cartridge

two cylinders at high pressure (2200psia). The pressure regulator and indicator are installed at the top of the cylinder. The regulator controls outgoing pressure of the gas and the pressure indicator shows the pressure of the cylinder as well as the outgoing gas. When the cylinder valve is open, hydrogen gas comes out through the in-line filter to meet the necessary purity (99.95%) for the fuel cells. Hydrogen velocity fuses and flame arrestor is installed for safety. The former blocks the Hydrogen flow when the flow rate exceeds a preset value and the latter quenches any flame that may occur inside the Hydrogen pipe. An electronic flow meter indicates the flow rate of the gas and it generates an electric signal for the monitoring system. A second pressure regulator is placed to step down the pressure further. Two-way ball valves are connected to make it possible to control the gas flow manually. Finally, Hydrogen gas is supplied to each fuel cell at the pressure of 7.5psig (55 Kpa-g). Electronic mass flow meter monitors the Hydrogen flow rate to the fuel cell stack. Detailed specification for the fuel cell stack is presented in the Table 3.2. Fig 3.7 shows the V-I characteristics of the SR-12 fuel cell stack and Fig 3.8 shows its power versus current curve.

3.6 Conclusion

A fuel cell powered, line-interactive UPS system has been discussed in detail. The approach provides stable power to the load when the utility is interrupted. Also, this approach verifies the possibility that the fuel cell can replace conventional UPS power

sources such as engine generators, batteries and flywheels. A supercapacitor module is incorporated to overcome the transients such as instantaneous power fluctuations, slow dynamics of the fuel preprocessor and overload conditions. In conclusion, an environmentally friendly and clean power back-up system has been proposed and its validity and feasibility has been verified through the simulation.

Fig. 3.6 Fuel cell system installed in the Power Electronics & Fuel Cell Power System Laboratory of Texas A&M University.

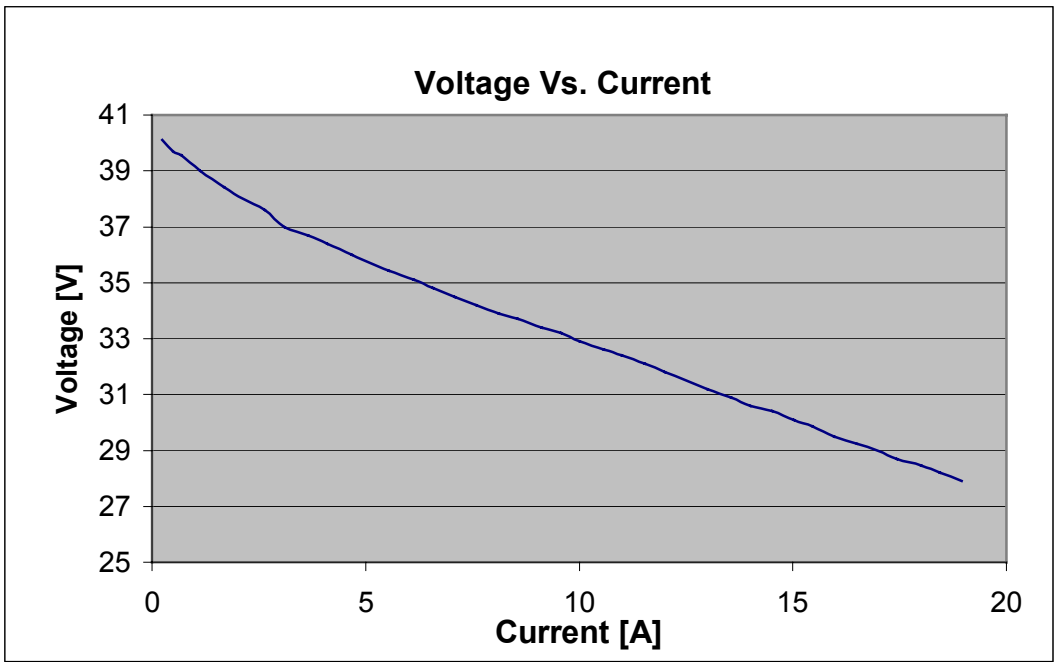

Fig. 3.7 Voltage versus current curve for the SR-12 fuel cell stack

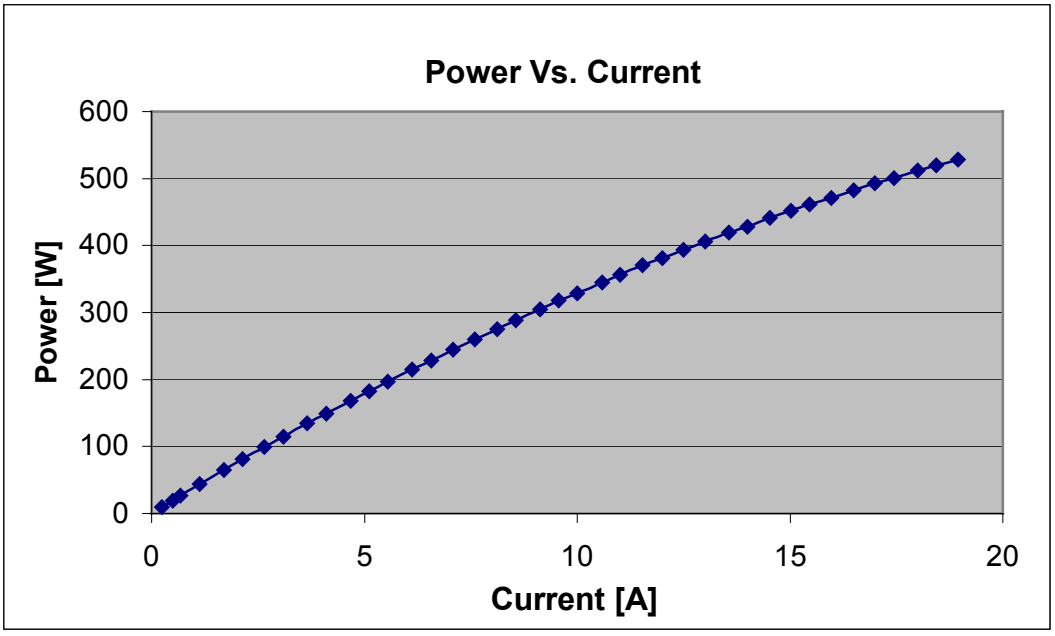

Fig. 3.8 Power versus current curve for the SR-12 fuel cell stack

CHAPTER IV

AN ADVANCED POWER CONVERTER TOPOLOGY TO SIGNIFICANTLY IMPROVE THE CO TOLERANCE OF PEM FUEL CELL POWER SYSTEMS

4.1 Introduction

In addition to the fuel cell stack itself; a fuel cell power system consists of a fuel processor and other subsystems to manage air, water, thermal energy, and electric power conditioning unit to produce ac output (Fig. 4.1). The fuel processor is one of the most crucial parts of the fuel cell power system in that this makes it possible to use the hydrogen rich fuels, such as methanol, gasoline, diesel, or gasified coal, thereby assuring the fuel flexibility. However, as seen in the Fig. 4.1, the fuel processor takes up considerable amount of volume, weight and cost in the system, thus it is desirable to reduce the requirement of the fuel processor such as reformers.

As the fuel cells are becoming more acceptable, it is observed that the fuel cell starts to replace the conventional power sources such as ICE (Internal Combustion Engine), batteries or generators. Among the various kinds of the fuel cells, Polymer Electrolyte Membrane Fuel Cells (PEMFC) is the preferred choice in many applications including: home power generating units and automobiles. However, there are still many obstacles that prevent fuel cells from playing a major role in electrical power production.

One of the problems in reforming natural gas (which is widely available and supplied to many homes today) is the presence of carbon monoxide (CO) in the hydrogen fuel. CO, a by-product of the reforming process, can poison the fuel cell by blocking the Pt-Ru electro-catalyst and can drastically decrease the output voltage and hence the power output. Many natural gas reformers (adiabatic) developed to date can produce as little as 10 parts per million (ppm) of CO. However, these reformers are expensive, the amount of CO produced is not always consistent, and even small amounts of CO may be detrimental to the performance (operating life) of the PEM fuel cell power system. It has been shown in literature that creating anode over-potential can electro-oxidize CO from the surface of the electro-catalyst and improve the performance [25]. Furthermore, references [13,25] (conducted on a single cell) indicate that pulsing the cell with positive current spikes can be effective in improving the cell CO tolerance.

In view of the above results, this chapter proposes an advanced power converter topology to significantly improve the CO tolerance on PEM type fuel cell power systems. In the proposed method an additional two-stage dc-dc converter with a supercapacitor module is connected in parallel with the back-end dc-dc boost converter of the fuel cell. This two-stage dc-dc converter draws a low frequency (0.5Hz) pulsating current of specific amplitude (20-30 [A]) to create sufficient anode over potential to electro-oxidize the CO from the fuel cell catalyst. The resulting system is shown to produce increased power (up to 50%) when supplied by hydrogen fuel with 500 parts per million (ppm) CO. The advantages of the proposed method are:

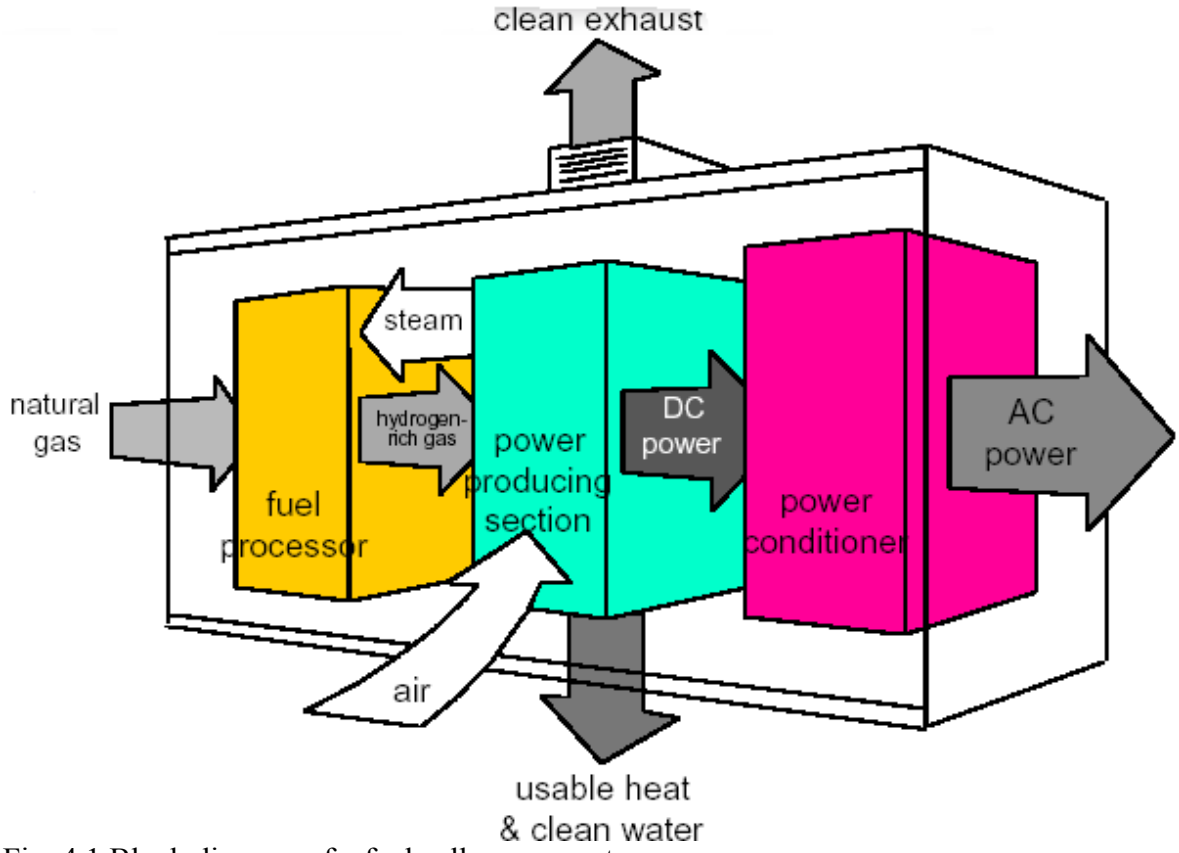

Fig. 4.1 Block diagram of a fuel cell power system

(a) A CO tolerant PEM fuel cell power system is more robust and lower in cost, since it facilitates the usage of cheaper natural gas to hydrogen reformer technologies.

(b) The method easily adapts to different CO concentration levels present in the hydrogen fuel and is controllable via closed loop.

(c) Extended operating life of the fuel cell power system can be potentially realized with the proposed strategy.

Experimental results show the effectiveness of the proposed electrical pulsing technique. Also the simulation results of the proposed power converter topology prove the feasibility of the proposed scheme.

4 2. Background Information on CO Poisoning and Methods to Prevent It

Figure 4.2 shows the typical configuration of a single PEM fuel cell. In the fuel cell structure catalyst is an essential part. Catalysts, such as platinum (Pt) are added to the anode and cathode of a PEMFC to obtain a high reaction rate at low temperatures. Pt based alloys are an effective catalyst at the anode connected to the fuel cell because hydrogen oxidation occurs abundantly on these surfaces. However, CO present in the hydrogen fuel adsorbs on the platinum alloy surface due to its strong affinity, thereby halting the hydrogen oxidation reaction by blocking the adsorption site [13, 25].

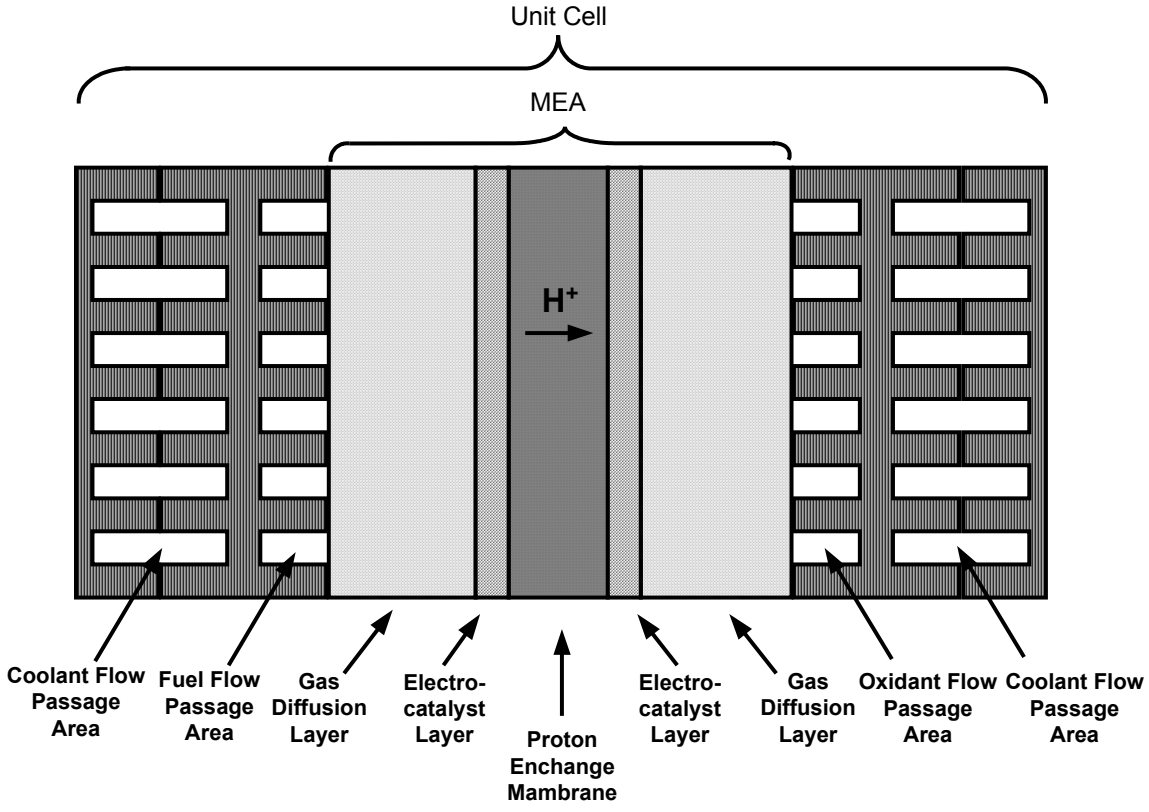

Fig. 4.2 Typical configuration of a single PEM fuel cell

This phenomenon is referred to as CO poisoning. PEM fuel cells typically run at temperature around 60-80 C° where they exhibit long-term stability. At this temperature, the CO will adsorb as (4.1) and strongly bind to catalyst. This halts the hydrogen oxidation reaction (4.2) occurring at the anode of the fuel cell, as only a small fraction of the catalyst sites is left free for the hydrogen oxidation.

$$CO + Pt \Rightarrow CO_{ads} \quad (4.1)$$

$$H_2 + Pt \Rightarrow Pt + 2H^+ + 2e^- \quad (4.2)$$

Thus this leads to a significant reduction in fuel cell output voltage and hence the output power. For a PEMFC to operate as desired, the CO must be cleaned from the catalyst surface.

Several methods have been suggested to solve this problem [11-12]. One solution to mitigate the effect of CO poisoning is to use alloyed catalysts such as Pt/Ru, Pt/Mo, Pt/Ru/Mo, Pt/Sn and etc., which exhibit improved CO-tolerance [11]. This is the most convenient approach because it does not introduce any additional steps or hardware. It is quite effective to handle a reformate containing less than 10 ppm CO, but it is not adequate when the CO concentration is higher. In the presence of higher CO concentration, an additional step involving bleeding an oxidant into the anode compartment has been suggested [12]. The bleeding oxidants such as air, oxygen, or hydrogen peroxide chemically oxidize CO to CO2 and thus lowers its concentration. However, since the only a small part of the oxidants participates in the oxidation

process, the remaining oxidant chemically combusts with hydrogen. This combustion reaction lowers the fuel efficiency typically on the order of 2% for 5% air bleeding. [11-12]. Also the above solutions contribute to higher cost.

Interesting results can be found from the literature [13,25] that at very high anode overpotential, CO oxidation occurs by the process described below. In reaction (4.3), the CO_{ads} is oxidized to CO_2 by means of water activation by the catalyst, where oxygenated species OH_{ads} are formed from water present in the reaction zone (4.4).

$$OH_{ads} + CO_{ads} \Rightarrow CO_2 + H^+ + e^- \quad (4.3)$$

$$Pt + H_2O \Rightarrow OH_{ads} + H^+ + e^- \quad (4.4)$$

Thus it can be inferred from the above that it is possible to remove the CO from the surface of the catalyst, if sufficient anode overpotential is generated. This can be achieved by the proposed circuitry to generate the pulse current from the fuel cell described in the section 4.4.

4.3 Fuel Cell Polarization Curves with CO Contents in the Hydrogen Fuel.

4.3.1 Experimental Set-up and Method

Fig 4.3 shows the 300W PEM fuel cell system implemented for this experiment. The fuel cell stack was manufactured by BCS fuel cells Inc and its specification can be

found in the Table 4.1. The stack is composed of 24 cells including four cooling cells and water-cooled. The temperature of the stack is maintained in between 60-65°C by a controller, which controls the water pump through the SSR (solid state relay) and the speed of the fan. This controller also controls the solenoid valve to purge the stack periodically. Air is supplied to the cathode through the compressor and the airflow rate is monitored by the flow meter attached at the front panel. Pressure indicator indicates the backpressure of the fuel cell stack and it is maintained at 5 psi by the needle valve during the experiment. Hydrogen leak detector is used to sense the hydrogen leak and if there is any leak, hydrogen is blocked by the solenoid valve controlled by the relay installed

Table 4.1 BCS PEM fuel cell specifications

Manufacturer	BCS Fuel Cells Inc.
Output Voltage	12 [V] at 25 [A]
Output Power	300 [W]
Number of Cells	20 Cells
Cooling	Forced Flow (Water-Cooling)
Area of the Membrane	64 [cm^2]
Anode Catalyst Loading	0.25 [mg/cm^2] Pt/Ru
Pressure	5-10 [psi] for anode and cathode
Operating temperature	60-65 °C

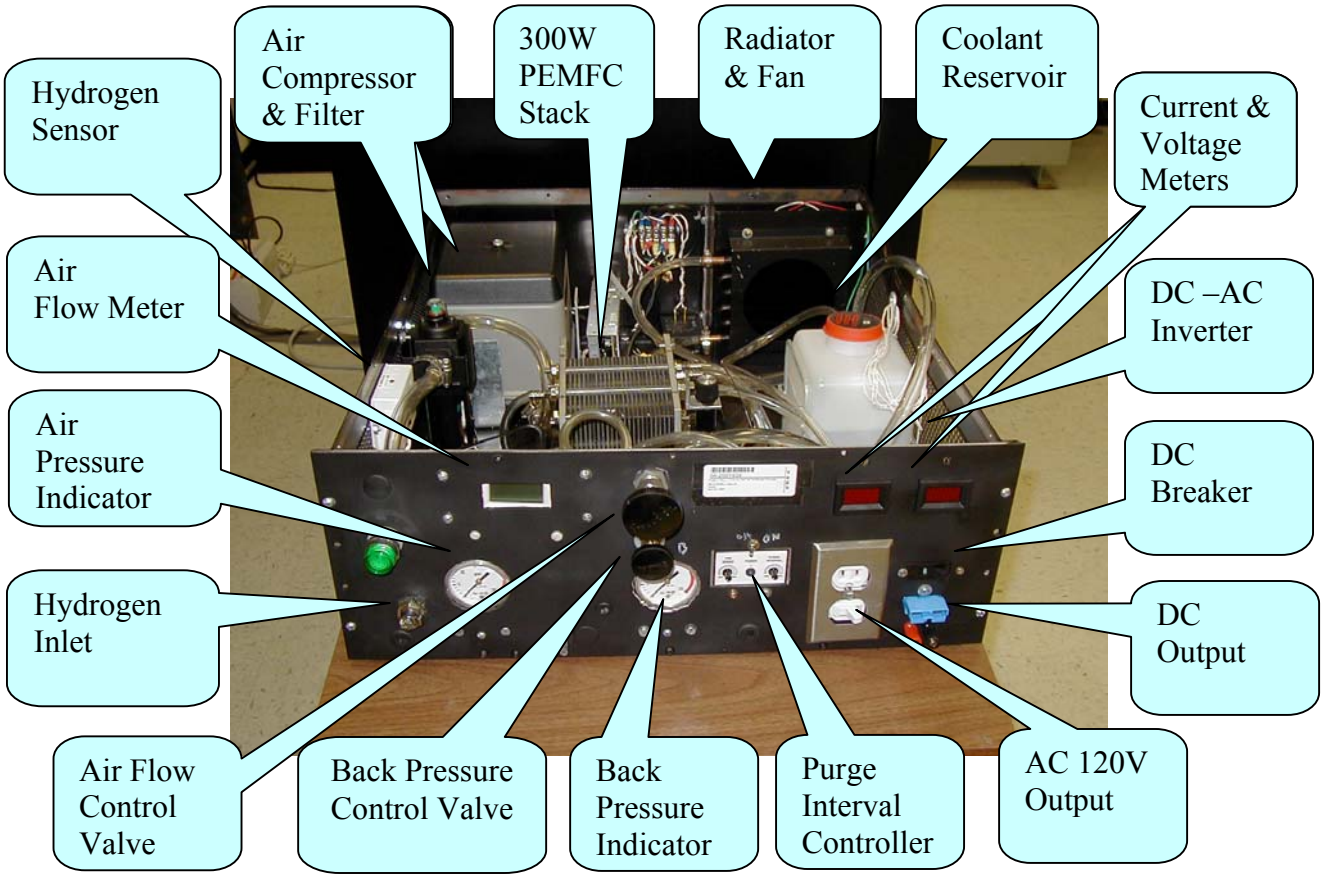

Fig 4.3 Implemented 300W PEM fuel cell system with a DC-AC inverter

inside the hydrogen leak detector. An electronic programmable load (Chroma 63202) is connected to the terminal of the fuel cell stack. First experiment was performed to verify the effects of the CO on the performance of a 300W fuel cell and the validity of the proposed pulsing technique At the beginning, pure hydrogen was supplied to the fuel cell stack and the stack was running with 50% load for an hour until the temperature of the stack gets to its steady-state value (60°C). Then, the load was varied from the no load to full load and the current and output terminal voltage were recorded.

After the results with pure hydrogen were recorded, the premixed H2/500 ppm CO, as confirmed by HP Gas Products Inc., was introduced to the fuel cell stack. Since the gas supply system has two intakes, one connected to the pure hydrogen cylinder and the other to the premixed H2/500 ppm CO cylinder, it was able to alter the fuel by blocking one cylinder and opening the other. During the course of experiments, seamless operation of the fuel cell system was achieved while supplying power to the load and thereby all the experiments could be performed without stopping the fuel cell stack.

As soon as the CO was introduced, immediate voltage drop was observed. It continued for about 40 minutes and the voltage was finally stabilized on a certain voltage. After then the same experiments were performed to get the polarization curve under the presence of CO in the fuel.

4.3.2 Experimental Results

Fig 4.4 shows the V-I polarization curves of the fuel cell stack with pure hydrogen and premixed H2/500 ppm CO. In this case, about 50% of the voltage drop is observed at the full load. Fig 4.5 shows the output power curves of the fuel cell stack. The output power decreases significantly when the fuel cell stack runs with hydrogen fuel with 500 ppm CO. Fig. 4.6 (a) and (b) show the output voltage drop and the corresponding available output power in per-unit due to 500 ppm CO in the fuel at the different loads.

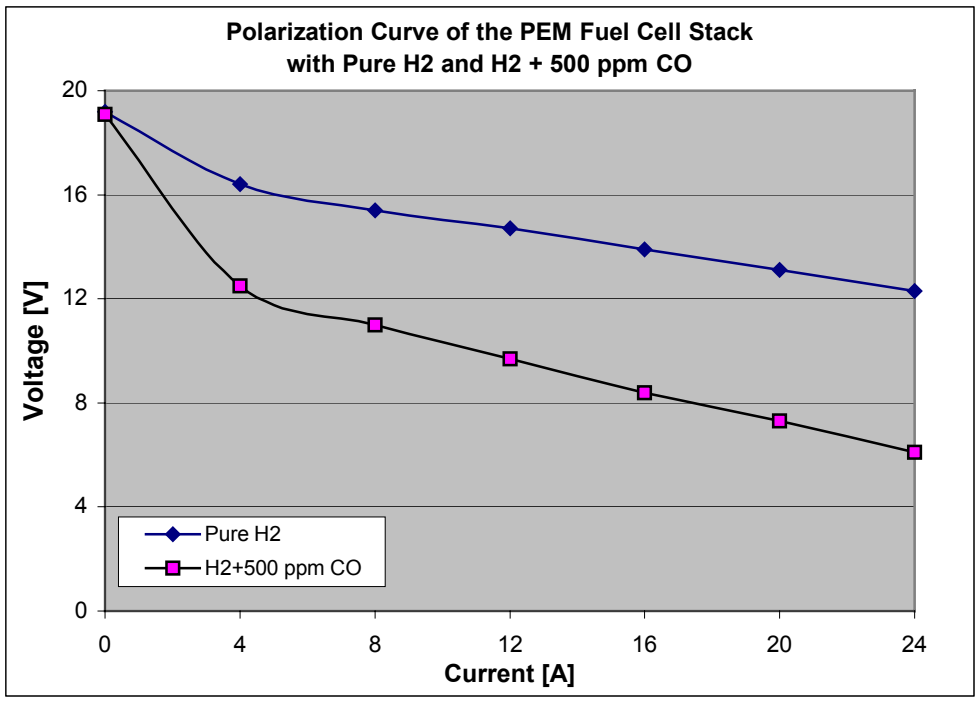

Fig. 4.4 Polarization curves of the fuel cell stack with pure hydrogen and hydrogen with 500 ppm CO

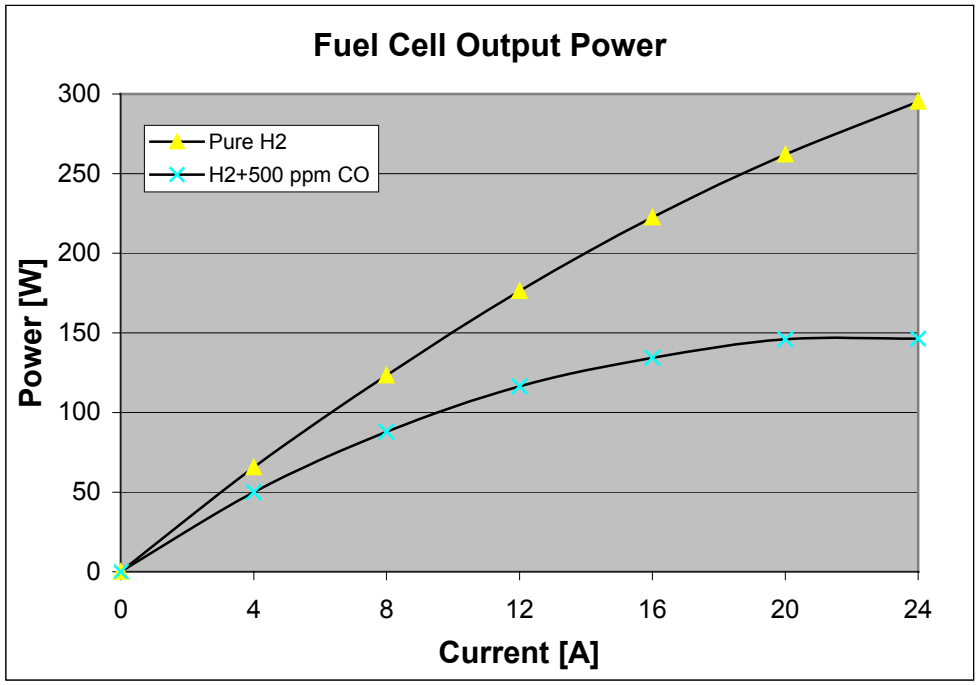

Fig. 4.5 Output power curves of the fuel cell stack with pure hydrogen and hydrogen with 500 ppm CO

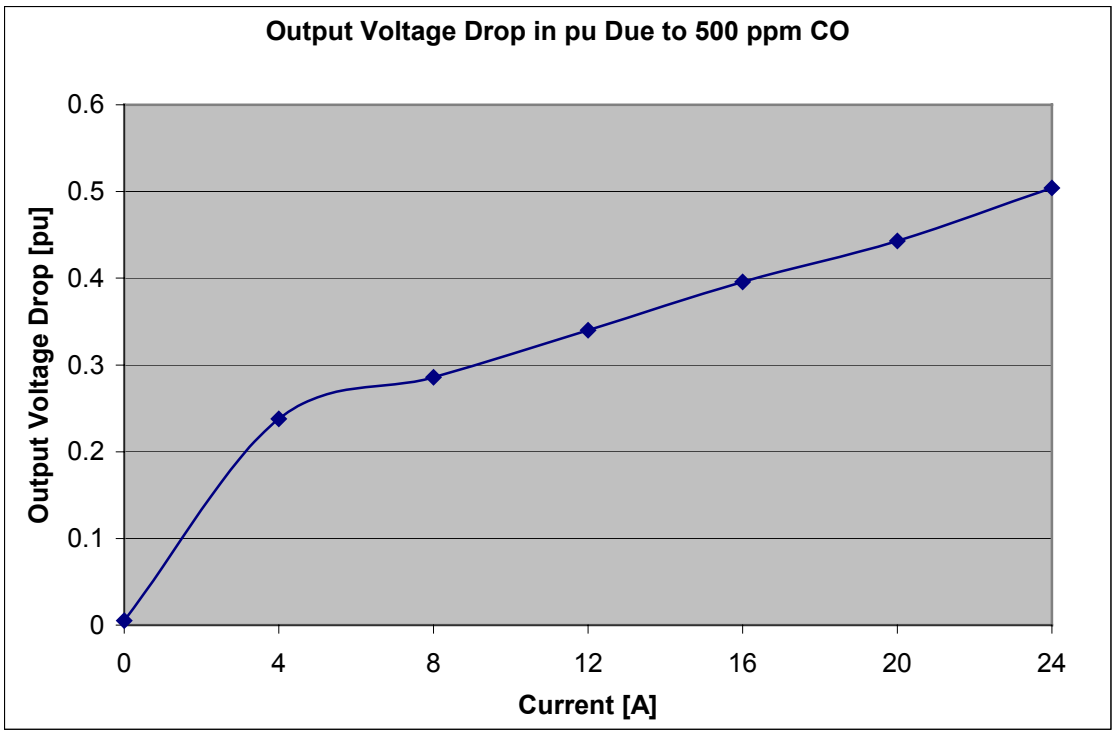

Fig. 4.6 (a) Fuel cell output voltage drop in pu (per unit) due to 500 ppm CO.

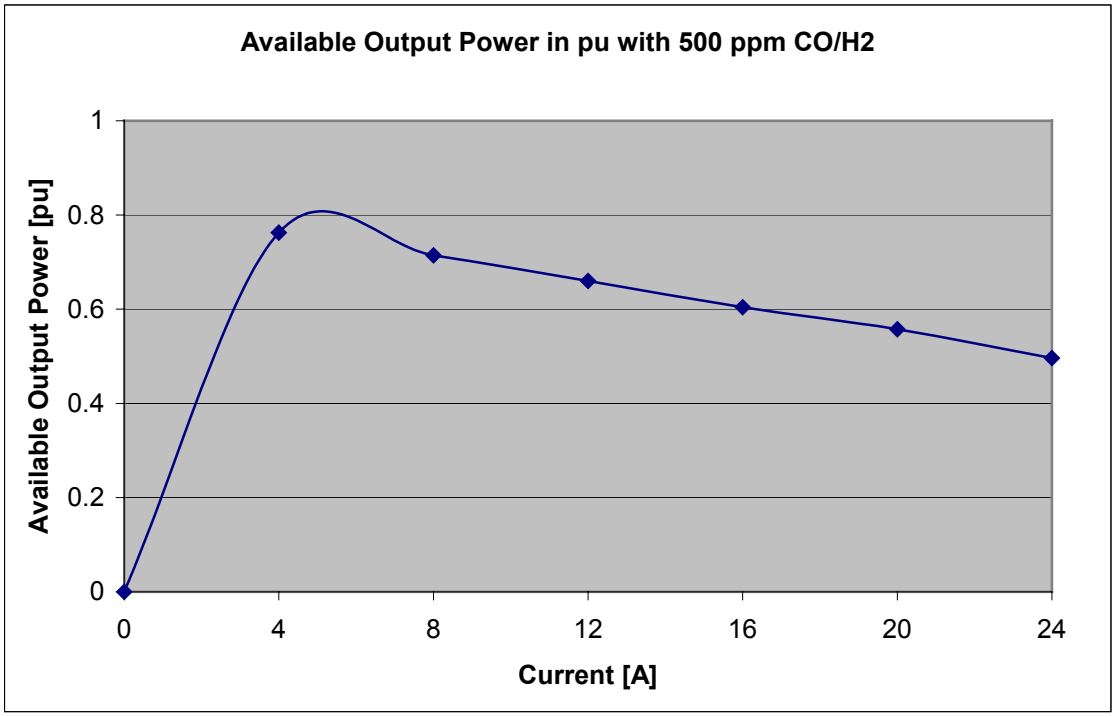

Fig. 4.6 (b) Available output power in pu (per unit) with premixed H2/500 ppm CO.

4.4 Proposed Solution to Improve the CO Tolerance of the PEM Fuel Cell.

4.4.1 Effects of the Pulsing Technique

As mentioned in the section 4.2, CO can be oxidized at very high anode overpotential and this can be generated by drawing the pulse current from the fuel cell stack. In order to verify the effects of the pulsing technique, electric pulsing was performed to the fuel cell stack by using a Programmable Electronic Load (PEL). In this experiment, the PEL draws the suitable amount of dc current from the fuel cell stack as commanded and generated the pulse current of specific pattern as well.

Fig. 4.7 shows the effect of the pulsing technique. At the beginning of the experiment, the fuel cell was supplied with pure hydrogen and was connected to an electrical load of constant current source drawing 10.2 [A]. The fuel cell output voltage was 15 [V] at an output power of 149.8 [W] (see Fig. 4.4 V-I polarization curve). After operating under pure hydrogen for sufficient length of time, hydrogen with 500 ppm CO was introduced into the fuel cell stack. The output voltage of the fuel cell was observed to decrease and finally stabilized to 10.3 [V] at a power output of 104.7 [W] (Fig. 4.7 (a)). Therefore, introducing 500 ppm CO (while supplying a constant current source of 10.2 [A]) contributed to a reduction in output power from 149.8 [W] to 104.7 [W], a significant 30.1% decrease. In Fig. 4.7 (b), the output load current was pulsed from 10 [A] to 30 [A] at a frequency of 0.25Hz with 5% duty ratio pulse. The top trace of Fig. 4.7 (b) clearly demonstrates that the fuel cell output voltage recovers immediately due to

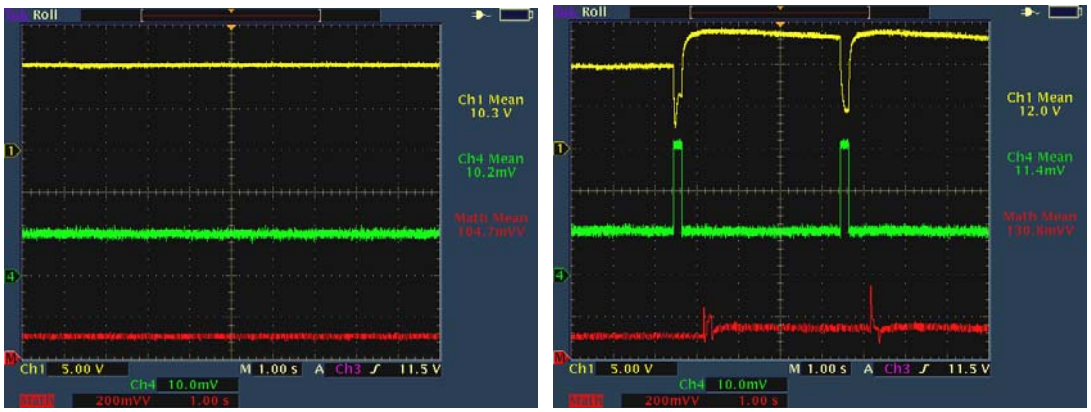

(a) (b)

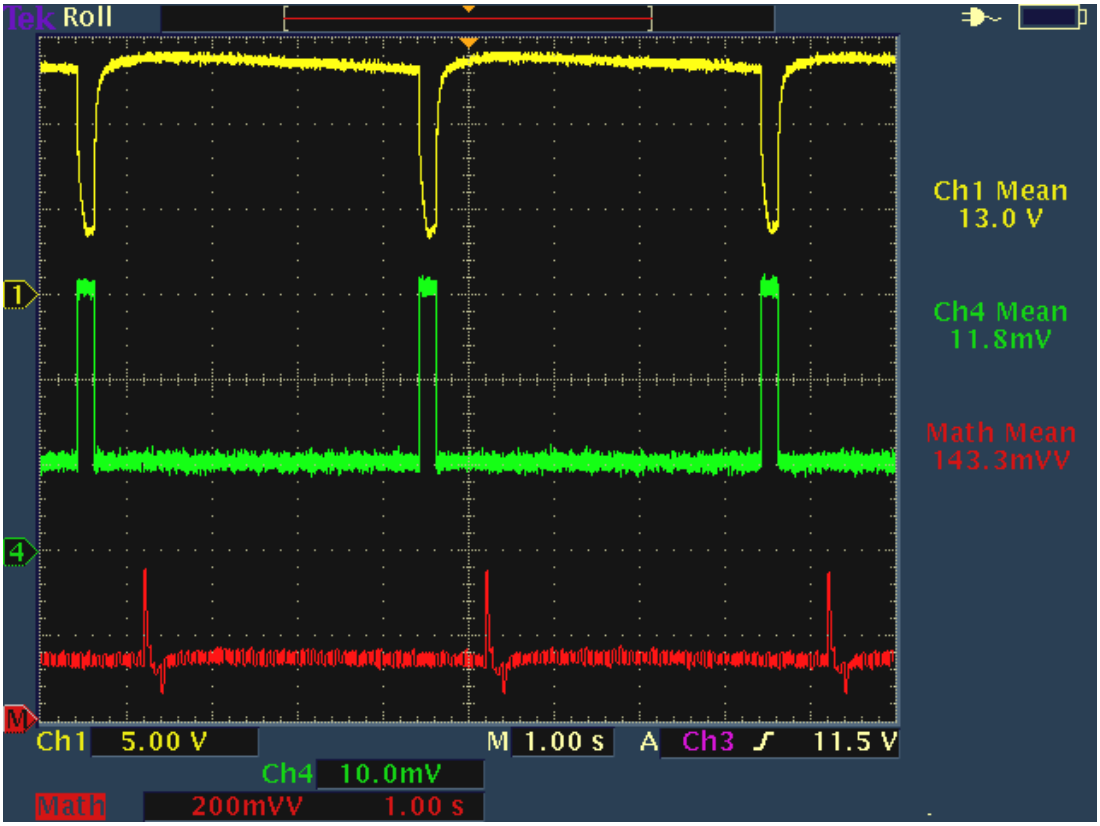

(c)

Fig. 4.7 Effects of the pulsing technique. (a) Fuel cell is supplying 10.2 [A] load with hydrogen with 500 ppm CO. (b) Effect of 5% duty cycle pulse of 30 [A] peak at 0.25Hz (c) Steady state performance of the fuel cell with hydrogen with 500 ppm CO when output current is pulsing: 5% duty cycle, 30A peak at 0.25Hz

pulsing and subsequent electro-oxidation of the CO. Fig. 4.7 (c) illustrates stable operating point with 5% duty ratio and 0.25Hz pulsing as described above.

4.4.2 Optimum Pulse Pattern

In the previous section, it has been proven that the electrical pulse is an effective means to remove the CO from the surface of the catalyst and thereby significantly increases the output power of the fuel cell stack under the presence of the CO in the hydrogen. Fig 4.8 shows the effect of pulse width on the fuel cell output voltage and the power when the fuel cell stack is supplied with premixed H2/500 ppm CO.

Fig 4.8 (a) shows the results obtained with pulses, which have same amplitude (20 [A]) but different pulse width at a frequency of 0.25Hz. As seen in the figure, the resulting average output voltages are different depending on the pulse width. Thus, in order to find out the optimal parameters for the pulse, it is required to investigate about the relationship between the effectiveness of the pulse and its parameters such as frequency, duty and amplitude.

The results shown in the Fig 4.9 have been obtained from the experiments performed with the pulses of different parameters. Fuel cell stack was supplied with premixed H2/500 ppm CO and the pulsing was performed. It is seen from the graph that the best result has been obtained by the pulse with 10% duty (200msec) at 0.5 Hz.

Figure 4.10 shows the results obtained by the pulses with same frequency and duty (0.25Hz, 10 %), but different amplitude. The optimum pulse amplitude that gives the maximum output power is different depending on the operating point. When the load

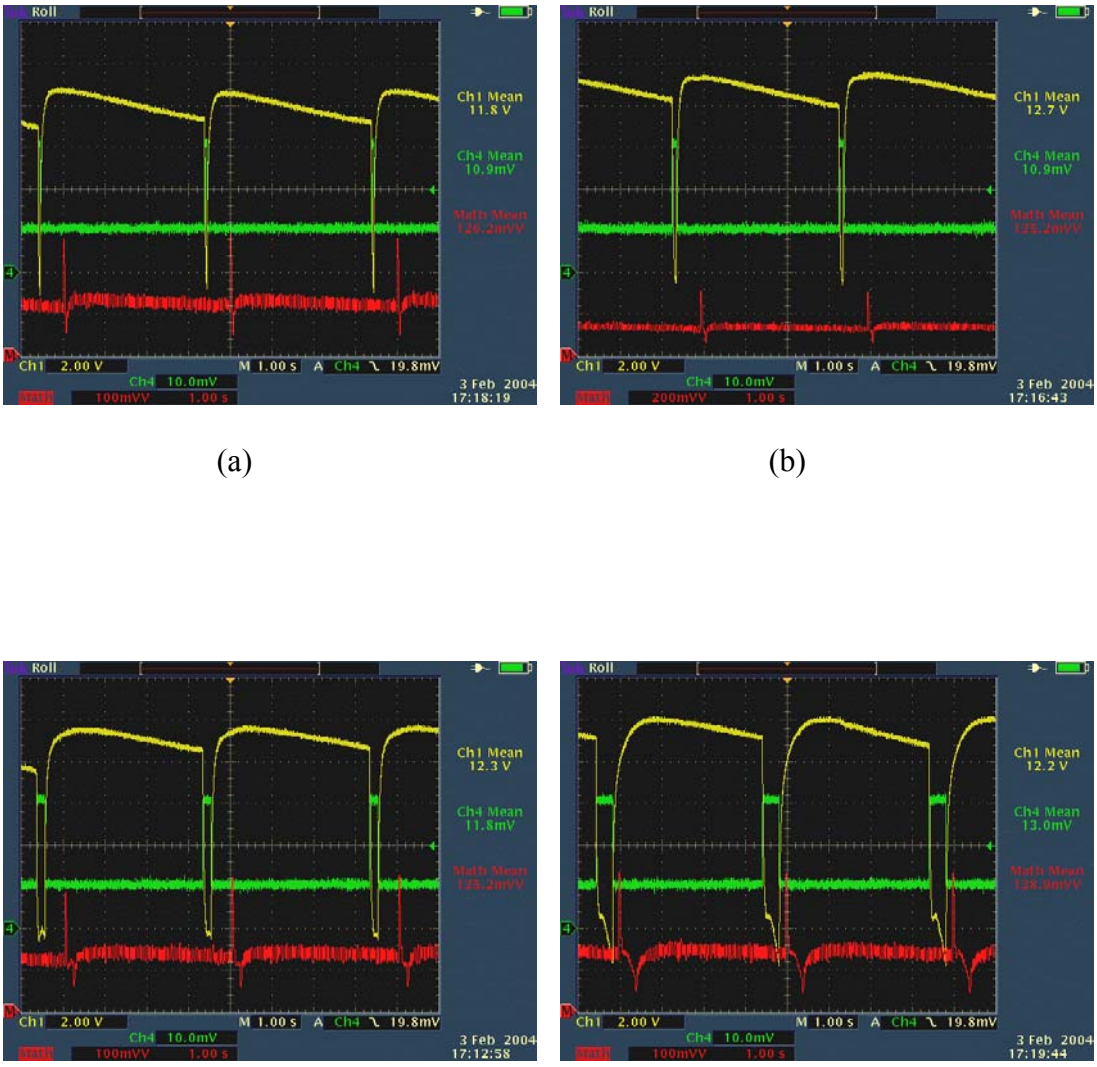

(a) (b)

(c) (d)

Fig. 4.8 Effects of the parameter variation in pulsing technique. (When the fuel cell is supplying 10 [A] with hydrogen containing 500 ppm CO) (a) 0.25 Hz, 1.25% duty, 30 [A] peak amplitude pulse is applied (b) 0.25 Hz, 2.5% duty, 30 [A] peak amplitude pulse is applied (c) 0.25 Hz, 5% duty, 30 [A] peak amplitude pulse is applied (d) 0.25 Hz, 10% duty, 30 [A] peak amplitude pulse is applied

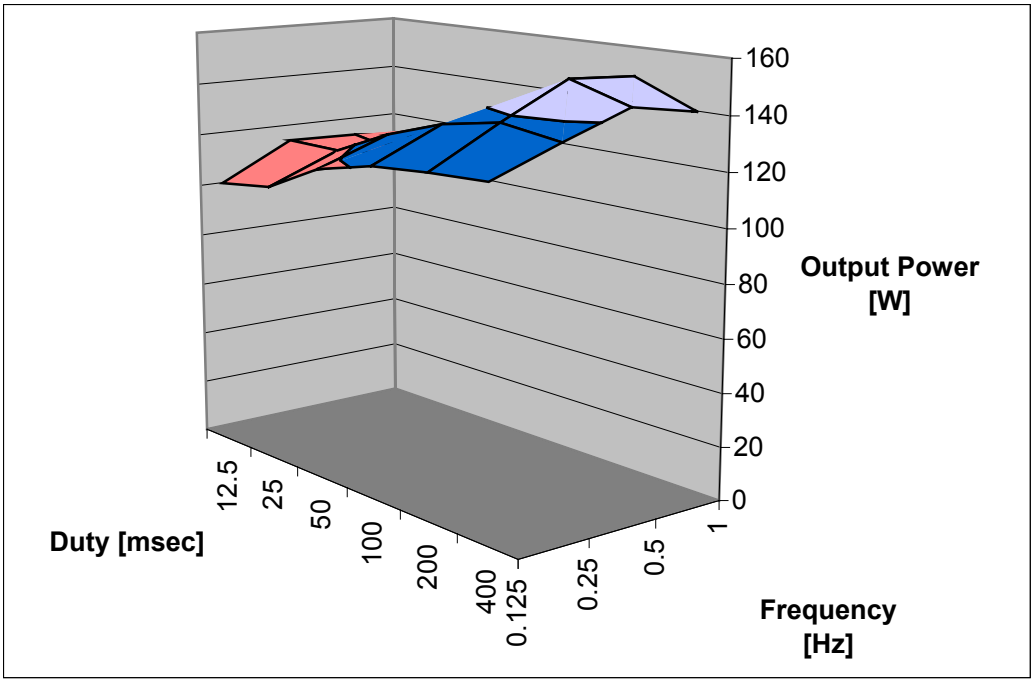

Fig. 4.9 Fuel cell output power obtained by the pulses with varying parameters (frequency and duty)

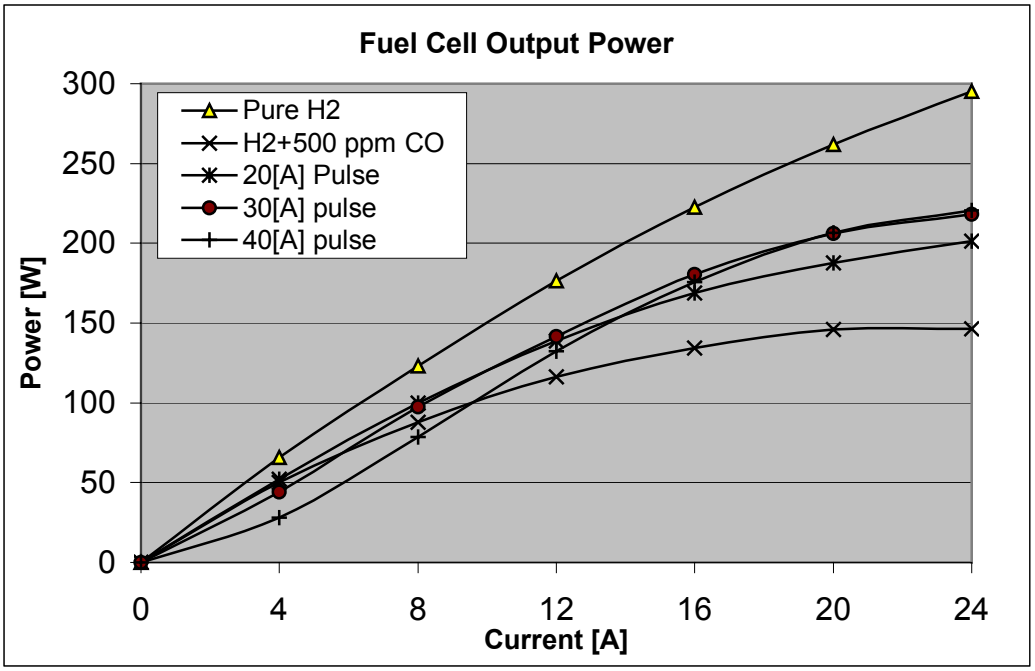

Fig. 4.10 Fuel cell output power obtained by the pulses with same frequency and duty (0.25 Hz, 10 % duty), but different amplitude

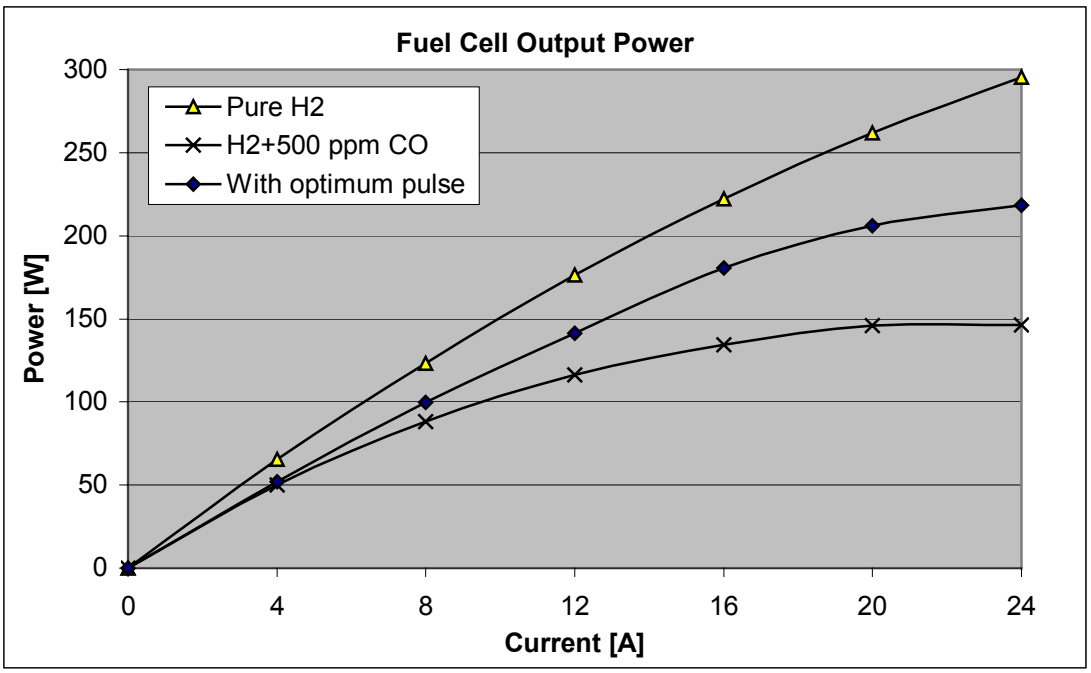

Fig. 4.11 (a) Effects of the pulsing technique with optimum pulse pattern according to the load

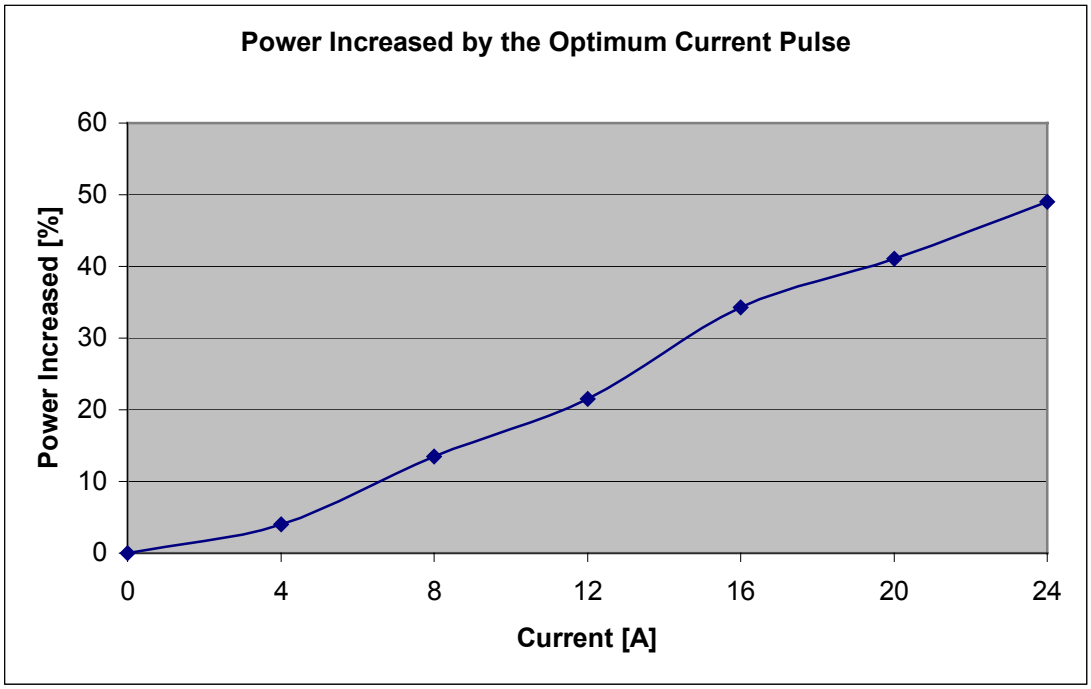

Fig. 4.11 (b) Power increased with optimum pulse pattern according to the load

is less than 40 [%], the optimum pulse amplitude is 20 [A] and it is 30 [A] to give the optimum result in the load range between 40 [%] and 80 [%]. In the load range higher than 80 [%], almost same results were obtained with the pulse of 30 [A] and 40 [A]. Thus, in conclusion, for the fuel cell stack used in this experiment optimum pulse amplitude is 20 [A] for under 40 [%] load and 30 [A] for over 40 [%] load.

Figure 4.11 (a) shows the output power of the fuel cell stack when the optimum pulse is applied according to the load. As seen in the figure 4.11 (b), up to 50 [%] of the lost power can be recovered by the pulsing technique. This means that the requirement of the reforming system can be reduced significantly with this technique and hence the cost of the fuel processing system.

In the power conditioner for the fuel cell, the DC-DC conversion stage is essential for most applications due to its wide variation of the output voltage. As described in the previous section, pulsing the cell with positive current pulse can electro-oxidize the CO on the surface of the catalyst and thereby improve the performance of the fuel cell operating under the presence of the CO in the hydrogen fuel. In the section 4.4.1, it has been proven that the optimum pulse for the fuel cell stack used in this experiment is 0.5 Hz pulse of 20 [A] with 10 % duty under 40 [%] load and .0.5 Hz pulse of 30 [A] with 10 % duty over 40 [%] load. Figure 4.12 shows the shape of the optimum current pulse. This positive current pulse can be generated by the proposed topology (Fig 4.13) and thus the method suggested in this chapter is clean, fast, and reliable.

4.5 Detailed Circuit Topology to Achieve the Pulsing Technique

4.5.1. Proposed Power Converter Topology for Pulsing

In order to generate the anode overpotential to effectively electro oxidize the CO, optimum pattern of the current pulse should be drawn from the PEM fuel cell stack and this energy should be returned to the load since this current pulse is drawn only to remove the CO regardless of the load demand. However, if this energy is directly released to the output dc capacitor, it will significantly increase the voltage of the dc link and the voltage control loop of the boost converter cannot function properly due to this sudden voltage rise. Thus, it is required to have the energy buffer to release this energy to the dc link without significantly increasing the voltage.

Fig. 4.13 shows the proposed power converter topology. An additional two-stage dc/dc converter with a supercapacitor module is connected to the fuel cell. One is used to

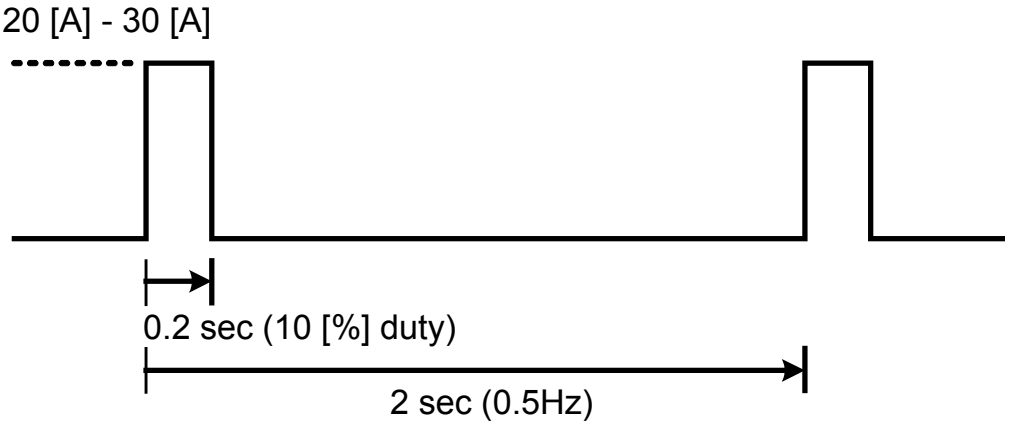

Fig. 4.12 Optimum current pulse pattern

generate the current pulse and the other to slowly release the energy to the 42 V dc-link. A supercapacitor module is employed in between two converters to store the energy drawn from the fuel cell in the form of current pulse.

The operation of the system can be summarized as follows; When the CO sensor senses the CO contents in the hydrogen fuel, the sensor generates and transfers a signal to the controller for pulsing. The converter 1 generates the optimum pattern of the current pulse and this current pulse is stored into the suprercapacitor module, thereby raising the voltage of the supercapacitor. When the voltage of the supercapacitor module reaches to a certain voltage (for example 45V), then the converter 2 starts to release the stored energy in the supercapacitor to the 42V dc-link. Since the voltage of the supercapacitor does not need to be controlled, only the current control loop is required for both converter 1 and converter 2 to generate the required shape of the current.

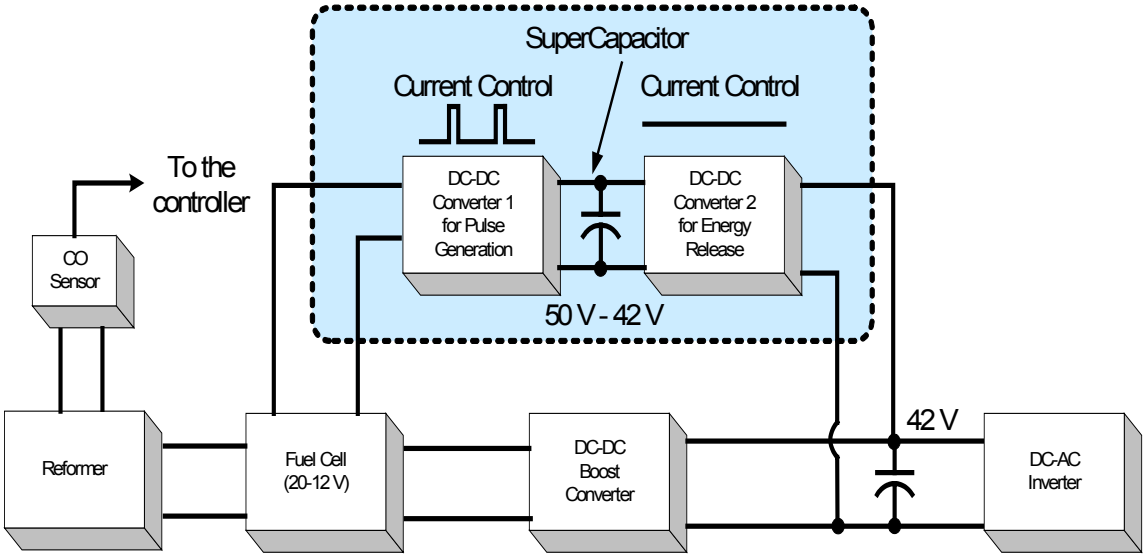

Fig. 4.13 Proposed power converter topology for pulsing

4.5.2 Simulation Results of the Proposed Scheme

Figure 4.14 shows the simulation results of the proposed scheme. Figure 4.14 (a) shows the inductor current of the dc/dc boost converter. The converter supplies the current demanded by the load (10[A]). As the pulsing starts by the proposed scheme, the optimum current pulse (0.5 Hz, 10 % duty, 20 [A]) is drawn from the fuel cell stack through the dc/dc converter 1 (Fig. 4.14 (b)) and this energy is stored in the supercapacitor module. Then, the stored energy is released to the 42V dc-link through the converter 2 in a slow manner (Fig. 4.14 (c)). Thus the shape of the total current

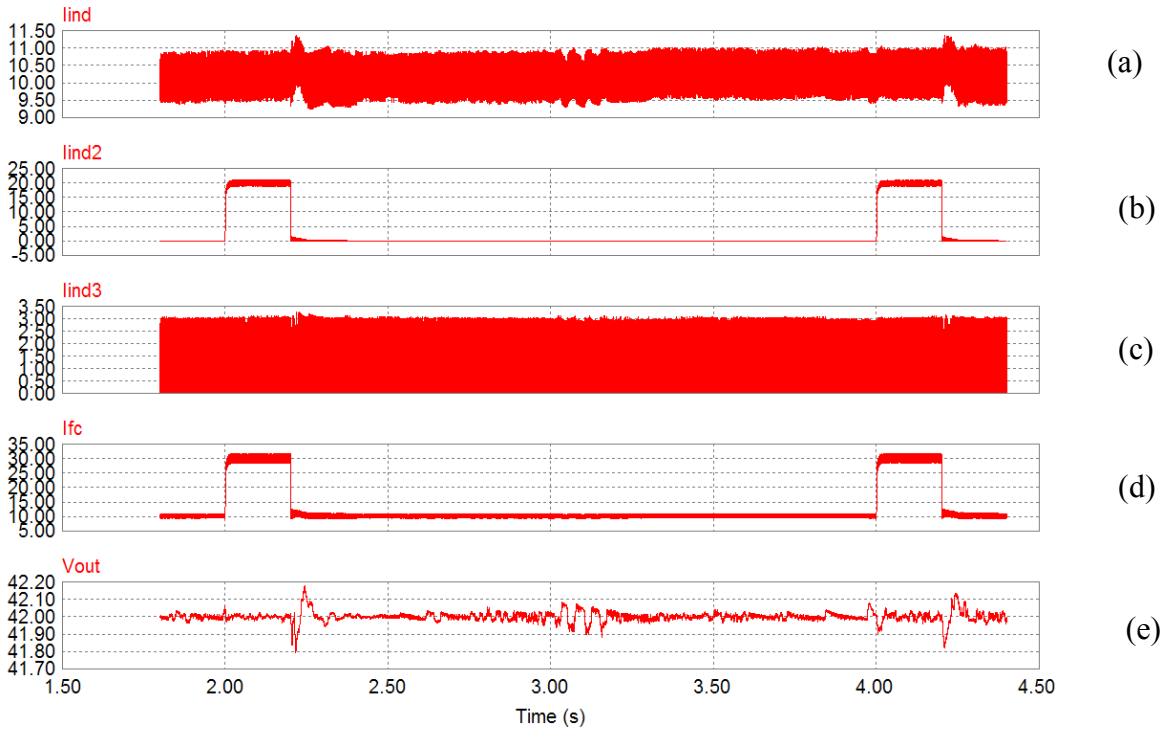

Fig 4.14 Simulation results of the proposed scheme.

drawn from the PEM fuel cell stack is as Fig 4.14 (d). The anode overpotential is created by the pulse current and the output power is increased by the subsequent electrooxidation of the CO. Due to the proposed scheme and the control strategy, the output voltage of the dc capacitor is properly maintained at the desired value of 42 V (Fig 4.14(e)).

4.6. Conclusion

In this chapter, an advanced power converter topology to improve the CO tolerance of PEM fuel cell power systems has been shown. Since the current pulsing technique can be achieved by the switching power devices and simple control circuits, the proposed method is clean, fast, reliable and cheap. The results obtained demonstrate up to 50% increase in the output power due to the proposed scheme and control strategy. It is considered that the proposed scheme contributes to a significant cost reduction in fuel processing unit by reducing the requirement of the expensive fuel processor.

CHAPTER V

CONCLUSIONS

5.1 Conclusions

In order for the PEM fuel cells to play an important role as a primary energy source in the future, several technical challenges should be overcome. The challenges include high cost of the system, slow dynamics of the fuel cell when it is incorporated with the reformer, limited overload handling capability and the requirement of the high purity for the fuel. This research has shown that those challenges can be overcome by selecting a suitable topology for the power conditioning system, combining the fuel cell with auxiliary power source such as supercapacitor and utilizing the inherent nature of the fuel cells.

In the section II, an impedance model of the PEMFCS has been developed to explain the electrical characteristics of the fuel cell. It has been shown experimentally that the ripple current (120Hz) of PCU (Power Conditioning Unit) can contribute to up to 10% of a reduction in the available output power of the fuel cell and increased distortion of terminal voltage. This result helps the power electronics designer to design the cost-effective fuel cell power conditioner by suggesting the optimum limit for the ripple current.

In the section III, a fuel cell powered UPS topology has been discussed and detailed design example has been provided. For the fuel cell to be used as an emergency power source, it is necessary to use the line-interactive topology to ensure the seamless power supply. Instantaneous power fluctuation due to load step change and/or overload can be compensated by the energy stored in the supercapacitor module. The validity and feasibility of an environmentally friendly and clean power back-up system has been verified.

In the section IV, an advanced power converter topology to improve the CO tolerance of PEM fuel cell power systems has been proposed. The CO tolerance of the PEM fuel cell can be significantly increased by this proposed topology. The experimental results show that up to 50% of the lost output power due to CO can be restored by the proposed scheme. Thus the proposed scheme can achieve a significant cost reduction in the PEM fuel cell power generation unit incorporated with fuel processors such as reformers.

In conclusion, this research contributes to the performance improvement of the PEM based fuel cell power systems in term of cost, efficiency and functionality.

5.2 Suggestions for Future Work

Continuation of the work presented in this dissertation can be divided into two categories. First, it is required to find the optimum way to prevent the detrimental effects caused by the ripple current for the fuel cell power systems. As shown in the section II,

the PCU ripple current (120Hz) contributes to power reduction and terminal voltage distortion of the fuel cell [26-28]. Thus, for fuel cells powering a single-phase AC load, it is recommended to install an active or passive filter to mitigate the effects of the ripple current.

However, both types of the filter have their own advantages and disadvantages. The passive filter is simple in design and easy to install, but additional losses within the L-C filter become a concern and contribute to a lower PCU efficiency. While the active filter requires more components and complex control, it has less loss than the passive filter. Thus, based on the results obtained in the section II, optimum type and parameter of the filter can be determined.

Second, the power converter topology presented in the section IV and reference [29] needs to be implemented to prove the feasibility of the proposed system. It is also required to investigate about the optimum pulse pattern for different CO concentration levels present in the hydrogen fuel. The cost comparison between the conventional fuel cell power system employing a fuel processor [30-31] and the proposed system needs to be performed to estimate the benefit of the proposed scheme in term of the cost.

REFERENCES

[1] Leo. J. M. J. Blomen and M. N. Mugerwa, *Fuel Cell Systems*, New York and London: Plenum Press, 1993.

[2] B. K. Bose, " Energy, Environment, and Advances in Power Electronics," *IEEE Trans. on Power Electronics*, vol. 15, no. 4, pp. 688-701, July 2000.

[3] M. W. Ellis, M. R. Von Spakovsky and D. J. Nelson, "Fuel Cell Systems; Efficient, Flexible Energy Conversion for the 21st Century," *Proceedings of the IEEE*, vol. 89, no. 12, pp. 1808-1818, December 2001.

[4] C. Boyer, *"Special Topics; Fuel Cell Technology,"* CHEN 689-Class Notes, Texas A&M University, College Station, 2002.

[5] M. W. Chase Jr,. *NIST-JANAF Thermochemical Tables*, 4th Edition, Washington D.C: American Institute of Physics for the NIST, 1998.

[6] R. S. Gemmen, "Analysis for the Effect of the Ripple Current On Fuel Cell Operating Condition," *Proceedings of the ASME 2001 IMECE*, New York, NY, pp 1-11, November 2001.

[7] E. Santi, D. Franzoni, A. Monti, D. Patterson, F. Ponsi, and N. Barry, "A Fuel Cell Based Domestic Uninterruptible Power Supply", *IEEE Applied Power Electronics Conference and Exposition, APEC '02 Proceedings,* Dallas, TX, pp. 605-613, March 2002.

[8] M. Pagano and L. Piegari, "Electrical Networks Fed by Fuel-Cells for Uninterruptible Electrical Supply," *Proceedings of the 2002 IEEE International Symposium*, Los Alamitos, CA, vol. 3, pp. 953-958, May 2002.

[9] G. V. Sukumara, A. Parthasarathy and V. R. Shankar, "Fuel Cell Based Uninterrupted Power Sources," *International Conference on Power Electronics and Drive Systems*, Sanjib, Singapore, vol. 2, pp. 728 –733, May 1997.

[10] N. Kato, T. Murao, K. Fujii, T. Aoiki and S. Muroyama, "1 kW Portable Fuel Cell System Based on PEFCs," *Telecommunications Energy Special, TELESCON,* Dresden, Germany, pp. 209 –213, May 2000.

[11] Z. Qi and A. Kaufman, "CO-tolerance of Low Loaded Pt/Ru Anodes for Fuel Cells," *Journal of Power Source*, vol. 113, pp. 115-123, 2003.

[12] T. Zawodainski and T. Springe, "R&D on Optimized Cell Performance for Operation on Reformate and Air," *OAAT Annual Review*, Los Alamos National Laboratory, June 2000.

[13] A. H. Thomason, "Increasing the CO Tolerance of PEM Fuel Cell via Pulsing and Sustained Potential Oscillations," Master's Thesis, Texas A&M University, College Station, December 2003.

[14] G. Maggio, V. Recupero and L. Pino, "Modeling Polymer Electrolyte Fuel Cells: An Innovative Approach," *Journal of Power Source*, vol. 101, pp. 257-286, 2001.

[15] J. C. Amphlett, R. F. Mann, B. A. Peppley, P. R. Roberge and A. Rodrigues, "A Model Predicting Transient Responses of Proton Exchange Membrane Fuel Cells," *Journal of Power Source*, vol. 61, pp. 183-188, 1996.

[16] M. D. Lukas, K. Y. Lee and H. Ghezel-Ayagh, "An Explicit Model for Direct Reforming Carbonate Fuel Cell Stack," *IEEE Transactions on Energy Conversion*, vol. 16, no. 3, pp. 289-295, September 2001.

[17] J. M. Correa, F. A. Farret and L. N. Canha, "An Analysis of the Dynamic Performance of Proton Exchange Membrane Fuel Cells Using an Electrochemical Model," *IECON '01, The 27th Annual Conference of the IEEE*, Denver, CO, pp. 141-146, November 2001.

[18] P. Enjeti and W. Choi, *Chapter 8.2: "Power Conditioning Systems for Fuel Cell Systems," Fuel Cell Handbook*, Sixth Edition, US Department of Energy, 2002.

[19] DOE Future energy challenge 2001 and 2003, *Low cost fuel cell inverter design competition*, http://www.energychallenge.org.

[20] S. B. Bekiarov and A. Emadi, "Uninterruptible Power Supplies: Classification, Operation, Dynamics and Control," *IEEE Applied Power Electronics Conference and Exposition, APEC '02 Proceedings*, Dallas, TX, pp. 597-604, March 2002.

[21] Department of Energy, "Fuel Cells: Opening New Frontiers in Power Generation," http://mfnl.xjtu.edu.cn/gov-doe-netl/publications/brochures/brochure_toc.html, November 1999.

[22] J. H. Dymond and E. B. Smith, *The Virial Coefficients of Pure Gases and Mixtures, A Critical Complication*: Oxford, Oxford University Press, 1980.

[23] J. M. Smith, H. C. Van Ness and M. M. Abbott, *Introduction to Chemical Engineering Thermo Dynamics*, New York: McGraw-Hill, 1996.

[24] R. S. Pieere, "CS51227 in a 112W Boost Converter Application," On Semiconductor, Application Note 8035D, www.onsemi.com, November 2000.

[25] L. P. L. Carrette, K. A. Friedrich, M. Huber, and U. Stimming, "Improvement of CO Tolerance of proton exchange membrane fuel cells by a pulsing technique," *Phys. Chem*., pp. 320-324, 2002.

[26] W. Choi, G. Joung, Jo. W. Howze and P. Enjeti, "An Experimental Evaluation of the Effects of Ripple Current Generated by the Power Conditioning Stage on a PEM Fuel Cell Stack," *Journal of Materials Engineering and Performance*, vol. 13, no. 3, pp 257-264, June 2004.

[27] W. Choi, Jo. W. Howze and P. Enjeti, "Development of an Equivalent Circuit Model for a Fuel Cell to Evaluate the Effects of Inverter Ripple Current," *APEC Conference*, Anaheim CA, pp 355-361, February 2004.

[28] W. Choi, G. Joung, Jo. W. Howze and P. Enjeti, "An Experimental Evaluation of the Effects of Ripple Current Generated by the Power Conditioning Stage On a PEM Fuel Cell Stack," *Abstracts of the Fuel Cell Seminar 2003*, Miami Beach, FL, pp 29-32, November 2003.

[29] W. Choi, J. A. Appleby and P. Enjeti, "An Advanced Power Converter Topology to Significantly Improve the CO Tolerance of PEM Fuel Cell Power Systems," to be published at *2004 IEEE/IAS Annual Meeting*, Seattle, WA, October 2004.

[30] M. Todorovic, L. Palma, W. Choi, C. Dowling, P. Enjeti and et al, "Development of a Low Cost Fuel Cell Inverter System with DSP Control for Residential Use," *Proceedings of the Fuel Cell Seminar 2003*, Miami Beach, FL, pp 27-32, November 2003.

[31] W. Choi, Jo. W. Howze and P. Enjeti, "Fuel Cell Powered UPS Systems: Design Considerations," *PESC 2003 IEEE 34th Annual Conference*, Acapulco, Mexico, vol. 1, pp 385-390, June 2003.

VITA

Woojin Choi received the B.S. and M.S. degree in electrical engineering from Soong Sil University in 1990 and 1995, respectively. From 1995 to 1998, he was with Central R&D Institute of Daewoo Heavy Industries, Ltd., Incheon, Korea, where he was engaged in research and development of spindle (Induction Motor) drive and permanent magnet synchronous motor (PMSM) drives for CNC machines. In 1998, he joined Signet Corp., where he developed the battery charger for the battery car and average voltage regulator (AVR). In September 1999, he began his doctoral program at Texas A&M University in the area of power electronics. He has been working as a Research Assistant in the Power Electronics and Fuel Cell Power System Laboratory of electrical engineering and conducting some research on developing the power electronic architecture for fuel cell application. In addition, he has done some teaching assistant activities during his stay at TAMU. His research interests are primarily in advanced power converter and inverter architecture for fuel cell applications, fuel cell modeling and simulation, switching mode power supply design, application of DC/DC converters, and electric hybrid vehicle.

He can be reached by e-mail at cwj777@ee.tamu.edu. His permanent address is: Soojung Apt. A-1208, Youido, Youngdeungpo, Seoul, 150-883, Republic of Korea.